Doctoral Dissertations

Student Theses and Dissertations

Fall 2017

LHD vibrations analysis and numerical modeling during operations

Kgosietsile Kolobe

Recommended Citation

LHD VIBRATIONS ANALYSIS AND NUMERICAL MODELING DURING

OPERATIONS

by

KGOSIETSILE KOLOBE

A DISSERTATION

Presented to the Faculty of the Graduate School of the

MISSOURI UNIVERSITY OF SCIENCE AND TECHNOLOGY

In Partial Fulfillment of the Requirements for the Degree

DOCTOR OF PHILOSOPHY

in

MINING ENGINEERING

2017

Approved by:

Dr. Nassib Aouad
Dr. Daniel Stutts
Dr. Paul Worsey
Dr. Lana Alagha
Dr. Grzegorz Galecki

ABSTRACT

Load-haul-dump vehicles (LHDs) are extensively used as primary loaders in mining operations. LHDs have proven to be vigorous, extremely productive and reliable in mining applications. They have a wide range of tramming capacities that have enabled them to become an essential component in the hard rock mining industry.

Increased mining economic challenges and global competition means the mining industry has to maximize productivity by cutting down operating and capital costs. Also, improvements in safety standards have led to the demand for safer and efficient machines.

LHD operators are at a high risk of whole-body vibrations (WBVs) exposure leading to musculoskeletal disorders (MSDs) over long exposure periods, and elevated lower back and neck injuries. Thus, there is a health and safety concern among LHD operators. Despite manufacturer's emphasis on ergonomics, there is lack of adequate fundamental vibration models of large mining equipment accessible to the public.

This research focused on developing valid analytical and numerical models for determining the vibration propagation in LHDs. Also, this research pioneered the development and analysis of comprehensive dynamic virtual models of LHDs with detailed vibration analysis of the operator-seat interface. The introduced LHD virtual prototype has a total of 24-DOF and captures the complex vibration mechanics of the LHD, with emphasis on vibrations reaching the operator seat-interface in the three dimensions (3D), x, y and z-directions. The RMS accelerations recorded at the operator-seat interface are 0.62 m/s^2 in the x-direction, 0.51 m/s^2 in the y-direction, and 1.01 m/s^2 in the z-direction which exceed the ISO-2631 comfort level.

ACKNOWLEDGEMENTS

TABLE OF CONTENTS

Page

LIST OF FIGURES

LIST OF TABLES

NOMENCLATURE

Symbol	Description
m_1	LHD Body, Front Wheel Base and Loading Bucket
m_2	Operator's seat
m_3	Front Wheel Assembly- Tires and Wheels, ($m_3 = m_3^{right} + m_3^{left}$)
m_4	Rear Wheel Assembly- Tires and Wheels, ($m_4 = m_4^{right} + m_4^{left}$)
m_5	Operator's cabin
I_5	Moment of Inertia about the Center of mass of LHD
K_1	Stiffness constant for the seat suspension
K_2	Stiffness constant for the suspensions between the front wheels and the body
K_3	Stiffness constants for the suspensions between the rear wheels and the body
K_4	Stiffness constants for the front tires
K_5	Stiffness constants for the rear tires
C_1	Damping coefficient for the seat suspension
C_2	Damping coefficient for the suspensions between the front wheels and the body
C_3	Damping coefficient for the suspensions between the rear wheels and the body
C_4	Damping coefficient for the front tires
C_5	Damping coefficient for the rear tires
a	Distance between front wheel assembly and the center of mass of LHD

b	Distance between rear wheel assembly and the center of mass of LHD
m	Single particle mass
r	Position vector
$\dot{r}$	Velocity vector
t	Time in seconds
t_0	Initial time in seconds
$q_i(t)$	Time dependent generalized coordinates
$\dot{q}_i(t)$	Time dependent generalized velocities
$\ddot{q}_i(t)$	Time dependent generalized accelerations
$Q_i(t)$	External force applied to the system
$z_i(t)$	Vertical displacements
$\dot{z}_i(t)$	Vertical velocities
$\ddot{z}_t(t)$	Vertical accelerations
$F_i(t)$	Applied forces
$\theta(t)$	Chassis pitch angle
$q_i(0)$	Initial displacement
$\dot{q}_i(0)$	Initial velocity
τ	Random time in seconds
K_i	Stiffness coefficient
C_i	Damping coefficients
V	Potential energy, $V = 1/2kr^2$
T	Kinetic energy, $T = 1/2m\dot{r}^2$

L	Lagrangian,	$L = T - V$
R	Dissipation energy,	$R = 1/2C\dot{r}^2$
W	Work done on a particle	
g	Gravity	m/s^2
δ	Dirac delta	
β	Rayleigh damping coefficient	
$[M]$	Mass matrix	
$[K]$	Stiffness matrix	
$[C]$	Damping Matrix	
λ	Lambda	$\lambda = \omega^2$
ω	Frequency of oscillation	
ω_n	Natural frequency (rad/sec)	
f_n	Natural frequency (Hz)	
ω_d	Damped frequency	$\omega_{di} = \omega_{ni}\sqrt{1 - \zeta_i^2}$
ϕ_i	Phase angle	$\phi_i = tan^{-1}\left(\dfrac{\zeta_i}{\sqrt{1-\zeta_i^2}}\right)$
ζ_i	Damping ratio	$\zeta = \dfrac{c}{c_c}$
Z_i	Amplitude	
$[M]^{-1}$	Mass inverse matrix	
$[I]$	Identity matrix	
$[A]$	Dynamic matrix	$[A] = [M]^{-1}[A]$

$DET(\ )$ Determinant of matrix ( )

$\hat{u}_i(t)$ Eigenvectors, Normal modes

$[P]$ Modal matrix $[P] = [\{\hat{u}\}_i]$

$[P]^T$ Transpose of the modal matrix

$[\Omega]$ Diagonal matrix of $\omega_i^2, [\Omega] = \lfloor diagonal\ of\ \omega_i^2 \rfloor$

$N_i(t)$ $N_i(t) = \sum_{j-1}^{n} u_{ji} F_j(t)$

RHS Right – hand – side of an equation

LBP Low back problems

CG Center of gravity of the sprung mass

1. INTRODUCTION

1.1. BACKGROUND OF THE RESEARCH PROBLEM

On many occasions, large mining machinery generates high vibration frequencies during daily operation. These vibrations affect the efficiency and the life cycle of the machinery, as well as impact the operator's health due to long-term exposure. Since the majority of these machines require direct human intervention during operation, human operators are at high risk of being subjected to harmful vibration frequencies. Long-term exposure to these vibration frequencies leads to whole-body vibrations (WBVs) and musculoskeletal disorders (MSDs) (T. Eger et al., 2006). LHD operators may have high risks to injuries because of the postures they have to maintain when they operate the equipment (Eger, 2006). About 4% to 7% of the labor force in USA, Australia, and Canada, is affected by WBVs (Bovenzi, 1998). With an increased demand for more advanced mining machines in terms of safety, productivity, and efficiency, it is very important that vibration sources are identified and studied intensively to understand them with a practical aim to reduce their propagation. Despite the recent emphasis on ergonomics from the original equipment manufacturers, a lack of adequate fundamental vibration models of large mining equipment means vibration problems still exist and are rendering these large machines unsafe and less efficient. It is necessary to understand the dynamics of LHD vibrations while in operation because they render both underground and surface mining equipment less productive and affect efficiency as well as the health and safety of operators of such big machines.

LHD vehicles are very important in trackless mining, and about 75% of underground metal mines in the world use them to remove rocks from small drives, large tunnels, and wide excavations (Ratan, 2013). These machines are subjected to high levels of vibrations during operation. Thus, there is a need to build a dynamic virtual model that would help to solve vibration problems and reduce human exposure to harmful frequencies. This virtual model would pave the way for vibration solutions in LHD operations that would help create much safer and more efficient machines in the future. It would also help mitigate whole body vibrations (WBVs) that may result in operator fatigue and musculoskeletal disorders in the long term.

The human body can safely attenuate vibration frequencies, but the vibration frequency spectrum between 1 Hz and 20 Hz forces the human body to vibrate in a harmful way (Kitazaki and Griffin, 1998; Thalheimer, 1996). This resonance on the human body may lead to structural damage and health problems such as pains in the lower, spinal degeneration, neck problems, and headaches. Previous vibration studies focused on the vibrations of cars, trucks, and trains on how they respond to the vibrations from different road conditions. Other studies such as military applications focused on whole-body vibrations with operating fighter jets and helicopters. There is no fundamental research that studies LHD vibrations in mining applications and human exposure to these vibration frequencies as well as, MSDs. This novel work would expand the frontiers to better understand LHD vibrations and to help create a safer and healthier work environment that contributes to the overall efficiency of the LHD vehicle as well as creation of comfortable working conditions for operators of these mining machines.

1.2. STATEMENT OF THE RESEARCH PROBLEM

LHD vehicles are used as the main loading machines in underground mining, surface mining, and construction applications because they are highly versatile with low operating costs. These loading machines have proven to be very vigorous, extremely productive, and reliable in underground mining, surface mining, construction, and tunneling applications. Since these machines have very good tramming capacities and are easy to service, they have become a vital piece of equipment in the mining, tunneling, and construction industries. With an increased demand for high-performance loading machines in these industries, LHDs are highly employed because of their high productivity and maneuverability. Mining, tunneling, and construction industries also seek to eliminate the potential accidents and health problems resulting from these machines by emphasizing their safety during the manufacturing process. About 75% of underground metal mines in the world use LHDs to remove rocks from small drives, large tunnels, and wide excavations as illustrated in Figure 1.1 (Ratan, 2013).
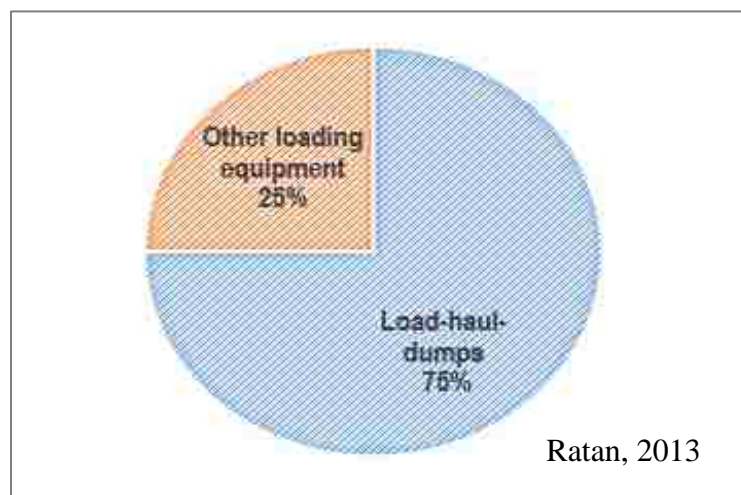
Figure 1.1. Use of LHDs in trackless mining around the world

In addition to equipment performance, a safe operation protocol plays an important role in the overall productivity of the equipment. The use of LHDs in mining operations exposes operators to high vibration frequencies, and this is detrimental to the operators' health and safety. Since LHDs require human intervention within the machine during operation, human operators are at high risk of being exposed to high levels of vibrations during machine operation. Exposure to these high vibration levels lead to operator fatigue and ultimately MSDs. The forces generated during LHD vehicle operation create high frequency shock waves that lead to extreme vibrations that expose operators to WBVs and long-term injuries. Despite recent original equipment manufacturers' (OEMs) efforts and emphasis on ergonomics and seat design, a lack of adequate fundamental vibration models of large mining equipment means these problems still exist. This has resulted in unsafe work environments for the operators who use these powerful machines. LHDs face these vibration problems that are widespread through the mining, tunneling, and construction industries.

The human body harmlessly attenuates most vibration effects acting on it, but exposure to excessive machine vibrations has a significant impact on human health. For instance, Kitazaki and Griffin (1998) showed that frequency spectrum between 1 Hz and 20 Hz affects the human body, and causes the pelvis and spine, to vibrate in a way that eventually leads to health problems such as back pains, spinal problems, headaches, neck and leg problems, and dysfunctional nervous system. Beevis and Foreshaw (1985) and Shwarze et al. (1998) showed that frequency zone of 1 Hz to 20 Hz affects the human backbones and this results in spinal health disorders. Thus, there is a need for research in the field of LHD vehicle vibrations to fully understand the vibration spectrum generated while operating these machines with a practical aim to isolate the harmful frequencies.

1.3. RESEARCH OBJECTIVES

The ultimate goal of this research is to develop valid analytical and numerical models for describing the LHD vehicle vibrations in mining, tunneling, and construction industries during operations. Developing valid analytical and numerical models for describing the LHD vehicle vibrations would help facilitate better design and mitigate vibration problems in the mining industry. The goal of this research will be achieved by focusing on three main areas of the load-haul-dump (LHD) vehicle while in operation. These three major areas are:

1. Identifying the forces acting on LHD vehicles while in operation and linking them to the impact forces propagating throughout the entire LHD vehicles and ultimately reaching the operator-seat interface of the LHD vehicles.

2. Developing complete analytical vibration models used in describing vibration problems encountered in LHD operations.

3. Creating an LHD virtual prototype model to simulate various frequency exposures upon operations.

This research will pioneer the development and analysis of comprehensive dynamic virtual models of LHDs for underground mining operations with detailed vibration analysis on vibrations reaching the operator's seat on LHD vehicles. Figure 1.2 illustrates the major categories involved in vibration modeling in underground mining operations used throughout this research study. This figure shows a flowchart of objectives for solving the LHD vibration problem.
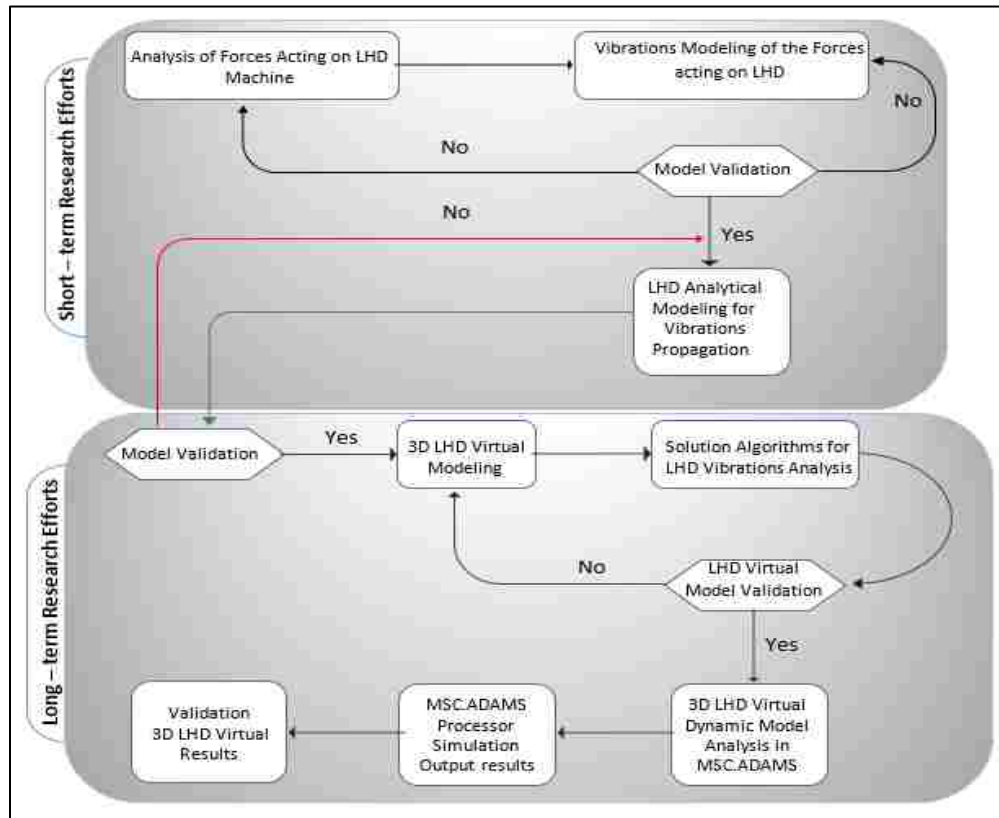
Figure 1.2. Flowchart of objectives to solve the LHD vibrations problems

The forces acting on the LHD vehicle will be analyzed by establishing FBDs of various machine components. These identified forces acting on the LHD vehicle while in operation will be modeled and analyzed. The modeled forces will be verified before LHD analytical modeling for vibration propagation is conducted. The model will then be validated, and 3D virtual modeling on MSC.ADAMS will follow. Solution algorithms for LHD vibration analysis will be performed, and the 3D model will be validated. Simulations of the virtual LHD 3D model will be conducted under various operating conditions, and then the results will be analyzed.

1.4. PROPOSED RESEARCH METHODOLOGY

This research focuses on developing a methodology to identify harmful frequencies on LHD vehicles while in operation. The aims of this research would be achieved by identifying the forces acting on the LHD vehicle and understanding how these forces propagate throughout the machine up until the operator-seat interface. Free body diagrams of an LHD vehicle would be established to identify all the forces acting on various machine components. The mechanics of an LHD vehicle is composed of a multi-degree of freedom system (MDOF) connected together by joints and spring-damper systems. Once all the forces acting on various components of the machine have been identified, equations of motion (EOMs) for various components would be derived using Newtonian-Lagrangian formulation. Moreover, valid mathematical models for describing the propagation of vibrations in LHD vehicles would be developed on MAPLE® to identify the frequencies spectrum on the machine and filter the harmful frequencies. A Virtual 3D model of the LHD vehicle would also be built on MSC.ADAMS® to identify the harmful vibrations LHD operators are exposed to during operation. The standards of permissible vibrations a human body is allowed to be exposed to as set by the International Standards Organization (ISO) would be used as a benchmark to the exposure limit to vibrations by the human body for this research. The forces generated and their corresponding vibration frequencies while the LHD vehicle is in operation will be mathematically modeled.

The LHD vehicle is a complex machine that is made up of rigid body components linked together via joints to build one unit. The mathematical models developed would capture the forces acting on the LHD vehicle. The virtual LHD model is built by connecting the different body parts of an LHD vehicle or rigid body components together using joints. The different components that are analyzed are the driver's cabin, seat, LHD body, front

wheels, and rear wheels of the LHD vehicle. These different parts have dimensions, material properties, masses, and inertial properties and are not allowed be deformed by external forces. In this study, Lagrangian formulation is used to derive the equations of motion (EOMs) that govern the vibrations of various LHD components. The equations of motion derived using Lagrangian formulation are second-order ordinary differential equations (ODEs). These EOMs are derived for each identified LHD component. The resulting set of EOMs is then solved for the frequencies of vibration using MAPLE® software.

The results from using the numerical modeling methods on MAPLE® software will be compared to the virtual prototype LHD model built on MSC.ADAMS®. Once validated, a complete and detailed virtual prototype model will be built and simulated in MSC.ADAMS®. The approach entails first drawing the different parts of an LHD vehicle on MSC.ADAMS/View, assigning dimensions, material properties, masses, and inertial properties, and then linking them with the relevant joints and spring-damper system to mimic the real life scenario. This complete dynamic virtual prototype would capture the three-dimensional displacement, velocities, accelerations, profiles, as well as, moments and forces acting on various LHD components such as the body, the cabin, the tires, and the operator-seat interface.

External forces will be applied on the model bucket to account for the material loaded into the LHD bucket when it is in operation. MSC.ADAMS/View evaluates the reaction forces in the joints for each component, as well as reaction forces corresponding to all spring-damper systems involved. After the virtual model has been completed by connecting all components together, static equilibrium simulation is performed with the initial conditions to ensure that all the system forces are balanced. A static equilibrium is

basically undertaken to expose any mistakes made in the geometry of the different LHD model components. A dynamic simulation then follows, and it reduces some initial transient system responses. A static equilibrium is carried first, and then it is followed by a dynamic equilibrium.

The virtual models will be validated using the experimental results from a research study conducted by T. Eger et al. (2006). These researchers came from various mines to study the health effects LHD operator get exposed to during operations. They conducted experimental results on different models of LHDs to find the vibration frequencies that reach the operator-seat interface of the LHDs while in operation. T. Eger et al., (2006) asked for help in conducting their study from northern Ontario mine companies. The actual experimental testing was conducted at five mine sites. They selected and tested different models of LHDs that had haulage capacities greater than 4.6 m^3, and they also tested six LHD vehicles with haulage capacities less than 4.6 m^3. The LHDs chosen were used to load muck in underground mines. The results of the vibration measurements from this research will be compared to the ISO 2631 guidelines recommended for operating heavy machinery.

1.5. ACADEMIC AND INDUSTRIAL CONTRIBUTIONS

Mining operations seek to be safe, efficient, and highly productive to compete economically. Thus, this research aims at advancing the knowledge of both surface and underground heavy mining machinery vibrations with a practical aim of improving such machines. This research offers great importance to the study of innovation process in the field of heavy mining machinery. Undertaking this research will help improve the scholarly

contribution of universities to innovation-based growth in the field of machine vibrations and offer a long-term perspective to the development of industrial vibrations mitigated machinery. This research also provides a robust training ground for future entrants into the industry workforce, resulting in an educated workforce.

Historically, university research-trained students have proven to be very beneficial to the industry, and this research offers an opportunity to such an important training. Vibrations generated while LHD vehicles are in operation have never been studied to promote solutions that could reduce MSDs and WBVs on LHD vehicle operators. The primary aim of this research is to develop a complete analytical model of the LHD vehicle during operations and solve the MDOF vibration model in order to expose the harmful frequency spectrum at the operator-seat interface of the LHD. The successful completion of analytical modeling will create a basis to further study the vibration problem and complete a 3D virtual model. Once the vibrations problem is understood, the results would help create a safer and healthier work environment and contribute to the overall efficiency of the machine, as well as comfortable conditions for the operators, leading to improved efficiency operations. Vibrations-mitigated machines could be built from the successful solutions of this research and significantly improve productivity of the load, haul, and dump activities in mining. The maintenance costs of machines would be affected and preventive maintenance could be scheduled accordingly, which will affect machine availability and longevity.

1.6. ORIGINALITY OF PHD RESEARCH

This research will advance the body of knowledge on the vibration mechanics of LHD vehicles in a new, innovative way. No prior virtual prototyping has been done on

LHD vehicles, and the results of this novel work will generate LHD models that will be tested for extreme vibration conditions. These virtual models will not expose human operators to harmful vibration shock waves unlike experimental data collection conducted by operating actual LHD vehicles. Successful completion of a 3D virtual model would create a basis for understanding the vibration behavior of other heavy mining, construction, and tunneling machines. There is a lack of numerical models in the literature to understand the propagation of vibrations on LHD vehicles until they reach the operator-seat interface. Thus, the results of this research would add new information to the body of knowledge to better understand LHD vehicle vibrations. Complete analytical vibration models have not been developed for LHDs, and the successful results of this research can be extended to other mining equipment, tunneling, and construction machines.

1.6.1. Research Frontier. This research study would provide the basic fundamentals of the behavior of LHD vehicle while subjected to vibrations while it is in operation and advance the frontiers in mitigating vibration problems on LHDs. Development of a complete analytical vibrations model has not yet been done for LHDs. This research work will pioneer the development and analysis of comprehensive dynamic virtual models of load-haul-dump vehicles. Successful completion of 3D virtual model would create a basis for understanding the vibrations behavior of other heavy mining, construction, and tunneling machineries. The built 3D LHD model would be tested for severe operating conditions in a virtual environment instead of subjecting human operators to harmful vibrations during experiments conducted by human operators. The theoretical results of this research can be expanded to cover analysis on other heavy mining machineries such as front-end-loaders.

1.6.2. Analytical Analysis and Procedures. The aim of this research is to understand the vibrations generated while an LHD vehicle is in operation by providing a numerical tool that can help in identifying and determining the measurements of vibrations generated when an LHD vehicle is in operation and how they propagate until they reach the operator-seat interface. The results of the analytical models and the 3D virtual prototype are used to generate solutions to identify high vibration frequencies generated while the LHD vehicle is in operation. Harmful vibration frequencies will be identified without subjecting human operators to the harmful vibration effects that are associated with conducting site experiments.

LHD vehicle is made up of different components joined together to form a multi-body complex system. The different masses have different physical characteristics and different vibration frequencies. The LHD vehicle is dissected into different masses, which are analyzed by how they interact with each other by way of identifying the reaction and action forces acting on them. Free-body diagrams are drawn to derive a physical model used in deriving a numerical model. The forces identified on each LHD component using FBDs are used to derive the EOMs responsible for the rotational and translational behavior of the LHD components. In this analysis, it is assumed that there is always a linear vibration of the springs. It is also assumed that the displacements and rotations generated during LHD vibrations are very small compared to the LHD dimensions. Another assumption made is that the entire LHD system has viscous damping.

1.6.3. LHD Vibration Model. Vectorial and analytical methods were combined in deriving EOMs for the LHD vibration models. Lagrangian formulation was used in deriving EOMs for the LHD system during operations because it provides a powerful tool for deriving equations of motion for systems with multi-degrees of freedom. Mathematical

equations derived for this model were used to solve the free and forced LHD vibration problems. An LHD vibration virtual prototype was developed using MSC.ADAMS, and the method adopted for developing this model on MSC.ADAMS uses an approach for establishing a dynamic LHD model with a MDOFs system that simulates the real mechanical behavior of the LHD vehicle while in operation. LHD is made up of rigid-body parts that are joined together to form one solid complex machine. The model has fixed inertia and mass properties that are not affected by external forces. The virtual model built on MSC.ADAMS mimics the actual vibrations generated in LHD operations.

LHD components were drawn on MSC.ADAMS and assigned their corresponding masses, dimensions, and material properties. The different components of the LHD vehicle were assembled, and these components were connected together via joints and a spring-damper system to create a single unit virtual model. These different LHD components included the LHD body, the tire assembly, the cabin, and the operator seat. The ground was used a reference point of the LHD vehicle during analysis. Coordinates that define the direction of motion of the different LHD components were established in the three dimensions (3D) x, y and z-directions.

Figure 1.3 shows a wireframe schematic diagram of the LHD virtual model that was built on MSC.ADAMS to simulate the actual LHD vehicle vibration behavior while in operation. The generic model can capture vibration behavior of all the machine components and mimic the actual behavior of the LHD vehicle while in operation. This complex virtual model built on MSC.ADAMS will become a generic model that can accommodate various loaders for underground mining applications, as well as construction applications. The LHD virtual model built on MSC.ADAMS provides a powerful tool to

innovation-based technology in the field of heavy mining equipment design and optimization.
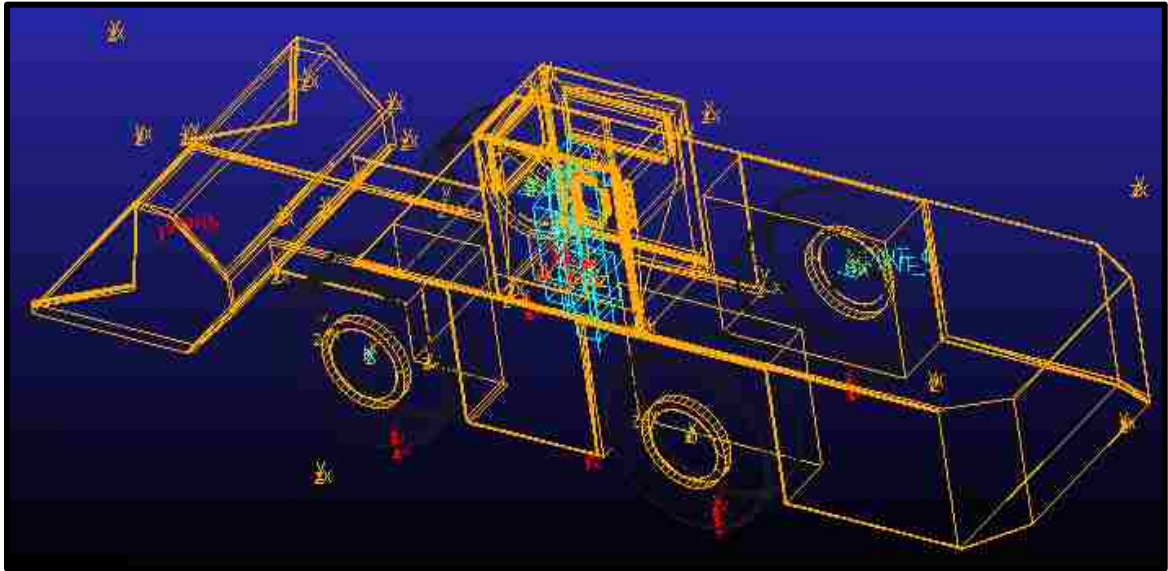
Figure 1.3. LHD vibrations model on MSC.ADAMS environment

The material that is loaded into the bucket of the LHD vehicle generates the vibration excitations on the machine during operations. These excitations cause the LHD vehicle to vibrate, and the vibrations generated propagate to the rest of LHD components and ultimately reach the operator-seat interface of the machine. These vibrations could lead WBVs and MSDs in the long run. The LHD vibrations virtual prototype built on MSC.ADAMS will provide a powerful tool in the field of LHD vehicle vibrations that would provide the basis for understanding the mechanical response of LHDs and other similar machines.

1.6.4. Technological Improvements. Once the vibration problems are understood throughout this study, the results will be used to improve the designs of a safer and more

efficient mining, tunneling and construction equipment with no vibrations problems while in operation. Success in building the LHD virtual model on MSC/ADAMS would mean that human operators will no longer be exposed to harmful vibrations shocks during operations. Furthermore, experiments would be conducted in virtual environments without subjecting test operators to harmful shockwaves during continuous improvement testing periods. Building vibrations mitigated equipment would result in a healthier work environment, improve the safety of the LHD during the various activities, as well as improve the performance of LHD operators.

1.6.5. Integration of Results to Current Designs. The results of this research study would serve as a basic guide to vibration control strategies, and help in developing vibration manuals that would serve as a guide during LHD vehicle manufacturing, and other construction, and tunneling heavy machinery. Once vibrations from LHD operations are understood, the results would affect new machine designs, as well as improve modifications on the current machine designs.

1.6.6. Scope of Research. The use of LHDs in the mining industry has risen because of their proven reliability in excavation and materials transport. It is estimated that 75% of underground metal mines in the world use LHDs to drive excavations (Ratan, 2013). These machines generate high-frequency vibrations during the loading, hauling, and dumping operations that becomes harmful to the operators. This vibration problem is encountered in both surface and underground mining operations. This original research is an effort aimed at implementing virtual simulation modeling to understand, identify and solve the high-frequency vibration problems resulting from operating this powerful mining machinery. This research is limited to LHDs in both underground and surface operations.

However, the theoretical results of this research study can be applied to the mining, tunneling, and construction machines to improve their overall safety and efficiency.

1.7. TECHNICAL BARRIERS

Large machines deployed in mining operations increase the operator's exposure to mechanical vibrations, and this affects the operator's health and safety over prolonged exposure periods. Among this large equipment, LHDs experience a high amount of vibrations while in operation. The shock waves are transmitted to the operator, affecting his or her health. This identified problem has to be understood fully in order to eliminate the LHD vibrations and to create a safer work environment in underground mining operations. The attempt to build a virtual analytical model for LHD vibrations, analyze it, and test it for severe operating conditions to solve the vibrations generated when LHDs are in operation has not been conducted yet. The major barrier of this research lies in the analytical modeling of the vibrations propagation within the LHD. This high-risk barrier comes with challenges of dissecting the LHD components and understanding the mechanical articulations and the relationship between the major parts to be able to express LHD motion analytically. This high-risk challenge will be tackled with the PI and researcher's expertise in mechanical engineering and machine design. Moreover, 3D virtual modeling and dynamic analysis has never been done before on LHD vehicles. The PI's expertise in 3D virtual dynamic modeling in MSC.ADAMS for other mining equipment would provide the basis for success in solving these critical issues during the long-term research efforts.

Thus, the technical barriers would be overcome by conducting analytical models for the vibrations that propagate throughout the LHD vehicle, ultimately reaching the

operator-seat interface and causing WBVs and MSDs. This research will build a virtual LHD model to provide a complete understanding of the behavior of LHDs under various terrain conditions. All the existing research studies and vibration models in literature lack one or more of analytical and virtual prototyping qualities. Moreover, no comprehensive work and analytical modeling has been done on LHDs in underground mining applications yet. Therefore, there is need for this research in order to isolate vibrations due to machine operations and create a safe work environment. This research will pioneer the development and analysis of comprehensive dynamic virtual models of LHDs for underground mining operations. The results of this research can be extended to front-end loaders and other construction equipment prone to vibrations during operations.

1.8. THE PHD PHILOSOPHY

It is very critical to understand the mechanics of LHDs in terms of the critical body components, articulations, dimensions, and the linkages, as well as the mechanical relationship between different machine components. The aim is to understand how different major components of the LHD vehicle interact with a practical aim to monitor how the vibration shock waves propagate throughout the LHD vehicle and ultimately reach the operator-seat interface of the machine.

1.9. DISSERTATION STRUCTURE

Section 1 gives an introduction to the research study conducted on LHD vehicles. It gives the details of the background of the research problem and introduces the LHD vehicles and the role that LHD vehicle play in the mining, construction, and tunneling industries. This introductory section highlights that LHDs produce high vibration

frequencies while in operation, and exposure to these vibration shock waves by human operators leads to operator fatigue and musculoskeletal disorders in the long run. Section 1 also outlines the research objectives and how these objectives will be achieved. Moreover, Section 1 covers the proposed research methods used in this study and the contributions of this research to academia and the industry. On the other hand, Section 2 gives a detailed literature review used during the course of this study. It covers the vibrations work that has been conducted on heavy machines and robotics and discusses what needs to be done in future vibration studies to expand knowledge on machine vibrations. Section 3 gives the details of vibration mechanics of LHD vehicle during operations. The force vectors acting on LHD vehicles during operations are discussed in this section. Section 3 also discusses the Lagrangian formulation as used in this research to derive the EOMs of the LHD system. Moreover, Section 3 covers vibration analysis of the 6-DOF LHD system, as well as the details of Lagrangian formulation used to derive the EOMs for the 6-DOF LHD system. The free and forced vibrations of the 6-DOF LHD system are also covered in this section. Section 4 gives a detailed analysis of the numerical techniques of LHD vehicle vibration mechanics while in operation. It also covers the stability of the model results, convergence, and error estimates. In addition, Section 4 explains the numerical integration methods used in MSC.ADAMS and gives details of building the virtual model and the associated simulations. Section 5 covers the virtual model constraints and MSC.ADAMS methodology used in LHD virtual model analysis. Section 6 discusses the details of the 24-DOF LHD virtual prototype simulation output results, and carries on discussions following the virtual model results. The LHD virtual model generated using MSC.ADAMS/View was simulated successfully for vibrations that reach the operator-seat interface of the LHD while in operation. This LHD virtual prototype

model reproduces the actual LHD vibration mechanical response during operations. The LHD virtual prototype has a total of 24-DOF and captures the complex vibration mechanics of the LHD vehicle while in operation, as well as vibrations reaching the operator seat-interface in the three dimensional directions (x, y and z).

Results from this research were compared to experimental results conducted by Eger et al. (2008) on various LHD models in section 7. The vibration shock waves reaching the operator-seat interface of the LHD vehicle while in operation were compared, and results from both studies had a convincing relationship. Section 7 also discusses how the research results were validated using the experimental results conducted on LHDs, and highlights the deviation between the simulated virtual LHD model and these experimental results.

Section 8 covers the research conclusions, discussions, and recommendations for future research in the field of LHD vibrations. The appendices, bibliography, and vita are attached at the end of the dissertation.

2. LITERATURE REVIEW

The importance of this research in mining operations is to maintain a comfort level in the work environment by ensuring a safe workplace with low level of vibrations induced by operating machinery. Although the body harmlessly attenuates most vibration effects, exposure to machine vibrations has a deep impact on human health. For instance, Kitazaki and Griffin (1998) showed that vibration frequencies that range between 1 Hz and 20 Hz are detrimental to the human health. These vibration frequencies cause the human body to resonate and cause structural damages, and damages to the organs. The human back is also affected and this leads to lower back pains, degeneration of the spine, neck pains and other problems that affects the nervous system in humans. Beevis and Foreshaw (1985) and Shwarze et al. (1998) showed evidence of back problems and spinal health problems in the same frequency zone.

2.1. ISO STANDARDS

Development of standardization is vital in running international trade of goods and services and in promoting cooperation at different levels of economic and technological activities worldwide. A private organization was established in 1947 in Geneva, Switzerland, to uphold the role of a worldwide federation of national standards. The International Organization for Standardization (ISO) has 162 member countries and holds annual meetings where international agreements are published as standards. The agenda at the ISO General Assembly focuses on ISO's annual reports, finances and ISO's strategic plans. The ISO has a counsel that is made up of principal officers and elected member bodies and had a Technical Management Board which meets several times each year to

address matters that concern the organization, strategic planning and technical work of the ISO. The ISO standards are developed by technical committees that are made up of experts from different sectors of the industry and business and these experts may be joined by other people with knowledge and experience from different industries and agencies. ISO has established more than twenty thousand standards that relate to manufactured products, technology, health care, agriculture and safety. ISO standards promote products and services that are safe and have good quality and reliability, and helps businesses improve productivity by reducing errors and wasted resources.

ISO will be used in this research study as a guideline to vibration exposure limits to the human body when operating mobile equipment. ISO 2631-1 (1997); focuses on capturing WBVs that human operators are exposed to while operating mobile equipment. ISO 2631-1 discusses the details of the types of WBVs that operators of mobile equipment get exposed to. These types of WBVs include transient, periodic and random WBVs. It analyses the degree of acceptable exposure limits and provides guidelines on how vibrations generated while operating mobile equipment affect the comfort and health of the equipment operators. The frequencies between 0.5 Hz to 80 Hz are considered for operator's comfort while operating mobile equipment. Also, frequencies between 0.1 Hz to 0.5 Hz are associated motion sickness (ISO-2631). ISO 2631-1 gives the details of how transducers are mounted the operators' body while measuring WBVs on mobile equipment. This part of ISO 2631 does not discuss how mechanical vibration affects the performance of equipment operators, and does not cover the mechanical vibration as a result of vehicle accidents. ISO 2631-1 considers motions that the human body gets exposed to through contact with surfaces during operations. The points of contact considered are the buttocks,

back, and feet of standing and seated persons. ISO 2631-1 will be used as the primary vibrations guideline in studying LHD vibrations in this research study.

ISO 2631-2 (2003) considers vibration in buildings in a range of 1 Hz to 80 Hz. This part of ISO 2631 discusses WBVs and shock that humans get exposed to while occupying buildings. ISO 2631-2 considers human comfort levels while occupying buildings and how people that occupy such buildings get irritated by the vibrations they are exposed to. Frequency weighting method is used in measuring vibrations in buildings and this method is discussed in details in ISO 2631-2. Frequency weighting method works in the frequency range between 1 Hz and 80 Hz and in this frequency range there is no need to define the postures of persons occupying the buildings. The concepts of ISO 2631-2 used for measuring the building frequency levels are also applicable to buildings that are still under construction and the buildings that are difficult to access. ISO 2631-2 is helpful in providing information that is helpful in identifying the structural flaws in buildings. This part of ISO 2631 does not deal with evaluating human safety and the health effects to humans from the WBVs experienced by human occupants of the buildings.

On the other hand, ISO 2631-4 (2001), focuses on evaluating human exposure to WBVs as a result of interacting with fixed-gateway transport systems. This part of ISO 2631 discusses the guidelines on mechanical shock that are adopted in evaluating the motions that the passengers and crew members of fixed-gateway transport system are exposed to while using this transportation system. ISO 2631-4 analyzes how these vibration motions affect the comfort levels of the passengers and crew members that use fixed-gateway transportation system. Also, part 4 of ISO 2631 helps in analyzing and evaluating designs of fixed-gateway systems for possible improvements. Evaluations conducted using part 4 focus on rotational motions, vibration impacts and repeated motions that passengers

and crew members get exposed to while using fixed-gateway transportation systems. ISO 2631-4 guidelines are meant to be used by the companies that own the fixed-gateway transportation systems. These guidelines are also intended as guidance while assessing motions that affect the human body in the *x*, *y* and *z* 3-imensional directions. ISO 2631-4 is not applicable to high transient vibrations that may cause human trauma or death. Frequency range that cause motion sickness is covered and this frequency range is identified as 0.1 Hz to 0.5 Hz. Frequencies experienced as in the vertical direction cause motion sickness.

ISO 2631-5 also deals with the evaluation of mechanical systems with emphasis on how humans get exposed to WBVs. Part 5 provides methods of studying vibrations that undergo multiple shocks. ISO 2631-5 measures the vibration levels that have multiple shocks at the seat pads of seated persons. The calculations conducted in evaluating the vibrations that reach the operator's back are based on the assumption that the person is subjected to vibration shocks while sitting in an upright position and this person consistently sits on the pad during the process of multiple-shock vibrations without rising up. The person has to maintain a single posture because a change in the posture of a person would influence the response of the spine to vibrations. ISO 2631-5 also discusses the details of the method that is applicable when the vibration shocks waves affect the lumber spine area of seated persons. The limitations of the models that deal with how the lumbar spine responds to vibrations that are used in ISO 2631 are given in 5.2. Caution is necessary when applying the method to extreme shock conditions.

Studying vibrations generated when the LHD vehicle is in operation and using ISO vibration guidelines for comparison forms the basis of this research. Once the vibrations frequencies of various components of the machine when it is in operation have been

identified using analytical and virtual models, the results would be compared to ISO standards to identify harmful vibration frequencies. The comparison of the LHD research results in this study, the LHD experimental results by T. Eger et al., and the ISO standards would provide a detailed guidance on how WBVs generated on LHDs affect the health and comfort of operators, as well as, the overall health of the LHD vehicle.

Eger et al. (2007) used ISO 2631-1 to predict the health risks as a result of operating LHDs. Their studies compared the LHD health risks using ISO 2631-1 and ISO 2631-5. Previous research work on studying WBV generated when operating LHDs have not used ISO 2631-5 standard for analysis. This study measured vibration level at operator seat interface of the machine, predicted the health risks as a result of operating LHDs and finally compared the health problems discussed by ISO 2631-1 and ISO 2631-5 to find if both approaches predict similar health risks. In this study, LHD operators were chosen, and WBV measurements were conducted based on ISO 2631-1 (1997). Accelerometers were mounted such that they were placed between the ischial tuberosities of the LHD operators. Then the vibration frequencies that reach the operator-seat interface of the load-haul-dump vehicle were measured in the *x*, *y*, and *z* directions of the established coordinate system. LHD operators performed their normal duties of loading, hauling, and dumping the rocks. The vibration data on LHDs was collected within a time limit of 2 hours. ISO 2631-5 guideline was used to provide guidance on assessing health effects LHD operators are subjected to as a result of multiple shocks to the lumbar spine. The study showed discrepancies on the health effects to the operators when comparing the health effects given by ISO 2631-1 analysis and ISO 2631-5 evaluation methods, and this lack of agreement is a concern. For example, the study they conducted showed that LHD operators experience low to moderate health risks to the lumbar spine that was reported while using ISO 2631-

1. While using ISO 2631-1, moderate health risks to high health risks were reported. Thus, there is a likelihood to misuse the standards and conclude that LHDs are safe and the vibrations reaching the operator-seat interface of the LHDs are harmless while using ISO 2631-5, and it can be concluded that there is extreme health risks while using ISO 2631-1 standard.

2.2. VIRTUAL PROTOTYPING

Most vibrations research analyzed the mechanical responses of small trucks, cars, and trains to the vibrations as a result of the operating conditions on the roads. Other studies, such as military applications, focused on whole body vibration with operating machinery such as fighter jets and helicopters. Many of the initial research studies were performed experimentally and without the benefit of analytical, numerical, and virtual dynamic analysis. Recently, virtual prototyping has found solid applications in the automotive industry, among others. The literature shows extensive work done using car dynamic virtual models. These models provide full understanding of vehicle behavior while subjected to different operating conditions, as well as mechanical responses of these vehicles during operations, but there is lack of virtual prototyping and vibration modeling in the mining industry in general (Aouad and Frimpong, 2008).

The PI (Aouad 2008) has pioneered efforts in virtual prototyping, numerical analysis and vibrations studies pertaining to human vibrations in mining. He has completed the required fundamental research on understanding the truck vibrations, and how these vibrations affect operators of the trucks due to the extreme shockwaves they are subjected to during shovel loading operations in surface mining operations. His research showed that the vertical root-mean-square (RMS) acceleration of the operator's seat can be as high as

3.56 m/s^2, which exceeds the ISO 2631 – 1 limits for extremely uncomfortable zones (> 2.5 m/s^2). This vibration level poses health and safety risks to operators over long-term exposure. Furthermore, the PI has conducted research studies for developing relevant technologies to reduce vibration exposures among truck operators due to high impact shovel loading operations (Aouad et al. 2011). The developed technology has led to the reduction of the vibrations reaching the operator-seat interface of the truck in the vertical direction of the operator's seat to less than 2.5 m/s^2, under the same operating conditions. The research built a 38-degree of freedom (DOF) dynamic virtual truck prototype model and simulated it for extreme ground conditions, which was used to aid the design of mitigating technology. Experimental analysis alone could not solve this problem due to the hazardous conditions that researchers will have to expose operators to as a result of the high level of vibrations during experimental measurements and the high costs associated with conducting a three-dimensional dynamic analysis on mining trucks. Furthermore, with the use of powerful computers, experiments conducted virtually are completed in a fraction of time compared to the actual setup and run time of the actual experiment.

Eger et al. (2005) measured the WBVs exposure levels experimentally on LHD vehicles. The study conducted by T. Eger et al. focused on understanding and exposing vibration frequencies that reach the operator-seat interface of LHDs while conducting the routine load, haul and dump operations. They used the different sizes and different models of LHD vehicles to conduct this research at the mine site. Their results showed that the operators are subjected to high levels of vibrations (1.18 m/s^2). But without a complete model to understand the vibration propagation, it is difficult to design mitigation measures. There is need to investigate the vibration propagation due to operating underground mining machinery with a view to help design engineering interventions. Analytical, numerical, and

virtual models are great tools for evaluating which intervention schemes will have the most effect for the least cost.

Other research studies have been conducted on the vibrations of various mechanical systems such as marine engines, diesel engines, high performance machines, gas turbines, armored tracked vehicles, navy ships, and industrial robots.

2.3. MACHINE VIBRATIONS

Chang and Hu (2010) developed a method that they used as a diagnosis tool for faults within the diesel engines. They used vibration frequencies generated by diesel engines while in operation in their study to detect faults within the diesel engines. This study conducted on diesel engines also uses blind source separation technique to collect data on mechanical faults within diesel engines. The vibration diagnosis method they developed to troubleshoot diesel engines uses a combination of time and frequency domains in vibration analysis. Chan and Hu devised a way to identify independent signal sources and they also discussed the importance of using vibration guidelines and the algorithms that optimize the vibration systems in troubleshooting diesel engines. They emphasized that marine engines are subjected to harsh environmental conditions and are more likely to experience frequent breakdowns and thus affecting their operation and efficiency. There are many sources of vibrations on marine engines according to Chan and Hu, and these vibration sources include motions within the engine pistons, gas combustion chamber and the movement of valves within the diesel engines. It is difficult to filter vibrations and isolate them. Chan and Hu proposed BSS to account for the difficulty in isolating vibrations and BSS is a method that processes the vibration signals from the diesel

engines and it is useful because it can measure the vibration signals that have been detected without the knowledge of the sources of the signal.

Homic (2010) studied the components that make up diesel engines and how they respond while subjected to vibrations during operations. The study he conducted on diesel engines focused on the diagnostic information and maintenance data of diesel engines. In addition, Homic also studied the vibration mechanics of the dampers within the diesel engines. They study he conducted was successful in proving that the vibrations generated while diesel engines are in operation result in the movement of the crankshafts within the engines in the three dimensional direction. Homic stated that the crankshafts are mostly affected by the vibrations because the vibrations they are subjected to torsional motion generated within the combustion engines. This study suggests that in order to minimize vibration impacts on torsional dampers, the engine crankshafts have to be installed at the free end of the engines. This approach improves the efficiency and durability of the engines. Also, the use of multiple cylinder in the diesel engines of the ships leads to vibrations that significantly affect the lifespan of the engine and the propulsion system of the of the ship, as well as other engine parts. The results of the study Homic conducted show that it is important to monitor the mechanical state of the diesel engines by focusing on the condition of torsional dampers used in the manufacturing of diesel engines. If the condition of the dampers is not monitored, there is a high possibility that the dampers will be damaged and the lifespan of the engine will be shortened due to excessive and undamped vibrations generated within the engines.

Hara, Furukawaand, and Shoda (1995) conducted a study to examine the main engines. The study they conducted focused on the engines that have shafts with longer strokes. T. Hara et al. developed a vibration analysis on engines by using building block

approach. The building block approach (BBA) they introduced is efficient in reducing engine vibrations. The aim of their study on engine vibrations was to develop algorithms used in predicting engine vibrations generated while engines are in operation. T. Hara et al. were successful in verifying the accuracy of the BBA approach they developed by conducting further vibration analysis on predicting the effects of vibrations using BBA. They concluded that it is important to accumulate data on damping effects of the engines to improve the accuracy of the results using BBA.

Moreover, Rusinsk, Odyjas, and Pietrusiak (2013) have conducted a study on the vibrations of high-performance machines. High-performance machines are prone to many different dynamic effects that can lead to vibrations of the entire structures or their local parts. The mistake that is common during manufacturing of high performance machines is usually failure to incorporate the mechanisms that would deal with the effects of the dynamics within the mechanical systems of the designs. The other reason is that dynamic effects are still difficult to recognize and thus are difficult to consider at the designing stage. Their study stresses that it is very important to provide proper and quick correcting actions to prevent costly failures or catastrophic breakdowns. Their first step is to identify reasons of problems. They do this with the use of on-site tests and advanced calculations based on theories of vibrations or numerical analyses (FEM, CFD etc.). The numerical analyses are frequently used for such purposes due to a wide range of applications available in systems such as nonlinear or linear, static or dynamic, dynamic response, frequency analyses, and many more. When the problem is properly identified the next step is to provide correct actions to bring the object to normal and safe operational mode. There are no universal solutions for all identified issues. Experience says that each case has to be investigated separately due to many differences in excessive vibrations, effects and possible ways of

solutions. At this stage of investigations numerical analyses are commonly used. When the problem is identified, it is possible to use numerical simulations of the object to incorporate modifications and calculate the effects of changes. The advantage of such an approach is that there is a numerical model of existing problematic object, which is verified by on-site measurements, and with such a tool it is possible to perform various modifications and choose the best solution to eliminate problems in operation.

Mel Maalouf (2005) conducted a study on monitoring the vibrations of gas turbine that focused on the differences between aero derivative and industrial gas turbines. This study outlines that industrial gas turbines and aero-derivative turbines are constructed differently and have different mechanical structures as well as, different maintenance requirements. Because of these mechanical differences, industrial gas turbines and aero-derivative use different vibration monitoring systems. This study focused on understanding these mechanical differences and studying the most common ways that aero derivative and industrial gas turbines use to monitor vibrations they are exposed to during operations. Maalouf discusses that there could be some improvements made to enhance the approaches used in monitoring the vibrations conditions of the aero derivative and industrial gas turbines. The simplest way proposed to monitor gas turbine vibrations is by making sure the filtered vibration signals, acceleration signals, and velocity signals are all fed into the vibration monitoring system. Another approach to monitoring gas turbine vibrations that the study proposes is to improve the seismic transducers within the turbines by mounting these seismic transducers near the embedded bearings and near the vibration source. Aero derivative gas turbines are typically subjected to steady-state vibration of 20 g's or higher and the accompanying vibration peaks as high as 100 g's occur most of the time. These vibration peaks introduce several mechanical problems and turbine fatigue problems and

this in most cases triggers false alarms of the vibration monitoring systems. The best practice to counteract this problem is by installing transducers without moving parts within the gas turbine and fixing the system's interface modules in areas that do not experience vibrations.

Chuan and Ann (2010) also conducted a study on reducing the vibrations of armored tracked vehicles. It important to monitor the vibration levels on armored vehicles. The vibrations generated on armored vehicles could affect the health problems and fatigue. The vibrations generated while armored vehicles are in operation also affect the mechanical response of the vehicles and their reliability since it causes some breakdowns. The study on vibrations generated on armored vehicles by Chuan and Ann (2010) proposed three vibration evaluation approaches. The study proposed the following ways to reduce vibration levels on armored vehicles:

➢ The source approach

➢ The path approach

➢ The receiver approach

Vibration tests were conducted to verify results of the proposed approaches. Vibrations affect the longevity of mechanical systems and these approaches aim at reducing vibration levels on armored tracked vehicles. Reducing vibration levels on armored vehicles combines these approaches. The armored vehicle study conducted showed that the approaches used are able to reduce the vibration level on armored vehicles to 0.63 m/s^2 at all the crew stations. Acceleration of 0.63 m/s^2 is a typical benchmark adopted in the assessment criteria of health risks. In conclusion, the discussed approaches are successful in reducing vibration levels on armored tracked vehicles and will be needed for consideration in the future designs of armored platforms.

Basten and Berkhoff (2010) conducted a study on analyzing the vibrations generated on navy ships. The structural design of navy ships is such that they have low underwater signature and most navy ships are equipped with two trains within the propulsion system. These ships also have large gearboxes which enhances their capability to use the diesel engines. The engines and gearboxes on navy ships are installed on springs to reduce the vibrations that the engine, and gearbox are exposed to while the navy ship is running. There is a coupling installed between the navy ship engine and the gear box to isolate vibrations generated between the engine and the gearbox. In overall, the coupling and the springs installed are successful in isolating the vibrations generated while the navy ships are in operation. Both engines and the gearboxes are mounted on springs for vibration isolation. Tonal frequencies occur at low frequencies within diesel engines and this increases the acoustic signatures. The vibration frequencies generated are related to the 3rd engine order, and the vibrations frequencies of this nature are hard to solve using passive methods. In this study active control shakers were used to reduce vibrations generated within the engine by acting as opposing forces that lower vibration levels. In their analysis, they developed a model gearbox and analyzed it for vibration frequencies. The input parameters that were used in the model gearbox to mimic the actual gearbox include the mass, moments of inertia, joints and springs used for the gas turbine and diesel engines. The actuator position was chosen, and the required forces, and other parameters were calculated depending on the number of sensor positions from the measurements of gearbox vibrations. Simulations were performed to deduce the best positions for the sensor positions and a conclusion was finally drawn that the active control vibration system is more efficient in reducing the underwater acoustic signature.

Brüel and Kjær (2001) have conducted a study on vibration as a machine condition indicator. In their study, they outline that avoiding vibrations on mechanical designs is difficult. The vibrations within mechanical structures could result from manufacturing flaws, contact of parts in motion within mechanical systems, forces that are out of balance within the machine components that are oscillating or rotating. It is possible for small vibrations within a mechanical system to excite the resonant vibrations of the system and amplify the structural vibrations to high and destructive levels. Their study has shown that machines give warning signals by way of unusual vibrations and sounds before breaking down and these warning signs usually repeat long enough before a mechanical structure fails. Brüel and Kjær found out that the defects within most machines are accompanied by an increase in vibration levels within the machine. This increase in vibration levels can be monitored and used as diagnostic tool for machine condition. This vibration monitoring can be conducted my measuring the vibration levels on the external surfaces of the machines. The study they conducted discusses the significance of planned preventive maintenance of machines to avoid unnecessary and costly breakdowns. The vibration frequency spectrum generated on machines while in operation during normal running conditions could be used as condition monitors for such machines. This frequency spectrum can then be used as a guideline to any vibration deviation spectrum occurring on the machines. Planned machines vibration diagnosis can then be conducted by generating frequency plots of the machine, and necessary remedial action can then be introduced to fix the machines before major breakdowns.

Wang (2010) conducted a study to find out if noise and vibrations generated while operating vehicles have influence on the overall performance of vehicles. Wang emphasizes that vehicle noise and vibration refinement are related to the vehicle

development process. Thus, it is very important that vehicle vibration and noise are refined in the early stages of vehicle designs. Refining noise and vibrations generated on vehicles while they are in operation helps in optimizing vibration mechanisms of vehicles, and this is required for the constantly rising market competition in the automotive. There is a rising number of powertrains that are incorporated on vehicle programs and diesel-powered engines are the best options in the automotive industry. The use of diesel powered engines adds to the noise and vibration challenges that already exist in the automotive industry. These noise and vibration problems need to be solved during the vehicle manufacturing and design stages. The rattling sounds of the engines and other vehicles parts must be eliminated, and the vibration sources must be prevented in order to produce high quality vehicles that can withstand competition in the global market. Spring-damper systems and engine mounts are introduced in vehicles to reduce the vibration frequencies generated while the vehicles are in operation. Vibrations generated on vehicles affect vehicle comfort, safety, and maintenance. Vibrations prone vehicles are less reliable and unsafe than other vehicles that generate less vibrations while in operation. The study by Wang introduced more methods to control vehicle vibrations. These methods are:

➢ Automated microprocessor transport control

➢ Automatic adjustment of bias response

➢ Automatic adjustment of frequency response

Ganeshraja and Dheenathayalan (2014) studied the vibrations generated on a grinding machine. It is difficult to measure the vibrations on a grinding machine according to Ganeshraja and Dheenathayalan. The vibrations on grinding machines are mostly caused by misalignment of the parts within the grinding machines, and the unbalanced forces that are generated while the grinding machine is in operation. The misalignment is commonly

noticeable by careful observation of the motion of the grinding wheel while it is in operation. The misaligned grinding wheel produces a wavy motion while it rotates during operation. The vibrations generated during grinding work are reduced by introducing rubbers that act as dampers within the grinding machine, and any vibrations generated in the grinding machine could be measured using a vibrometer. The dampers introduced within the grinding machine are used isolate the vibrations, and these rubber dampers are elastic in nature, and are capable of absorbing the energy of a mechanical system. The vibrations generated within a grinding machine affect the safety and the productivity of a grinding machine. These forced vibrations need to be eliminated by proper alignment of the grinding wheel. Proper alignment of the grinding wheel prevents the eccentric motions of the grinding wheel and improves the accuracy of the grinding machine (Inaskai and Yonetsu, 1969, Gawlak, 1984). Other causes of forced vibrations within the grinding machines include the hydraulic systems that are used to promote motion of mechanical parts within the grinding machine. The vibrations from the floor that the grinding machine is installed on also contribute the overall system vibrations. Conducting maintenance well on time could help to eliminate vibrations by detecting them before they cause major damages to the grinding machines.

Mohammadi (2011) states that vibrations monitoring is a common approach used to detect mechanical faults in machines that experience a lot of rotary motions while in operation. Using the information of vibrations generated on rotary machines is an efficient technique that is commonly used for vibrations analysis of machines, and maintenance scheduling. Once the components that cause rotary motion within a machine deteriorate, they vibrate in an eccentric motion and produce different vibratory characteristics that deviate from the known vibration characteristics of a normal functioning machine. The

different components that aid rotary motion of a mechanical system wear off as they continue to operate, and this leads to uncharacteristic movements within mechanical systems. These components could be the bearings, gears and shafts that rotate within a machine. Once these components rotate and vibrate differently, it is an indication of faults within the machine. Thus, it is simple to monitor the mechanical faults of a system by analyzing the system's vibration signature. The signals received from machines while in operation are difficult to analyze because they are usually combined with noise. Machines that are complex and have multi-degree of freedom systems are even more difficult to analyze because each individual component has different equations of motion. The best way to solve this difficulty is by mounting the vibration sensors very close to the target machine components. Two alternative methods can be used to solve this problem. These approaches are:

- ➢ Blind source separation – This approach uses statistics and numerical methods developed such as independent component analysis (ICA) in separating signals from different vibration sources.
- ➢ The last approach is to use the specifications and signal characteristics of vibrations that are produced by the different machine components and compare the signals generated in normal and faulty conditions.

2.4. VIBRATIONS IN ROBOTICS

Tsai et al. (2013) proposed a method that is used in reducing the vibrations caused by the deflections within the robot arms. The method they proposed for reducing end-effector vibrations uses an iterative learning control (ILC) technique that reduces the vibrations that are caused by the deflections of the flexible joint within the robot

manipulators. This study used a 6-degree of freedom robot that has vertical linkages in conducting the tests aimed at reducing the end-effector vibrations of the robot arm. The vertical links used were long and too flexible and this affected the precision of the end-effector. The kinematics of vibration within the robot arm determine the control action that is applied to actuation DOF to account for the link of deflection used. The results of the simulations conducted indicate that the proposed technique is efficient in reducing the vibrations experienced by the effector-end of the robot arm. This study suggests that ILC technique is efficient for improving the capability of the end-effector on large robots that are made up of links that vibrate because of the joint flexibility.

The study conducted by Itoh and Yoshikawa (2003) focused on a way to eliminate vibrations generated at the waist level of a robot arm. This study focused on the waist axis on a robot with a practical aim to eliminate the transient vibrations generated while operating the robot. The study used a technique uses a model control to introduce damping to the robot waist axis. To use the model-based control method, the velocity of the load acting on the robot has to be estimated, and this estimated velocity is then changed to the motor shaft speed. The technique is based on a model control in order to establish the damping effect on the mechanical part. Using this model, the velocity of the load is estimated, which is converted to the motor shaft speed. A velocity difference between the speed of the shaft and the speed of the estimated load is then computed dynamically, and adding the calculated velocity difference to the command helps to reduce the transient vibrations that occur within the robot at waist axis of the robot arm. This technique is effective because it increases the cut-off frequency of the robot system, and also the technique increases the damping effect of the robot at the robot waist axis. The robot arm in this study has 5 DOF and it is equipped with a gear reducer that has a harmonic drive.

Conducting simulations of the control model and conducting experiments yields results that prove the effectiveness of the control results in reducing the vibrations of the robot at the end-effector. The control model used in this analysis can be taken from experimental or robot design data.

Moreover, Deein, Mitsantisuk, Naksuk and Kunieda (2014) conducted a study on reducing vibrations for a welding robot using disturbance observer. In order to design an effective vibrations control for industrial robots that can be precisely controlled by position, an effective control method that can be controlled effectively by position has to be established. In this study an effective method that uses resonance control is established to reduce the vibrations and compensate error in the system using disturbance observer technique. This research presents the simulation of position control in 3-axis welding robot for application in the real system in further studies. Finally, the results of the simulation that represent the resonance control using disturbance observer can approach the requirements, and ultimately reduce vibration and position error in the system. In order to design an automatic welding control system that could replace manual welders, motion control of welding torch is important in controlling welding path and quality of weldments. In constant current, arc voltage is very important in the heat input control to estimate the penetration of melt pool because of heat input calculated from the measured values of arc voltage and arc current. Moreover, arc voltage and a model-based filtering techniques were be used to determine the length of the arc during the welding process. The proposed control method based on position control which considers the structure of resonance ratio control based on disturbance observer is an effective method, and this method can suppress vibration and compensate error in the robot system. Resonance frequency can be changed

according to the size of motor. Thus, the results show that this technique is applicable to the welding control system in the next experiments.

Tsetserukou, Kawakami and Tachi (2008) conducted a study that focuses on using dampers to control the vibration behavior of the robot arm. The aim of the study was to ensure that the new robot arm was safe to be used for conducting its tasks among humans in the workplace. The robot arm generates vibrations while in operation, and these vibrations are high in the joints of the robot arm because they carry a lot of load. The vibration shock waves generated while the robot arm is in operation affect the mechanical functions of the robot components, and this renders the robot arm less efficient in conducting its operations. A deteriorated robot manipulator also poses hazards to humans who interact with it during operations. Acceleration signal method is a useful tool introduced in this study to reduce the vibration frequencies generated on anthropomorphic robot arm. Also, the experiment conducted shows that the vibrations generated on robot joints can be reduced by adjusting the damping that is introduced to the robot joints. Tsetserukou et al. outline that the use of robotics to assist humans in most industrial activities has risen, and this increase in the use of robots calls for more research studies in the field of robotics. Also, improvements in robotics need to be made on how these robots and humans can safely work together in the workplace. For humans and robots to co-exist in the workplace there has to be improvements made to the ergonomics of the robots to ensure their cooperation with humans in executing daily tasks. The robot joints are flexible because of the mechanical connections, torque sensors, and the harmonic drives that are used to construct the joints. These mechanical characteristics of the robot joint introduce dynamic challenges on the robot which ultimately introduce unwanted vibrations to the robotic system. The robot arm in this study is modeled as a two-component system to

account for the mechanical effects of a flexible robot joint. The results from the experiment conducted by Tsetserukou et al. showed that improving the damping of the robot arm enhances the robot by reducing vibrations generated while it is in operation. Thus, introduction of efficient dampers to the robot joints would be very helpful in improving future research studies in the field of robot arm.

There is an increased competition in the field of robotics (Chun, 2000). Robotics is used in mining, construction, and manufacturing industries, and there is a need to design highly sophisticated robots that are safe and efficient in these industries. Because of high competition in terms of producing high quality products and services in the mining, construction and manufacturing industries, there is a need to improve the speed and accuracy of the robots used in order to improve productivity. The variations in the load that robots have to handle during operation result in unnecessary vibrations on the robots which renders them less accurate and unsafe. The vibrations generated cause the robot controllers to be unstable, and this instability affects the robot task execution task. The best way to reduce the vibrations generated while robots are in operation is through the introduction of a damping mechanism to the robot joints. A method that requires no additional actuators to suppress the vibrations generated while a robot is in operation is introduced by Chun. This method focuses on reducing unwanted vibrations by using the correct conditioning of the vibration excitations that are specified and applied to the payload. This method solves the problem of varying and flexible payloads that the robot manipulators carry while in operation. The best way to reduce vibrations on a robot joint is to filter out the trajectories of the robot joint that result from flexible payloads. This approach can be successfully applied to any flexible load that the robot manipulators carry while in operation to reduce the vibrations that the robot joint manipulators carry.

Due to costs and mission requirements, future space robots will be used to take the place of humans (Hanson, 1995). An important factor that is considered when robots are attached to the bases that are flexible like the space station freedom truss is the coupling that is introduced between the base and the robot. This coupling influences the performance of the robot, as well as the vibrations generated while the robot is in operation. When the robot moves, reaction forces and moments at the base of the manipulator excite flexible modes in the supporting structure that lead to end-effector tracking errors and performance degradation. Since redundant robots have the ability to track a desired end-effector trajectory while also optimizing secondary criteria, kinematically redundant robots are investigated in the current work as one means of reducing or eliminating the unwanted effects of flexible vibrations. Using local resolved acceleration control, energy dissipation control laws for the manipulator redundancies are derived and are theoretically and numerically shown to be effective for reducing vibration. However, owing to inherent singularity problems in local optimizations, excessively high joint velocities can occur. To overcome this problem, a fuzzy logic supervisor was designed and implemented to adaptively control the kinematic redundancies. Compared to the non-fuzzy solutions, the fuzzy solution is better at avoiding singularities while still decreasing flexible vibrations. Kinematic redundancies offer the ability to perform several tasks at once. In this research kinematic redundancies were used to solve a new research problem, namely flexible base vibration suppression. By using theoretical developments and through numerical simulations, it was shown that kinematic redundancies can reduce flexible vibrations if certain requirements are met. These requirements are as follows: (1) Sufficient robot joint damping is present to prevent instable motion, (2) the flexible velocities are measurable, and (3) the rank of the control influence matrix is larger than the number of task space

variables. If these conditions are not met (particularly conditions 1 and 3), the redundancies can still dissipate flexible energy, but stability and performance cannot be guaranteed. Numerical simulations were the only testing means available in this work. As a result, practical issues such as computation, system identification, and measurability were not considered to any great extent. Therefore, the next step in development should consider these as well other implementation issues.

Béarée (2014) studied a technique that focused on analyzing a way to reduce the vibration frequencies generated on undamped flexible joints of robots while in operation. The method Béarée introduced is called the jerk-shaped profile and it helps in vibration reduction within the undamped system that is subjected to vibrations resulting from the dynamics of the joint motions. Béarée (2014) used a technique called the jerk-limited profile to suppress residual vibrations that occur within the flexible joints. To understand how jerk-limited profile helps to reduce the joint vibrations, an input shaping formalism and an equivalent continuous filter are used. The success of jerk-limited profile in reducing the joint vibrations is used for formulating another criteria for further reducing the joint vibrations called the damped-jerk profile. Jerk-damped profile is more effective because it introduces dampers which absorb more mechanical energy of the system, and reduce the vibrations that the system is exposed to. The experimental and simulation results prove that damped-jerk profile that is introduced is more effective in reducing the vibrations in robots. If the system's dominant vibrations are not a result of external forces acting on the system, the system's vibrations can be reduced or eliminated using a reference trajectory. Experiments conducted on industrial robots have proven the effectiveness of the proposed approach and have shown that damped-jerk profile is capable of handling low—damped vibrations. This method of reducing the vibrations on robots is capable of canceling the

dominant vibrations within a vibratory system, and because of this, the method is recommended for reducing vibrations in industrial systems that require accuracy in positioning and high speeds.

Assad et al, (2009) studied an approach that uses two steps braking to reduce vibrations generated on a robot arm. This two steps braking approach is applicable to mechatronic and structural applications. The approach that was introduced by Assad is useful in applications that require high performance like medical imaging. Robot arms that are used in medical imaging were used as experimental validation tools for this new method. The two steps braking method used by Assad is robust and uses the normal vibrating behavior of a mechanical system to generate a profile that is used in monitoring residual vibrations, and reducing such undesired vibrations. The two steps braking approach is easy to develop and does not require addition of more actuators to the system. Validation of the two steps braking technique was made using the results of the simulations and experiments made on the Innova medical imaging robot.

2.5. VIBRATIONS IN ENGINES, MOTORS, JOINTS, AND BEARINGS

Tienhaara and Mikonaho (2014) conducted a research on engine dynamics and vibration control. They state that there is a rising demand in designing engines that produce less noise and low vibrations while in operation. Thus, this rising demand in manufacturing vibrations mitigated engines has led to an increase in more sophisticated vibration analysis approaches, and introduction of more robust vibration virtual models for vibration simulations. A practical way to reduce vibration frequencies is by isolating low natural frequencies of the system from the main vibration excitations of the system. Tienhaara and Mikonaho have found an effective way to reduce the vibrations of the system without

detuning its natural frequencies. They outline that a number of factors must be considered while making an effort to optimize the performance of a diesel engine. Tienhaara and Mikonaho analyzed the Eigenvalues, Eigenvectors, modal shapes, excitation forces, and the forced response of the vibration simulations in their complete vibrations analysis for the engine dynamics. In their analysis, they prefer using a tuned mass damper to reduce the system's vibrations instead of detuning the natural frequencies of the system because they outline that it is impossible to detune the natural frequencies of the system to eliminate vibrations. Where possible, the excitation forces that influence the motion of the system can be modified to reduce or eliminate vibrations. According to them, when it is not possible to tune the natural frequencies of the engine structure to avoid vibrations. When modifying the excitation forces is not possible, a tuned mass damper can be a good solution to reduce the engine vibrations. The study they conducted showed that the best position for a tuned mass damper is on the turbocharger of the engine because this position is where the system's amplitudes are highest on the engine, and this position is best for enhancing the efficiency of the damper. A properly tuned damper is effective in reducing the vibration frequencies generated while an engine is in operation (Tienhaara and Mikonaho, 2014).

Competition is growing in the engine design field to manufacture more efficient engine and enhance the vibration behavior of the engines. Therefore there is a rising demand for engines vibrations analysis to develop approaches that can improve the mechanical response of engines to vibrations. Ostman and Toivonen (2008) studied the vibration mechanics of internal combustion engines. The engine cylinder torque has to be constant to avoid generating unwanted torsion on the engine crankshafts. The creation of unnecessary torque on the engine crankshafts is a source of excessive vibrations within the engine. Excessive torsional vibrations speed up the wear and tear process of the essential

mechanical parts within the engine. Ostman and Toivonen introduce a new method that reduces the torsion motion of the engine crankshaft, and reducing the torsional vibrations that the engine is subjected to during operations. The method is called cylinder-balancing, and it reduces torsional vibrations generated on a medium speed internal combustion engines. Cylinder balancing approach was tested on a power plant engine and the results showed a significant reduction in the torsional vibrations of the Wartsila engine. Torsional vibrations can be addressed as a torsional vibrations problem using a model engine mechanics. Ostman and Toivonen (2008) further considered the temperature differences of the engine exhaust gas and solved the engine vibration problem as an optimization problem. The full-scale vibrations tests they conducted on Wartsila engine were successful in reducing the torsional vibrations generated within the engine.

Yipeng, Dayuan, Huijun and Xiuzhen (2014) have conducted a study on methods of reducing and controlling vibrations generated on diesel engines. Their study focused on the fuel injection system of the engine because it is critical part for running the diesel engine. In their study, they determined the vibrations and noise levels generated while a diesel engine is running using a numerical method. Yipeng et al. (2014) studied and established the relationship between all the engine components and determined all the external and internal forces causing the engine vibration excitations. They built the dynamic model of the pump and computed the accompanying mechanical response and the excitation forces generated. The finite element analysis method is used to determine the vibration response of the engine and the noise generated while the engine is running. The vibration analysis they conducted on 4102BG diesel engine was divided into fluid, and mechanical excitations. The results of the analysis showed more mechanical excitations when the frequency was below 500 Hz, and a wide range fluid excitation spectrum. The

constant pressure valve and a function cam were introduced into the engine to lower the force of the system. The final conclusion drawn from the engine analysis study by Yipeng et al. (2014) is that mechanical and fluid excitations can be significantly lowered using the two methods introduced.

Rabinovici (2005) conducted a study in an effort to find methods to solve the noise, torque ripples, and vibration problems on switched reluctance motors (SRM). Rabinovici found out that the effects of torque ripples are not connected to the noise and vibration effects of an SRM while in operation. Because the torque ripple effects are not related to the vibrations and noise generated within a motor, different methods are needed to solve the torque ripple effects generated while the motor is running. This study showed that the vibrations generated while a motor is in operation are related to the noise produced by the motor. Therefore, reducing the vibrations generated while a motor is in operation also solves the problem of the noise generated while a motor is running. Rabinovici (2005) introduced a technique that generated torque ripple, mechanical vibrations, and noise mitigation that used a multi-phase excitation of the switched reluctance motor. The problem of torque ripples generated on SRM is complex to solve and there should be a future research on torque ripple effects of SRM and optimization methods must be introduced to solve the torque ripple problem. Moreover, simulation methods must be introduced to the vibration study on SRM to understand the vibration mechanics and torque ripple effects generated while SRM is running. Rabinovici (2005) proposes that motors must be equipped with a specially designed accent on a three phase motor system. This would help to mitigate the vibrations, torque ripples and the noise generated while SRM is running.

Pöyhönen, Jover and Hyötyniemi (2004), conducted a study that was aimed at determining the vibration faults within an induction motor while it is in operation. The study conducted on induction motors focused on independent component analysis (ICA) of the induction motor. To improve the approach of motor fault diagnosis in this study, independent component analysis approach was applied to vibration measurements generated from a 35 Kw induction motor. The results show that ICA method improves the fault detection approach. Machines have complicated mechanical structures, and different components that generate unwanted vibration frequencies while the machine is running and these vibrates generated while the machine is operating can be useful in detecting faults that may damage the machine and render it unsafe. Thus, the frequencies generated while a machine is in operation during its normal condition are compared to the frequencies generated by a faulty machine and vibration frequency spectrum is generated that compares the frequency results of a faulty machine to the frequency results of a normal functioning machine. Comparison of the frequency spectrum from a normal and a faulty motor is based on an understanding that a faulty rotating machine displays distinctive vibration characteristics that are different from the vibration characteristics of a normal functioning machine. The mechanical parts of a normal machine experience wear and tear during the operating lifetime of a machine. The parts of the motor that experience wear and tear display distinctive vibration behavior and this affects the natural frequencies of the system. The characteristic vibration behavior displayed by worn-out motor parts becomes an important diagnostic feature in the assessing the health and safety of machines.

Hsueh (1998) conducted a study on ways to reduce the vibrations of main hulls using semi-active absorbers. The research conducted by Hsueh introduced semi-active absorber as a technique to be used for the reduction of vibration shock waves that the main

hull girders experience. The semi-active absorber is equipped with a control valve that is used to control the damper, and this control valve needs a small electrical power. A numerical analysis was conducted to analyze vibration response of the semi-active absorber while in operations. Numerical analysis conducted on these semi-active absorbers showed that they are effective in reducing the hull vibrations during operations. The semi-active absorber approach is useful in solving the vibrations generated on the hull because these vibrations are caused by periodic excitations. The passive absorbers are less efficient compared to the semi-active absorbers in reducing hull vibrations. The vibration problem as a result of multi-frequency excitations can be solved efficiently using the semi-active absorbers. Using semi-active absorbers to solve multi-frequency excitations produces the same results as using active absorbers. In conclusion, the semi-active absorbers are efficient in reducing the system vibrations, and the semi-active absorbers consume less power. This system can be used effectively to reduce vibrations that have high frequencies.

Passive Vibration Damping of the advanced photon source (APS) machine components study was conducted by Mangra, Sharma, Jendrzejczy (1996). The advanced photon source (APS) is a radiation facility that is designed to produce x-ray beams for use in many scientific research studies. In this facility, a positron beam is accelerated to 7 GeV and injected into the ultrahigh vacuum chamber of an 1104-m-circumference storage ring (SR). Approximately 1500 electromagnets are placed in 40 similar sectors of the SR to steer and focus the beam in a stable closed orbit. An extremely tight tolerance has been placed on the positron beam motion to prevent the emittance growth that degrades the brilliance of x-ray beams. One significant source of beam motion is the submicron-range vibration of the SR quadrupole magnets. The magnet vibration is induced by both the floor vibration of the SR tunnel and the flow-induced vibration of the water headers; the

specification for the acceptable SR quadrupole motion is an RMS displacement of less than 0.11 micrometer in the 450 Hz frequency range. Frequencies below 4 Hz are not included in this specification since the beam motion in this range can be corrected u sing the feedback system and corrector magnets. Above 50 Hz, the input excitation from the floor is usually insignificant and can be neglected. Viscoelastic damping pads have been shown to provide an attractive and cost-effective solution for passive vibration control of accelerator and beamline components. At the APS the damping pads reduced the Q of the storage ring girder- magnet assemblies from over 100 to 8, and their u se proved to be essential in meeting the stringent vibration specification. The simple design of the pads allows for their easy in-situ installation without interference with the alignment or vacuum connections of the components. This study concluded that the creep effects and radiation effects are not significant in causing vibrations that affect the damping effect of the pads.

Lacey (2008) conducted a research study on analyzing the vibrations generated on bearings. Rolling contact bearings are commonly used machines that require more rotary motion. The precision and type of bearings selected is very important in determining how reliable and efficient the bearings will in executing their intended tasks. The precision of the components that are used with bearing is a determining factor to the lifespan of these bearings. These components could be the nuts, bolts, shaft and spacers. The manufacturing industry has improved the designs of bearings and they last longer. Other factors that affect bearing life include temperature, poor lubrication and misalignment. These factors result in residual vibrations to the bearing. Vibrations monitoring is an important tool used in bearing fault diagnosis to detect wearing parts before they affect the entire system. Failure of bearings could affect the safety of the system and could lead to unnecessary downtimes.

2.6. WHOLE BODY VIBRATIONS AND MUSCULO SKELETAL DISORDERS

A study on multi-axis whole body vibrations was conducted by James P. Dickey et al. (2007) to find out how the level of discomfort is related to the total value of vibrations. Exposure to WBV in the industry causes injuries and discomfort, as well as, social and economic problems. Industries like mining and construction involve high levels of vibrations. Observation was made that statistically there is a difference in discomfort for the different axes of vibration. Their approach uses the equivalence between the axes for sinusoidal vibrations and it is an approach that has been adopted to measure vibration levels for field experiments. In their study, they exposed participants to two sample vibration conditions before the actual tests to help them define the comfort scale. The lowest vibration dose they were exposed to was 1.6 Hz and this is the vibration dose that most participants can't feel. 3.15 Hz was used as the highest vibration dose value and this is the vibration level that most participants reported as high. The vibration test order was made random for the different participants. This study showed that there is a significant relationship between the vibration axis and the vibration total value ranges. They concluded that the ISO-2631 standards need to be revised for vibrations that act in more than one direction, and an intensive evaluation needs to be conducted for uni-axis and multi axis vibrations in order to understand issues of intra-axis frequency and inter-axis direction sensitivity.

Blood, Ploger and Johnson (2010) made a comparison of three seats in order to study whole body vibrations on the operators of metropolitan buses during operations.

Their study compared two bus seats from two different manufacturing companies to find out the two seats exhibit performance variations in WBVs attenuation. The second goal of their study was to find out if a standard foam seat pan attenuates vibration

frequencies differently from a silicone foam seat pan. WBV is one of the high risk factors that contribute to low back disorders. This WBV also degrades other body parts by affecting the spinal cord, nervous system, gastrointestinal systems and endocrine functions. There are safety concerns as a result of WBVs that are caused by vibration frequencies that are equal to the resonant frequencies of the human body as these vibrations affect workers' ability to perform tasks. They state that back injuries significantly affect the workforce within the United States. Back injuries that take place in the workplace constitute 20% of the compensations claims of the US workers and contributes to about 40% of the compensation costs. In their research work they evaluated three different seats during metropolitan bus operation on chosen routes which comprised of old and new roads and some parts containing speed humps. The exposure to whole body vibration frequencies was measured using tri-axial accelerometers. The attenuations of each seat under investigation was determined by comparison of the bus floor vibrations and seat vibrations. Their results showed that there was significant WBV exposure differences as the bus drove on different streets and this difference occurred on all seats. Because of this, they propose administrative control that could assign different routes based on the types of the roads with an aim to reduce distribution of WBV exposures.

Friesenbichler, Lienhard, and Vienneau (2014) conducted a study to understand how vibrations transmit to the lower extremity soft tissues as a result of WBVs. In their study they evaluated the potential risks of WBVs by exposing sixteen healthy male participants to vibrations of different frequencies. They used accelerometers to measure the acceleration signals that reach the platform, as well as the vibrations on tissue compartments. They determined that triceps experienced high accelerations as compared to the corresponding accelerations measured for soft tissue injuries as described in the

animal studies experiments. They came with three findings from their study and the first finding was that, quadriceps, triceps, and femoris vibrate at higher peak accelerations, and also vibrate at higher peak amplitudes by comparison to the input at the WBVs platform. Also, the transmissibility of peak amplitude and acceleration decreases with an increase in input frequency through the platform. Lastly, they found out that the muscles mostly vibrate at the same vibration frequency that the platform vibrates. In conclusion, they determined that vibrations to the lower soft tissues depend more on the platform frequency and the specific muscle. From their research, the results showed that soft tissues are subjected to high vibration frequencies and high vibration amplitudes as compared to the vibration platform. There was more accelerations on the triceps than the related soft tissue injury in animal studies and this means there is a need to study long term vibration effects of WBVs exposure. Unwanted side effects of WBV may be modeled to eliminate unwanted side effects.

Eger et al. (2006) conducted a research to predict the how the health of the human operators of the LHDs is affected while operating these machines on a daily basis. Their study was focused on analyzing WBVs using ISO 2631-1 and ISO 2631-5 standards. Eger et al. (2006) predicted the health effects that result from operator interaction with LHD vehicles while in operation. Eger et al., 2006; and Village et al., 1989 found out that operators of LHDs in mining industries are exposed to WBVs and shockwaves when operating this heavy equipment. LHDs produce vibration frequencies that are detrimental to the health of the operators (Eger et al., 2006; and Village et al., 1989). The harmful vibration frequency spectrum generated lead to health problems that include among others, pain in the lower back, degeneration of the spine, neck pains and nervous system problems. Vibration frequencies that range between 1 Hz and 20 Hz are harmful to the human body

(Kitazaki and Griffin, 1998; Thalheimer, 1996). LHD operators experience an increased risk of experiencing neck pains and injuries to the lower back than other employees who do not operate LHDs in the mining industry (Eger et al., 2006; and Village et al., 1989). These researchers used the Vibration Analysis software that is a product of NexGen Ergonomics to conduct vibration analysis on different size LHDs. When applying the Great Britain research results to the U.S demographics it shows that an estimated 29 million U.S workers may have WBV in the workplace. About 1.2 million of these 29 million workers may have WBV exposures at significant levels to cause health problems and need help from professionals with a good knowledge on WBV.

Salmoni et al., 2007, conducted a case studies in assessing WBV challenges faced by the transportation industry. WBV reach hazardous levels heavy equipment industries and thus there is a need to measure vibration levels that result from operating equipment. It is very critical to understand occupational WBV exposures because there is a relationship between exposure to vibrations frequencies and medical problems in machine operators. The most common effect of exposure to high vibration levels is pains to the lower part of the human back (Boshuizen et al., 1990; Bovenzi and Hulshof, 1999; Hulshof and van Zanten, 1987; Palmer et al., 2003; Pope et al., 1998; Scutter et al., 1997; Seidel). It is estimated that 95,000 females and 444,000 males in the UK have lower back pains that are caused by WBVs (Palmer et al. 2003). Safety standards have been established to identify exposure limits above which the exposure limits are considered harmful to the operators because of this connection between operator's health and exposure to WBVs. This study showed the vehicle drivers are exposed to varying vibration frequencies while operating their vehicles to carry routine tasks. Because vibration frequencies can exceed the allowable limits that a human body can self-attenuate without causing health problems,

there is a need to continue measuring vibration levels that vehicle operators get exposed to while driving. Lack of knowledge about exposure to vibrations by operators is a big challenge facing most companies in conducting vibration field tests.

Joubert (2002) conducted a research study to control WBVs forklift drivers are exposed to. The aim was to reduce the severity of lower back pain forklift drivers are exposed that are associated with MSDs. Most efforts in these types of vehicles have focused on reducing vibrations produced during operating these machines with the use of suspended seats. These controls fail to take into account that the operators of these machines are part of the vehicle system and have different physical characteristics that contribute to the health outcomes they experience. The effects of WBVs that ultimately lead to MSDs include among others, lost time, illness, medical costs and reduced productivity in the workplace. Thus it is important to consider the safety and health aspects of the machines and incorporate them into the decisions to purchase these machines. The ergonomics, vibrations generated when the machine is in operation and the comfort of the machine to the operator need to be considered before buying these machines. Most research studies conducted have made recommendations about engineering solutions to vibrations as controls but these engineering solutions fail because of the complex components that make up an organizational system. The complexity and the attributes of individual operators of these machines contribute to the problem of WBVs and makes it difficult to solve.

None of these research studies have focused on the mechanical vibrations of load-haul-dump machines with a practical aim of solving the problem of unwanted vibrations generated and propagating throughout the machine when it's in operation. Thus lack of LHD virtual prototype models for testing the extreme vibrations generated when LHD

vehicles are in operations still exists and the problem of LHD vibrations is not fully understood. There is a need to solve the problem of LHD vibrations by creating numerical models that will be helpful to fully understand the problem. Existing literature lacks virtual models for vibrations and this research studies aims at creating and testing virtual LHD prototype for extreme vibrations that will eventually lead to health and safety problems.

2.7. RATIONALE FOR PHD RESEARCH

Vibration research studies have been conducted experimentally and analytically and they lack the virtual dynamic analysis. Tammy R. Eger (2008) and his research team studied the load-haul-dump vehicles and the health effects that operators get exposed to while operating small and large LHD vehicles. They used ISO 2631-1 and ISO 2631-5 in their study to understand the whole-body vibrations that reach the operator-seat interface of the LHDs. They measured the whole-body exposure levels at operator-seat interfaces and they were able to determine that LHD vehicle operators are exposed to high levels of vibrations. Their results indicated that LHD operators are affected by WBVs exposure during LHD vehicle operation. Vibrations study they conducted yielded good results but it lacked a complete virtual model that is useful in understanding how the vibrations shockwaves propagate throughout the entire LHD vehicle. Incorporating a complete virtual model in this research study would helpful for the designer to categorize the WBV exposure levels and be able to enhance LHD vehicle design to eliminate a possibility of detrimental health effects associated with WBV. According to Eger et al, 2006, postures that LHD operators sustain during LHD operations increases their risks to injuries and health problems. LHD operators may be at increased injury risks because of these postural demands, as well as WBVs they get exposed to that lead to MSDs.

There has not been any attempt at building a full virtual dynamic model for LHD operations and testing it for extremely severe operating conditions. A virtual model would provide an understanding of the dynamic behavior of LHD vehicle. Thus there is a need to have virtual prototyping where LHDs are fully modeled and tested to improve their designs. This research would provide the basic fundamentals of the behavior of LHD vehicle vibrations when it's in operation and pave way to the frontiers in mitigating vibrations problems in LHD vehicles. Moreover, this study would help in understanding the long term effects of exposure to LHD vibrations to operator's health. The results of this study would help in reducing or eliminating the unwanted whole-body vibrations that result from operating LHD vehicle and ensure conformity with the vibrations exposure limits set by the international standards organization. Once the vibrations that result from LHD operations have been identified and eliminated successfully, the result would be useful in facilitating better machine designs with less or no vibrations problems.

Vibrations research studies conducted have focused on vibrations of engines, high performance machines, gas turbines, armored tracked vehicles, navy ships and industrial robots. Many of these research studies were conducted analytically and experimentally and they lack dynamic analysis. Virtual prototyping contributes considerably in various regimes and specific situations and it has found good applications in automotive industry. It is important to conduct this research because its results would serve as a basic guide to vibrations control strategies and help in developing vibrations manuals that would serve as a guide during LHD vehicle manufacturing.

This research would contribute considerably to understanding LHD vehicle vibrations and to the overall behavior of complex dynamic systems in specific situations. Understanding the transmission path of vibrations is a major aim of this study and it's the

first step in determining necessity of mitigation majors and computerized vibrations analysis of LHD vibrations. The virtual simulator would be tested for operating conditions. This means that occupational hazards and unnecessary maintenance could be avoided by studying and understanding LHD vehicle vibrations. Vibrations problems are worth avoiding because the costs of dealing with them are very high and once LHD vibrations are understood the results would contribute to better design modifications.

Moreover, lack of data on a full LHD dynamic model in literature means there is a need for an extensive analytical work to be carried out to in order to be able to generate vibrations model from the Newton-Euler-Lagrange formulation which has proven its robustness and reliability. An analysis would be conducted that starts with dissecting LHD vehicle into different components and identifying all the forces acting on each component and ultimately building a 3D multi-body LHD vibrations model when it's in operation. MSC.ADAMS serves as one of the best tools to build and simulate the behavior of LHD vehicle when it's in operation.

3. VIBRATION MECHANICS OF LHD VEHICLE

3.1. FORCE VECTORS ON THE LOAD HAUL DUMP MACHINE

In order to analyze vibration propagation on LHDs, there is a need to define all the forces, internal and external, applied on each component of the machine. The right-hand Cartesian coordinate system was used in modeling the LHD vibrations. Figure 3.1 below illustrates the vector orientation in the *x, y,* and *z*-directions of the forces acting on LHD vehicle.
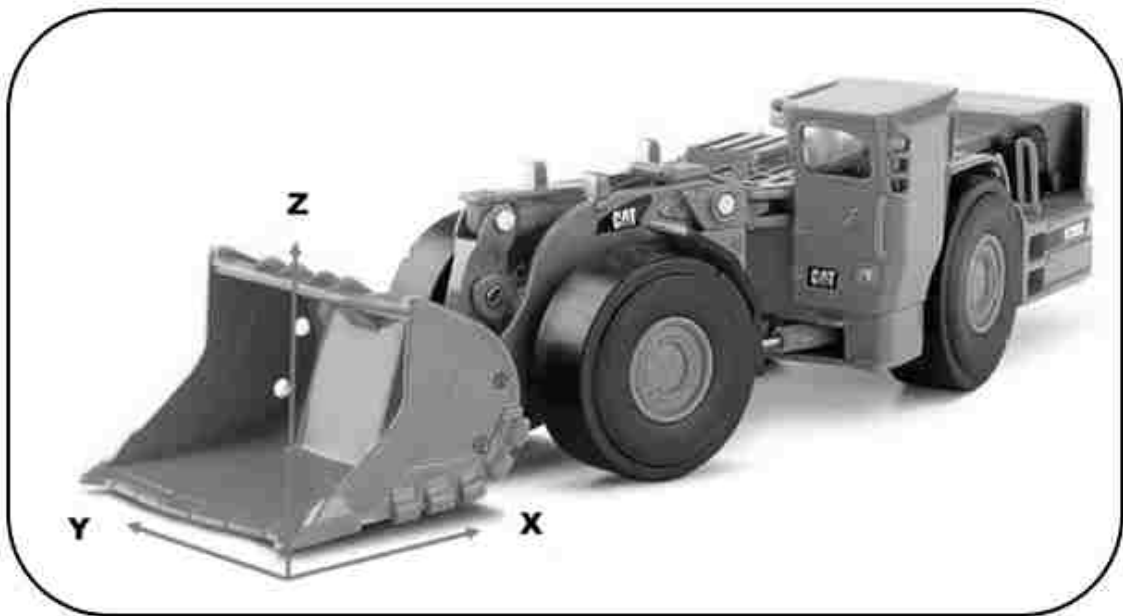
Figure 3.1. Vector orientation of the forces acting LHD vehicle

The forces acting in the vertical direction that produce the up and down motion are considered to be in the *z*-direction. When these forces are acting upward, they are considered to be in the positive *z*-direction, and when they act downward, they are

considered to be in the negative z-direction. The y-direction is into and out of the plane of the paper, and this y-direction represents the forces acting laterally and producing sideways motion on the load-haul-dump vehicle (from left to right side). The y-direction is positive into the paper and negative out of the plane of the paper. The positive x-direction is aligned across the paper to the right, and the negative x-is the opposite direction to the left across the paper. This x-direction represents the forces acting longitudinally on the machine that produce the back and forth motion.

The LHD vehicle will be broken down into different components during analysis. Various components would be assigned component properties, as described in Table 3.1. The LHD portion is made up of the front wheel base, the rear wheel base, and the loading bucket of the LHD vehicle, all of which will be considered to be a single rigid body that is assigned component symbol m_1. The operator's seat and the body mass of the operator will be combined and symbolized as m_2. The front wheel assembly is made up of tires and rims of all the front wheels, which are assigned mass, m_3. Similarly, m_4 is the rear wheel assembly, and it is made up of tires and rims of both the left and right rear wheels of the LHD vehicle. The operator's cabin is symbolized by m_4, and I_6 is the moment of inertia about the center of mass of LHD. The damping and stiffness coefficients for the seat suspension system are C_1 and K_1, respectively. Similarly, C_2 and K_2 are the damping and stiffness coefficients for the suspensions between the front wheels and the LHD body. Also, C_3 and K_3, are damping and stiffness constants for the suspensions between the rear wheels and the body. Conversely, C_4 and K_4 are the damping and stiffness coefficients for the front tires, and C_5 and K_5 are the damping and stiffness coefficients for the rear tires, respectively. The details of the component symbols and component descriptions are given in Table 3.1.

Table 3.1. Symbols and component descriptions used during calculations and on FBDs

Component Symbol	Component Description
m_1	LHD Body, Front Wheel Base and Loading Bucket
m_2	Operator's seat, mass of the operator
m_3	Front Wheel Assembly- Tires and Rims ($m_3 = m_3^{right} + m_3^{left}$).
m_4	Rear Wheel Assembly- Tires and Rims ($m_4 = m_4^{right} + m_4^{left}$)
m_5	Operator's cabin
I_6	Moment of Inertia about the Center of mass of LHD
C_1 and K_1	Damping And Stiffness Constants For the Seat Suspension Respectively
C_2 and K_2	Damping and Stiffness Constants for the Suspensions Between the Front Wheels and the body ($C_2 = C_2^{right} + C_2^{left}$) and ($K_2 = K_2^{right} + C_2^{Left}$)
C_3 and K_3	Damping and Stiffness Constants for the Suspensions Between the Rear Wheels And the Body ($C_3 = C_3^{right} + C_3^{left}$) and ($K_3 = K_3^{righT} + C_3^{left}$)
C_4 and K_4	Damping and Stiffness Constants for the Front Tires ($C_4 = C_4^{right} + C_4^{left}$) and ($K_4 = K_4^{right} + C_4^{left}$)
C_5 and K_5	Damping and Stiffness Constants for The Rear Tires ($C_5 = C_5^{right} + C_5^{left}$) and ($K_5 = K_5^{right} + C_5^{left}$)

Studying the mechanics of the LHD vehicle is very important to determine the vibration frequencies that affect the operator's health during machine operations. The mechanics of LHD vibrations is based on a multi-DOF system that is connected together by springs and dampers. The 6-DOF mathematical model system of LHD vibrations is developed using the Lagrangian formulation. The system developed is then solved for the vibration frequencies generated on different components while it is in operation.

3.2. GENERALIZED LAGRANGIAN FORMULATION

To be able to discuss vibrations of mechanical systems, mathematical equations need to be derived. After deriving these mathematical equations, they are used in analyzing the free and forced vibrations LHD problems. The derived equations are called equations of motion and describe the kinematics of systems under investigation. Lagrange's equations are used to derive the EOMs for the LHD system. These equations accommodate multiple degrees of freedom (MDOF). Thus, the Lagrangian formulation provides efficient resolution of the dynamics of systems vibrations. To derive these equations of motion using Lagrangian formulation, the kinetic and potential energy functions of the system, as well as the Rayleigh dissipation function, have to be computed first. The Rayleigh dissipation function is used to simplify the derivation of EOMs for mechanical systems that are damped.

Lagrange's equations of motion are derived using the following basics steps. The first step is to define the system's coordinate, identify all the independent components, and then draw the free-body diagrams for the different components. As a result, the number of DOF, will be defined based on the FBDs. The next step will be to compute the potential energy, kinetic energy and the Rayleigh dissipation function (V, T, and R) for the system. The partial derivatives of $V, T, and R$ are taken with respect to the generalized coordinates and velocities. The results of the steps above are then substituted into Lagrange's equations.

A free-body diagram will then be drawn for each component in the LHD system, showing all forces acting on it. This will be done by isolating each body within the LHD system ($m_1, m_2, m_3, m_4, m_5, I_6$), schematically representing all the forces applied on each component, including the forces that result from contact with other bodies within the

LHD system. It is important to analyze the motion of bodies in order to derive the accompanying EOMs. Vectorial methods and analytical methods are combined in deriving equations of motion for the vibration mechanics of the LHD vehicle.

Work done on the LHD system can be computed from the forces applied to the particle along an incremental change in the path of the particle. This work done on a particle is calculated by multiplying the applied force and differential displacement vector, as shown in Equation (3.1):

$$\Delta W = F \cdot dr \tag{3.1}$$

where an incremental change in path is denoted by dr, ΔW denotes an increment of mechanical work on a particle, and F denotes forces applied to the particle.

The kinetic energy, T, of a particle is equal to the rate of change in ΔW with time. An expression for kinetic energy can be expressed in Equation (3.2):

$$T = \frac{1}{2} M \dot{r} \cdot \dot{r} \text{ (for constant } M) \tag{3.2}$$

where M denotes the mass of the particle and $\dot{r}$ is a velocity vector.

For a rigid body, the kinetic energy can be calculated by adding up all the kinetic energies for all the individual particles. The kinetic energy equation then becomes as shown in Equation (3.3):

$$T = \frac{1}{2} \int_{body} \dot{r} \cdot \dot{r} \, dM \tag{3.3}$$

where dM denotes individual particles.

The potential energy, V, of a rigid body also plays an important role in this study. The applied force can be written in terms of special potential energy function or the gradient of a scalar energy function, $V = V(r, t)$, as shown in Equation (3.4):

$$F = -\nabla V \tag{3.4}$$

3.3. ANALYSIS OF THE 6-DOF LHD SYSTEM

The Lagrangian formulation has been used to derive a 6-degrees of freedom LHD system to analyze the vibration mechanics of the machine while in operation. The components under analysis are the LHD body (labeled as 1), seat (labeled as 2), front wheel assembly (left and right tires plus rims, labeled as 3), rear wheel assembly (left and right tires plus rims, labeled as 4), and the driver's cabin (labeled as 5). These components are linked together by the joint and spring-damper system as illustrated in Figure 3.2.
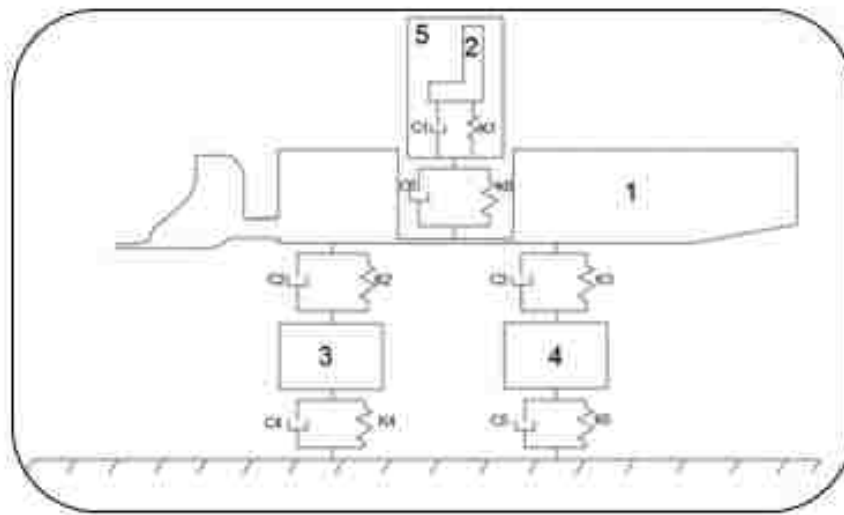
Figure 3.2. Free-body diagram of the LHD components showing spring-damper system

The equations of motion (EOMs) have been derived from the established free-body diagrams, and then solved for free and forced vibrations. After putting the equations of motion in a matrix form, the undamped free vibration problem is solved by equating the right-hand side (RHS) of the EOMs to zero. Equating the RHS to zero eliminates the damping from the system. This yields a homogeneous solution that has the natural frequencies of vibration. The forced vibrations problem is then solved, which leads to the particular solution for the LHD system under external forces $F(t)$ applied on the LHD bucket. The LHD mathematical model is based on the free-body diagram of LHD. Figure 3.3 shows all the forces acting on different LHD components. This free-body diagram serves as a tool used for identifying action and reaction forces and for deriving the equations of motion of the system.
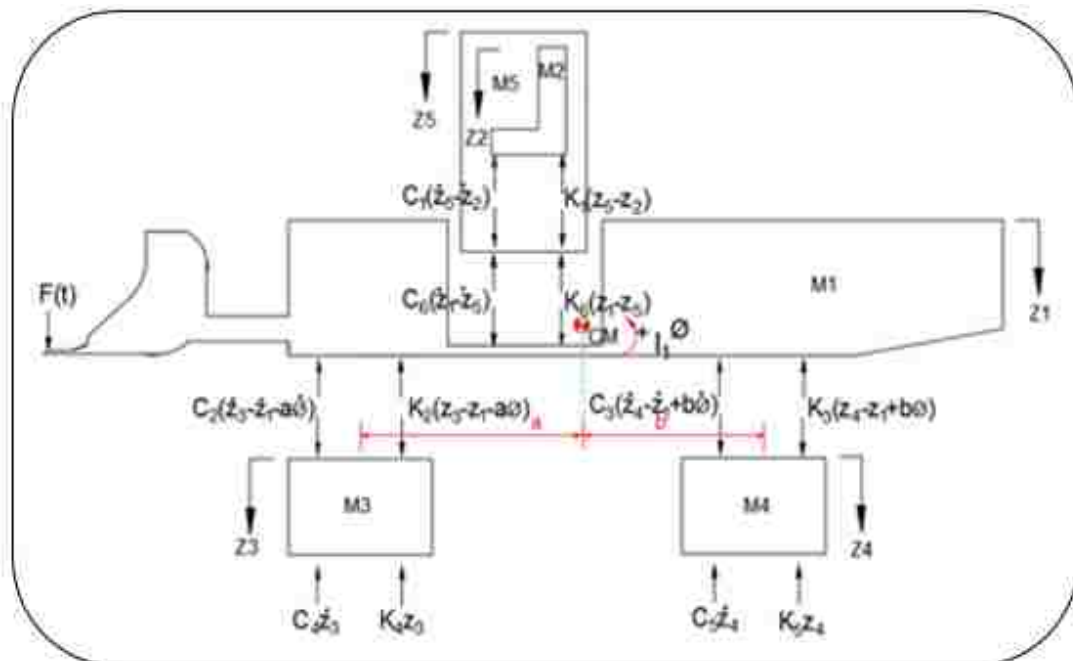
Figure 3.3. Free-body diagram of forces acting on each LHD component

Figure 3.3 shows the free-body diagram (FBD) of LHD model that describes how the vibrations generated while in operation are propagated throughout its body, and *F(t)* represents the external forces generated by the material that is loaded into the bucket of the machine. The forces F_{k1} and F_{c1} are action–reaction forces from the spring-damper system that connects the seat to the cabin, and F_{k2} and F_{c2} are action–reaction forces from the spring-damper system that connects the front wheels to the body of the LHD. Moreover, F_{k3} and F_{c3} are action–reaction forces from the spring-damper system that connects the rear wheels to the body of the LHD vehicle, while F_{k4} and F_{c4} are the reaction forces for the front wheels on the ground. Forces F_{k5} and F_{c5} are the reaction forces for the rear wheels on the ground. On the other hand, F_{k6} and F_{c6} are action–reaction forces from the spring-damper system that connects the cabin to the body of LHD the vehicle. The vibration shockwaves generated during LHD operations propagate through the different components of the LHD vehicle until they reach the operator-seat interface of the LHD.

3.4. NUMERICAL ANALYSIS FOR THE 6-DOF LHD MODEL

The 6-DOF model generates a set of six equations of motion with six unknowns for the LHD model while in operation. The input variables are the weights of different machine components, stiffness (*Ks*), and damping coefficients (*Cs*).

Lagrange's equation in its most familiar form is given by Equation (3.5):

$$\frac{d}{dt}\left(\frac{\partial L}{\partial \dot{q}_k}\right) - \frac{\partial L}{\partial q_k} + \frac{\partial R}{\partial \dot{q}_k} = Q_k^{nc}$$

(3.5)

A non-conservative force may be obtained from a potential energy function for the case of a viscous damping force. This potential viscous force is called the Rayleigh dissipation function, and the Rayleigh dissipation function for a single linear viscous damper is given by Equation (3.6):

$$R = \frac{1}{2} c \dot{x}^2 \qquad (3.6)$$

Lagrange's general formulation equation can be modified to account for the kinetic and potential energies of the system as described in Equation (3.7):

$$\frac{d}{dt}\left(\frac{\partial T}{\partial \dot{q}_k} - \frac{\partial V}{\partial \dot{q}_k}\right) - \frac{\partial T}{\partial q_k} + \frac{\partial V}{\partial q_k} + \frac{\partial R}{\partial \dot{q}_k} = F_k(t)$$

$$(3.7)$$

Because $\partial V / \partial \dot{q}_k$ and $\partial T / \partial q_k$ are independent of $\dot{q}_k$ and q_k, respectively, they are set to zero in Equation (3.7). Hence, the resulting equation reduces to

$$\frac{d}{dt}\left(\frac{\partial T}{\partial \dot{q}_k}\right) + \frac{\partial V}{\partial q_k} + \frac{\partial R}{\partial \dot{q}_k} = F_k(t)$$

$$(3.8)$$

Then, the kinetic energy, T, for the 6-DOF LHD system is given by Equation (3.9):

$$T = \frac{1}{2} m_1 \dot{z}_1^2 + \frac{1}{2} m_2 \dot{z}_2^2 + \frac{1}{2} m_3 \dot{z}_3^2 + \frac{1}{2} m_4 \dot{z}_4^2 + \frac{1}{2} m_5 \dot{z}_5^2 + \frac{1}{2} I_1 \dot{\phi}_1^2$$

$$(3.9)$$

Similarly, the potential energy, V, of the system is derived in Equation (3.10):

$$V = \frac{1}{2} K_1 (z_5 - z_2)^2 + \frac{1}{2} K_2 (z_3 - z_1 - a\phi)^2 + \frac{1}{2} K_3 (z_4 - z_1 + b\phi)^2 + \frac{1}{2} K_4 z_3^2 +$$

$$\frac{1}{2} K_5 z_4^2 + \frac{1}{2} K_6 (z_1 - z_5)^2$$

$$(3.10)$$

Next, the dissipation energy, *D*, of the system is computed and expressed in Equation (3.11):

$$D = \frac{1}{2}C_1(\dot{z}_5 - \dot{z}_2)^2 + \frac{1}{2}C_2(\dot{z}_3 - \dot{z}_1 - a\phi)^2 + \frac{1}{2}C_3(\dot{z}_4 - \dot{z}_1 + b\phi)^2 + \frac{1}{2}C_4\dot{z}_3^2 +$$

$$\frac{1}{2}C_5\dot{z}_4^2 + \frac{1}{2}C_6(\dot{z}_1 - \dot{z}_5)^2$$

(3.11)

The free-body diagrams from Figures (3.2) and (3.3) yield a set of second-order coupled differential equations that will be solved on MAPLE®. The Felberg fourth and fifth-order Runge-Kutta (RKF45) numerical method is used to solve these coupled differential equations because the 6-DOF LHD system did not exhibit stiffness. Using Lagrangian formulation, the input variables used to define kinetic, potential, and dissipation energies of the LHD model are used to generate a set of six equations of motion that describe the undamped free vibration system. The approach aims at finding the response of a free vibration system of an LHD vehicle with no damping. The undamped free vibration system yields a solution of natural frequencies, $w_{n,i}$ (*i=1,2....6).*

The equations of motion were derived for the 6-DOF LHD system. These EOMs were derived for each LHD mass based on the action–reaction forces acting on these components by way of contact with each other. The external forces acting on the LHD system were not considered for the free vibrations problem. This is because the free vibrations problem is only dependent on the physical characteristics of the LHD system and the initial excitations. The motion of a free vibration problem is not influenced by the external forces acting on the system.

Mass (m_1) is the body of an LHD vehicle and it experiences action-reaction forces because of its contact with the tire assembly and the cabin.

$$\frac{d}{dt}\left(\frac{\partial T}{\partial \dot{z}_1}\right) + \frac{\partial V}{\partial z_1} + \frac{\partial R}{\partial \dot{z}_1} = F_1(t)$$

$$(3.12)$$

$$m_1\ddot{z}_1 + \dot{z}_1(C_6 + C_2 + C_3) - C_2\dot{z}_3 - C_3\dot{z}_4 - C_6\dot{z}_5 + \dot{\phi}(C_2a - C_3b) + z_1(K_6 + K_2 +$$

$$K_3) \quad -K_2z_3 - K_3z_4 - K_6z_5 + \phi(K_2a - K_3b) = F_1(t)$$

$$(3.13)$$

Mass (m_2) is the driver's seat and the action-reaction forces on it are a result of contact with the cabin.

$$\frac{d}{dt}\left(\frac{\partial T}{\partial \dot{z}_2}\right) + \frac{\partial V}{\partial z_2} + \frac{\partial R}{\partial \dot{z}_2} = F_2(t)$$

$$(3.14)$$

$$m_2\ddot{z}_2 - \dot{C_1}z_5 + C_1\dot{z}_2 + K_1z_5 - K_1z_2 = F_2(t)$$

$$(3.15)$$

Mass (m_3) is the front wheel assembly and the forces acting on it are a result of contact with the ground and the LHD body.

$$m_3\ddot{z}_3 - C_2\dot{z}_1 + \dot{z}_3(C_2 - C_4) - C_2a\dot{\phi} - K_2z_1 + z_3(K_2 - K_4) - K_2a\phi = F_3(t)$$

$$(3.17)$$

$$\frac{d}{dt}\left(\frac{\partial T}{\partial \dot{z}_3}\right) + \frac{\partial V}{\partial z_3} + \frac{\partial R}{\partial \dot{z}_3} = F_3(t) = 0$$

$$(3.16)$$

Mass (m_4) is the rear wheel assembly and experiences the action-reaction forces due to interaction with the LHD body and the ground.

$$\frac{d}{dt}\left(\frac{\partial T}{\partial \dot{z}_4}\right) + \frac{\partial V}{\partial z_4} + \frac{\partial R}{\partial \dot{z}_4} = F_4(t) = 0 \tag{3.18}$$

$$m_4\ddot{z}_4 - C_3\dot{z}_1 + \dot{z}_4(C_3 - C_5) + C_3 b\dot{\phi} - K_3 z_1 + z_4(K_3 - K_5) + K_3 b\phi = F_4(t) \tag{3.19}$$

Mass (m_5) is the driver's cabin and it is in contact with the seat and the LHD body.

$$\frac{d}{dt}\left(\frac{\partial T}{\partial \dot{z}_5}\right) + \frac{\partial V}{\partial z_5} + \frac{\partial R}{\partial \dot{z}_5} = F_5(t) = 0 \tag{3.20}$$

$$m_5\ddot{z}_5 + C_1(\dot{z}_5 - \dot{z}_2) - C_6(\dot{z}_1 - \dot{z}_5) + K_1(z_5 - z_2) - K_6(z_1 - z_5) = F_5(t) \tag{3.21}$$

Moment (I_6) of inertia EOM about the center of mass is given by Equation (3.22)

$$\frac{d}{dt}\left(\frac{\partial T}{\partial \dot{\phi}}\right) + \frac{\partial V}{\partial \phi} + \frac{\partial R}{\partial \dot{\phi}} = F_5(t) = 0 \tag{3.22}$$

$$I_1\ddot{\phi} + \dot{z}_1(C_2 a - C_3 b) - C_2 a\dot{z}_3 + C_3 b\dot{z}_4 + \dot{\phi}(C_2 a^2 + C_3 b^2) + z_1(K_2 a - K_3 b)$$
$$-K_2 a z_3 + K_3 b z_4 + \phi(K_2 a^2 + K_3 b^2) = 0 \tag{3.23}$$

Once the equations of motions for the different LHD components have been derived using Lagrangian formulation, they are put together in a matrix form, and solved using MAPLE® for the natural frequencies of the LHD system. The equations of motion in the matrix form are given by Equation (3.24):

$$
\begin{bmatrix}
m_1 & 0 & 0 & 0 & 0 & 0 \\
0 & m_2 & 0 & 0 & 0 & 0 \\
0 & 0 & m_3 & 0 & 0 & 0 \\
0 & 0 & 0 & m_4 & 0 & 0 \\
0 & 0 & 0 & 0 & m_5 & 0 \\
0 & 0 & 0 & 0 & 0 & I_6
\end{bmatrix}
\begin{Bmatrix}
\ddot{z}_1 \\
\ddot{z}_2 \\
\ddot{z}_3 \\
\ddot{z}_4 \\
\ddot{z}_5 \\
\ddot{\phi}
\end{Bmatrix} +
$$

$$
\begin{bmatrix}
C_6 + C_2 + C_3 & 0 & -C_2 & -C_3 & -C_6 & aC_2 - bC_3 \\
0 & C_1 & 0 & 0 & -C_1 & 0 \\
-C_2 & 0 & C_2 - C_4 & 0 & 0 & -aC_2 \\
-C_3 & 0 & 0 & C_3 - C_5 & 0 & bC_3 \\
-C_6 & -C_1 & 0 & 0 & C_6 & 0 \\
aC_1 - bC_3 & 0 & -aC_2 & bC_3 & 0 & -a^2 C_2 + b^2 C_3
\end{bmatrix}
\begin{Bmatrix}
\dot{z}_1 \\
\dot{z}_2 \\
\dot{z}_3 \\
\dot{z}_4 \\
\dot{z}_5 \\
\dot{\phi}
\end{Bmatrix} +
$$

$$
\begin{bmatrix}
K_6 + K_2 + K_3 & 0 & -K_2 & -K_3 & -K_6 & aK_2 - bK_3 \\
0 & K_1 & 0 & 0 & -K_1 & 0 \\
-K_2 & 0 & K_2 - K_4 & 0 & 0 & -aK_2 \\
-K_3 & 0 & 0 & K_3 - K_5 & 0 & bK_3 \\
-K_6 & -K_1 & 0 & 0 & K_6 & 0 \\
aK_1 - bK_3 & 0 & -aK_2 & bK_3 & 0 & -a^2 K_2 + b^2 K_3
\end{bmatrix}
\begin{Bmatrix}
z_1 \\
z_2 \\
z_3 \\
z_4 \\
z_5 \\
\phi
\end{Bmatrix} =
$$

$$
\begin{Bmatrix}
F_1(t) \\
0 \\
0 \\
0 \\
0 \\
0
\end{Bmatrix}
$$

$$(3.24)$$

3.5. MODAL ANALYSIS FOR THE FORCED DAMPED LHD SYSTEM

Periodic vibrations of a body with an amplitude that decays with time are called damped vibrations. LHDs have a suspension system made up of springs and dampers, and the presence of dampers in LHDs means that once excited and allowed to vibrate freely, the amplitude of the LHD system will decay and the system will eventually come to rest.

This is because there is energy loss due to viscous damping. Damping affects the vibratory process of an LHD system by dissipating mechanical energy of a vibrating system into other types of energy such as heat energy.

The introduction of damping in computational analysis of the EOMs causes some difficulty in solving these equations. The resulting EOMs are coupled and difficult to solve. Rayleigh's dissipation function is introduced in the numerical analysis of the damped vibrations problem to simplify the derivation of the EOMs. Equation (3.25) is used to decouple equations of motion by Rayleigh equivalent damping, and it gives the damping matrix of a system that is written in terms of a linear combination of mass and stiffness matrices. The system in Equation (3.25) is said to possess Rayleigh proportional damping. Also, $\propto$ and β are the Rayleigh proportional damping factors.

$$[C] = \propto [M] + \beta [K] \qquad (3.25)$$

The damping matrix could be rendered diagonal when it occurs in a form that is proportional to the mass and stiffness matrices. The numerical analysis of a 6-DOF LHD system is considered to be composed of normal modes and time dependent generalized coordinates. The modal analysis solution is given by Equation (3.26):

$$\{z_i(t)\} = [P]\{q_i(t)\} = \sum_{i=1}^{6} \{\hat{u}_i(t)\} q_i(t) \qquad (3.26)$$

where $q_i(t)$ represents time dependent-generalized coordinates, $\hat{u}_i(t)$ represents normal modes, and P is the eigenvalue problem.

The methods that are used to calculate the modal masses and modal stiffness can be combined into a linear transformation given by Equation (3.27):

$$[P] = [\{\hat{u}\}_1 \ \{\hat{u}\}_2 \ \{\hat{u}\}_3 \ \{\hat{u}\}_4 \ \{\hat{u}\}_5 \ \{\hat{u}\}_6]$$

(3.27)

The columns of equation (3.27) consist of the system eigenvectors. Equation (3.27) defines the modal transformation matrix. Substituting (3.27) into the governing equation yields Equation (3.28):

$$[M][P]\{\ddot{q}\} + [C][P]\{\dot{q}\} + [K][P]\{q\} = \{F(t)\}$$

(3.28)

Pre-multiplying Equation (3.28) by P^T yields Equation (3.29):

$$[P]^T[M][P]\{\ddot{q}\} + [P]^T[C][P]\{\dot{q}\} + [P]^T[K][P]\{q\} = [P]^T\{F(t)\}$$

(3.29)

where $[P]^T[M][P] = [I]$, $[I]$ is the identity matrix, and $[P]^T[K][P] = [\Omega]$, and $[\Omega]$ is the diagonal of ω_i^2.

A rigorous analysis of an LHD system involves a computational analysis of the partial differential equations. Assuming that the damping matrix can be diagonalized, and using a normal coordinates system, the uncoupled system of equations of motion can be written as shown in equation (3.30).

In the case of proportional damping, the equations of motion of an LHD system may be uncoupled and recast into canonical form as shown in Equation (3.30):

$$\ddot{q}_i + 2\zeta_i \omega_i \dot{q}_i + \omega_i^2 q_i = N_I(t) \quad i = 1 \dots 6$$

(3.30)

A complete analysis of the LHD system is achieved by modeling the different components of an LHD vehicle as a lumped-mass system that is composed of 6-DOF. The 6-DOF LHD system is a second-order linear vibration system that can be mathematically modeled by ordinary linear differential equations of motion in the form of Equation (3.30).

3.6. FORCED VIBRATIONS OF THE LHD SYSTEM

Forced vibration occurs when an LHD system is subjected to external excitation that adds energy to the system. For the case of forced vibrations, the system's amplitude is dependent on natural frequencies of the system and the inherent damping in the system, as well as the frequency components present in the force exciting the system. The natural frequencies of the system are used to calculate the damped frequencies, and the initial conditions are used in Duhamel's integral to solve for the generalized displacements. Duhamel's integral, or the convolution's integral, is used to capture the total response of a system at a particular time. Duhamel's integral represents a particular solution of the differential equation of motion of a damped vibration system that is subjected to any excitation function. Equation (3.31) gives a general form of the solution:

$$q_i(t) = \frac{1}{\omega_{di}} \int_0^1 N_i(\tau) e^{-\zeta_i \omega_{di}(t-\tau)} sin\omega_{di}(t-\tau)$$
$$+ e^{\zeta_i \omega_{ni} t \left[\frac{q_i(0)}{(1-\zeta_1^2)^{1/2}} \cos(\omega_{di} t - \phi_i) + \frac{\dot{q}_i(0)}{\omega_{di}} sin\omega_{di} t \right]}$$

(3.31)

where ω_{ni} is the natural frequency of the system, ω_{di} is the damped frequencies of the system, $q_i(0) = \dot{q}_i(0) = \ddot{q}_i(0) = 0$ are the initial conditions of the system, and $t - \tau$ is the time elapsed of the impulse at a time τ. The total displacement q_i at any time t due to

the sum of impulses of the excitation function in the interval 0 to t is known as Duhamel's integral.

Equation (3.31) is used to define the natural frequencies, ω_{ni}, for the undamped free vibration problem, and the phase angle, ϕ_i, of the system:

$$\begin{cases} \omega_{di=} \omega_{ni}\sqrt{1-\zeta_i^2} \\ \phi_i = tan^{-1}\left(\dfrac{\zeta_i}{1-\zeta_i^2}\right) \end{cases}$$

$$(3.32)$$

Using the initial conditions in equation (3.31) and solving for the generalized displacements yields Equation (3.33):

$$q_i(t) = \frac{1}{\omega_{di}} \int_0^1 N_i(\tau)e^{-\zeta_i\omega_{di}(t-\tau)}sin\omega_{di}(t-\tau)$$

$$(3.33)$$

The results of Equation (3.33) are then used in Equation (3.26) which yields Equation (3.34). Taking the first and second derivative of Equation (3.34) gives velocity and acceleration as outputs:

$$\{z_i(t)\} = \sum_{i=1}^{6}\{\hat{u}_i(t)\}\frac{1}{\omega_{di}}\int_0^1 N_i(\tau)e^{-\zeta_i\omega_{di}(t-\tau)}sin\omega_{di}(t-\tau)$$

$$(3.34)$$

3.7. SUMMARY

Section 3 gives a detailed overview the vibration mechanics of LHD vehicle during operations. Force vectors on LHD vehicle were established, and the right-hand Cartesian coordinate system was used to model LHD vibrations. The LHD model was broken into

different components and analyzed. The different components under analysis were the tire assembly, the LHD body, the cabin, and the driver's seat. Dissecting LHD vehicle into different components is necessary for studying the vibration mechanics of the machine. Breaking down the LHD vehicle into different components helps in identifying harmful vibration frequencies that reach the operator-seat interface of the machine.

The mechanics of the LHD vehicle is based on a MDOF system that is connected together by joints, and spring-damper system to form a complex machine. Mathematical equations are derived for the LHD system to describe the kinematics of the different components of the machine. Vectorial and analytical methods are combined in deriving the EOMs for the LHD system. Lagrangian formulation was used to derive the EOMs that govern the LHD system because it provides efficient resolution of the dynamics of system vibrations and can handle MDOF systems. The kinetic energy, potential energy, and dissipation energy functions of the system have to be computed as the initial steps in deriving the EOMs that govern the system using Lagrangian formulation. Free-body diagrams are drawn for each dissected component of the LHD that schematically represent all the forces applied on each LHD component. The different forces are the action and reaction forces that result from the contact forces in an LHD system during operations. The external forces acting on the LHD system during operations are also considered.

The 6-DOF model generates a set of six equations of motion with six unknowns for the LHD model while in operation. The input variables are the weights of different machine components, stiffness constants, and damping coefficients. The EOMs derived from free-body diagrams are second-order coupled differential equations that will be solved on Maple®. The Felberg fourth-fifth order Runge-Kutta (RKF45) numerical method is used to solve these coupled differential equations because the LHD system did not exhibit

stiffness. The approach aims at finding the response of a free vibration system of the LHD vehicle with no damping. The undamped free vibration system yields a solution of natural frequencies, $w_{n,i}$ $(i=1,2....6)$.

4. NUMERICAL SOLUTIONS FOR VIBRATIONS MECHANICS OF LHD

It is important to understand all the numerical techniques used to study the LHD vibrations in this research work. The static, kinematic and dynamic analysis of the LHD model was conducted. Numerical analysis was conducted to verify the models and this chapter discusses the details of numerical solutions used in this research study to solve the problem of LHD vibrations during operations.

4.1. NUMERICAL METHODS USED IN LHD VIBRATION ANALYSIS

The RKF45 is a numerical method is used in this study for the solution of the equations of motion for the LHD vibrations numerical analysis. The EOMs derived for the LHD system are second-order coupled differential equations and they are solved on MAPLE®, which offers robust and efficient numerical algorithms for solving equations of motion. Normal-mode analysis and forced response analysis can be performed on MAPLE®. Conducting normal-mode analysis yields eigenvalues and eigenvectors of the LHD model at a specific operating point. The results of conducting normal-mode analysis are important because they help in analyzing the natural modes of vibration of the LHD system and they are useful in determining the dynamic characteristics of the LHD model. The result of eigenvalue analysis does not depend on specific excitations or external forces acting on the system. Eigenvalues analysis helps in estimating the mechanical behavior of the model when subjected to dynamic loads. Conducting frequency-response analysis is a useful criteria to find the steady-state response of the LHD model to external forces acting on the system.

Lagrangian formulation has been used to derive the EOMs for the 6-DOF LHD system. Lagrangian formulation was used because it can handle MDOF mechanical systems. Numerical analysis starts with a basic 6-DOF LHD system. The solution of the basic 6-DOF LHD system is then used to solve for the free undamped vibration LHD problem. Figure 4.1 illustrates the steps in solving undamped free vibrations LHD problem.
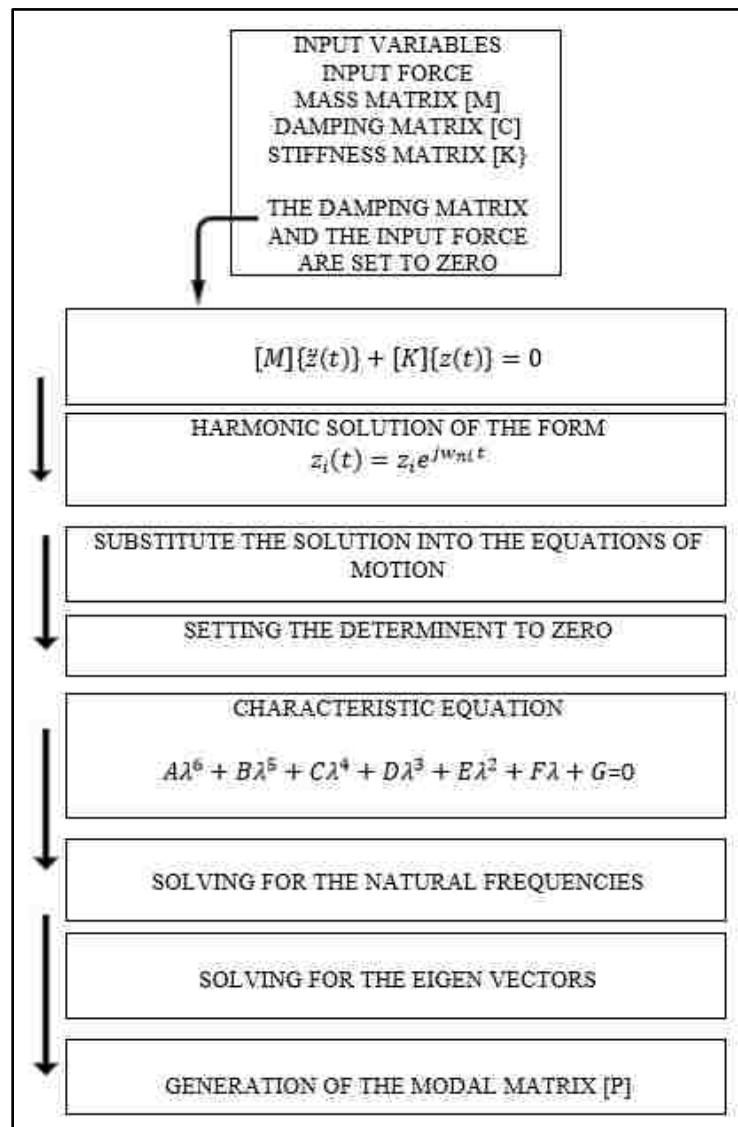
Figure 4.1. Steps in solving undamped free vibrations problem

The input variables used for defining the kinetic, potential and dissipation energies of the system are the input force $F(t)$, mass matrix $[M]$, damping matrix $[C]$, and a stiffness matrix $[K]$. The solution of undamped free vibrations is assumed to be harmonic. Therefore, substituting a harmonic solution into the equations of motion and conducting computational analysis yields a characteristic equation. The equations of motion are arranged in matrix form and solved for the undamped free vibration problem. The right hand side of the EOMs is equated to zero and the damping is eliminated from the system in the process. This yields a homogeneous solution with the natural frequencies of vibration. Normal-mode analysis is then performed. The Eigenvectors which correspond to natural frequencies are then normalized to create the modal matrix $[P]$. The modal matrix is used in deriving the solution of damped forced vibrations problem for an LHD vehicle.

Next, the study focuses on forced damped vibrations. The above steps are repeated but this time external forces acting on the LHD system when in operation are considered. The introduction of damping in computational analysis of the EOMs of LHD system adds some difficulty in solving these equations. The resulting EOMs are coupled and difficult to solve. Rayleigh dissipation function is introduced in the numerical analysis of the damped vibrations problem to simplify the derivation of the EOMs. The equation used to decouple equations of motion by Rayleigh equivalent damping gives the damping matrix of a system that is written in terms of a linear combination of stiffness and mass matrices. The LHD system is then said to possess Rayleigh proportional damping, and $\propto$ and β are the Rayleigh proportional damping factors. Figure 4.2 gives the basic steps in solving the forced damped vibrations problem.
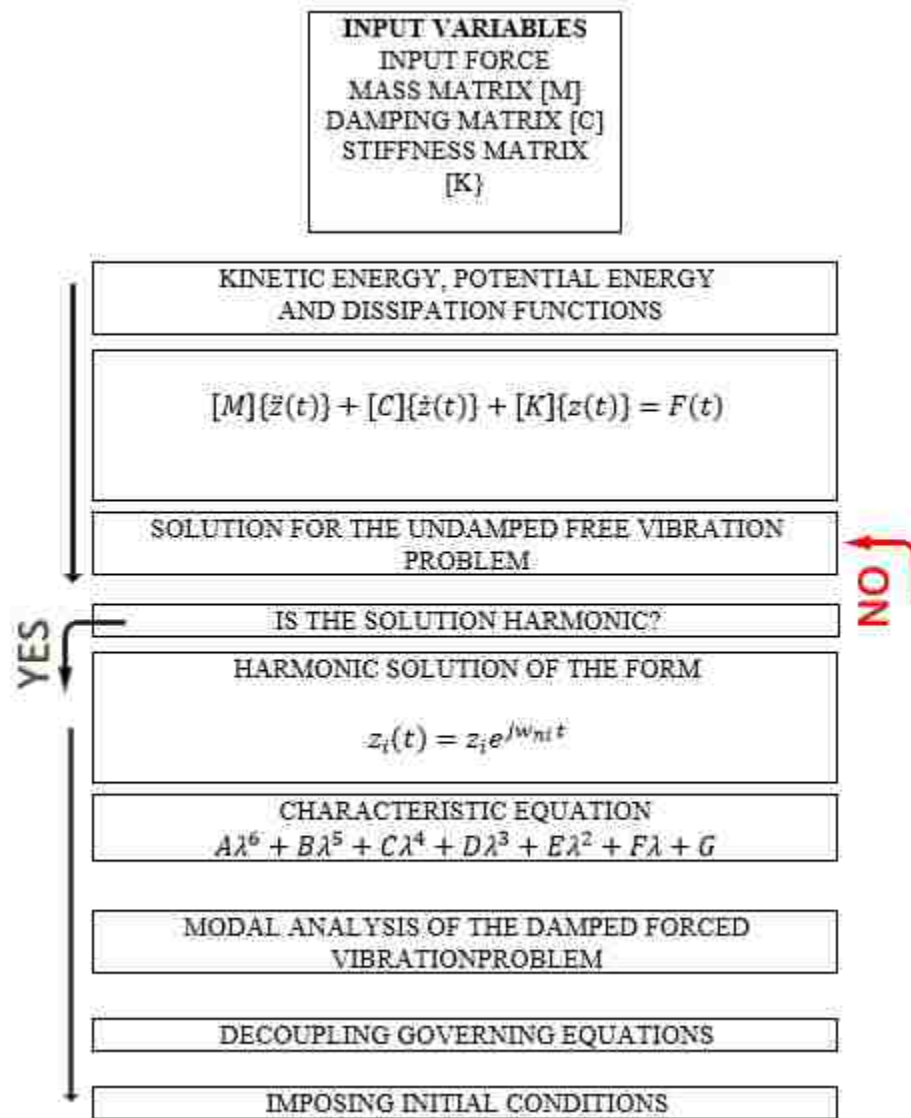
Figure 4.2. Steps in solving forced damped vibrations problem

The 6-DOF model generates a set of 6 equations of motion with 6 unknowns for the LHD model while in operation. To derive the equations of motion using the Lagrangian formulation, the kinetic and potential energy functions of the system, as well as the Rayleigh dissipation function have to be computed first.

The input variables are the weights of different machine components, stiffness constants and damping coefficients, *Ks* and *Cs* respectively. Figure 4.3 gives the steps for the general solution of 6-DOF LHD system.

INPUT VARIABLES
GENERALIZED
COORDINATES
GOVERNIG EQUATIONS

MODAL ANALYSIS OF THE FORCED DAMPED SYSTEM

HARMONIC SOLUTION OF THE FORM
$$z_i(t) = z_i e^{jw_{ni}t}$$

SOLUTION OF THE FORM
$$z_i(t) = [P]\{q(t)\} = \sum_{i=1}^{6} \{\Omega\}_i q_i(t)$$

SUBSTITUTING THE SOLUTION INTO THE EQUATIONS OF MOTION MULTIPLYING BY THE TRANSPOSE OF MODAL MATRIX, $[P]^T$

DECOUPLING EQUATIONS OF MOTION BY RAYLEIGH EQUIVALENT DAMPING

$$[C] = \propto [M] + \beta[K]$$

$$\ddot{q}_i + 2\zeta_i \omega_i \dot{q}_i + \omega_i^2 q_i = N_I(t)$$

$$i = 1,2,3 \dots 6$$

USE DUHAMEL'S INTEGRAL TO SOLVE FOR q_i $i=1,2,3 \dots 6$

$$\{z(t)\} = \sum_{i=1}^{6} \{\hat{u}(t)\} q_i(t)$$

Figure 4.3. General numerical analysis steps for the LHD vibrations problem

4.2. STABILITY, CONVEGENCE AND ERROR ESTIMATION

The Runge-Kutta Fehlberg method is an adaptive time-stepping method that was used in this study. This method uses a fourth-order and fifth-order Runge-Kutta methods that show some calculations of $f(t, y)$ to reduce the number of calculations of f per time step to 6 instead of 10 that are normally required for a pairing of fourth-order and fifth-order methods. The default error estimates of Runge-Kutta methods were used in this study. These default error estimates are 10^{-7} for the absolute error, and 10^{-6} for relative error tolerances.

For the general approach, y_n is calculated, which is an approximation of $y(t_n)$. Then $y+1$ is calculated, which is an approximation of $y(tn+1)$. These are calculated using two stepping methods that have different accuracies. One method is pth-order accurate and the other is $(p+1)$st-order accurate. This means that the local truncation error in these methods is $O(h^p)$ for the fourth-order Runge-Kutta method, and $O(h^{p+1})$ for the fifth-order Runge-Kutta method. In general, it is impossible to determine the global error of a given method, thus, the local truncation error is used because of the challenge presented in determining the global error. An important advantage of Runge-Kutta-Fehlberg method is that only six function evaluations per step are needed, whereas an arbitrary combination of Runge-Kutta methods of orders four and five need a total of ten evaluations. Exactly four function evaluations are required for the fourth-order method and six function evaluations are needed for the fifth-order method. The fourth-order method denoted by M_1, is given by equation (4.1):

$$y_{n+1} = y_{n+h} \sum_{i=1}^{5} a_i k_i(x_n, y_n; h)$$

(4.1)

and the fifth-order Runge-Kutta method is given by equation (4.2):

$$\tilde{y}_{n+1} = y_{n+h} \sum_{i=1}^{6} b_i k_i(x_n, y_n; h)$$

(4.2)

where

$$k_1(x, y; h) = f(x, y)$$

$$k_i(x, y; h) = f\left(x + C_i h, y + h \sum_{j=1}^{i-1} d_{ij} k_j\right), 2 \leq i \leq 6$$

In order to attain a sufficient condition for convergence, it is necessary that all the coefficients of the Runge-Kutta Fehlberg methods are consistent and add up to one. The Runge-Kutta-Fehlberg methods produce stable results because they are consistent and a small change in the initial conditions produces correspondingly small changes in subsequent approximations. These methods are convergent, and this is a condition necessary for stability.

4.3. NUMERICAL INTERGRATION METHOD USED IN MSC.ADAMS

The Runge-Kutta-Fehlberg method (denoted RKF45) was used to integrate the differential equations that govern the LHD system. RKF45 are a class of formulas used for the approximate numerical integration on non-stiff initial value problems. RKF45 method creates approximate solutions of systems of autonomous ordinary differential equations using implementation of the Runge-Kutta-Fehlberg method of order 4 and 5. RKF45 has a procedure to determine if proper step size is being used. Two different approximations are made at each step and compared for solution. This method solves ordinary differential equations (ODEs) with approximate error estimations.

RKF45 method embeds the fourth-order integration step into fifth-order step and allows to perform adaptive step size control without the need for re-evaluation. The solution procedure is a Runge-Kutta-Fehlberg method whose implementation is provided by routine RKF45 written by H.A. Watts and L.F. and L.F Shampine. RKF45 can only handle ordinary differential equations (ODEs) and cannot handle differential algebraic equations (DAEs). Also, RKF45 uses coordinate partitioning method that eliminates constraint equations from the equations, and it reduces a system of differential algebraic equations to compact form of ordinary differential equations. This is achieved by selecting degrees of freedom that will change most during the simulation constraints. The coordinate partitioning approach calculates the dependent displacements, the accompanying time derivatives, accelerations and Lagrange multipliers after each successful integration step. ADAMS/solver keeps independent coordinates constant and adopts Newton-Raphson iterative method to find the dependent coordinates.

4.4. NUMERICAL SOLUTION FOR THE 6-DOF LHD SYSTEM

The equations of motion derived for the LHD system are second-order coupled differential equations. The six coupled equations of motion for the LHD system cannot be solved analytically. Thus, numerical solution techniques are used to solve the 6-DOF LHD system of undamped free vibration problem. The derived equations of motion are written in an expanded matrix form of 6x6 mass, damping, and stiffness matrices that are multiplied by 6x1 acceleration, velocity, and displacement vectors respectively, and equated to a 6x1 force vector.

$$
\begin{bmatrix}
m_1 & 0 & 0 & 0 & 0 & 0 \\
0 & m_2 & 0 & 0 & 0 & 0 \\
0 & 0 & m_3 & 0 & 0 & 0 \\
0 & 0 & 0 & m_4 & 0 & 0 \\
0 & 0 & 0 & 0 & m_5 & 0 \\
0 & 0 & 0 & 0 & 0 & I_6
\end{bmatrix}
\begin{Bmatrix}
\ddot{z}_1 \\ \ddot{z}_2 \\ \ddot{z}_3 \\ \ddot{z}_4 \\ \ddot{z}_5 \\ \ddot{\phi}
\end{Bmatrix} +
$$

$$
\begin{bmatrix}
C_6 + C_2 + C_3 & 0 & -C_2 & -C_3 & -C_6 & aC_2 - bC_3 \\
0 & C_1 & 0 & 0 & -C_1 & 0 \\
-C_2 & 0 & C_2 - C_4 & 0 & 0 & -aC_2 \\
-C_3 & 0 & 0 & C_3 - C_5 & 0 & bC_3 \\
-C_6 & -C_1 & 0 & 0 & C_6 & 0 \\
aC_1 - bC_3 & 0 & -aC_2 & bC_3 & 0 & -a^2 C_2 + b^2 C_3
\end{bmatrix}
\begin{Bmatrix}
\dot{z}_1 \\ \dot{z}_2 \\ \dot{z}_3 \\ \dot{z}_4 \\ \dot{z}_5 \\ \dot{\phi}
\end{Bmatrix} +
$$

$$
\begin{bmatrix}
K_6 + K_2 + K_3 & 0 & -K_2 & -K_3 & -K_6 & aK_2 - bK_3 \\
0 & K_1 & 0 & 0 & -K_1 & 0 \\
-K_2 & 0 & K_2 - K_4 & 0 & 0 & -aK_2 \\
-K_3 & 0 & 0 & K_3 - K_5 & 0 & bK_3 \\
-K_6 & -K_1 & 0 & 0 & K_6 & 0 \\
aK_1 - bK_3 & 0 & -aK_2 & bK_3 & 0 & -a^2 K_2 + b^2 K_3
\end{bmatrix}
\begin{Bmatrix}
z_1 \\ z_2 \\ z_3 \\ z_4 \\ z_5 \\ \phi
\end{Bmatrix}
$$

$$
= \begin{Bmatrix}
F_1(t) \\ 0 \\ 0 \\ 0 \\ 0 \\ 0
\end{Bmatrix}
$$

(4.3)

Equation (4.3) can be presented in a compact form as shown in Equation (4.4) below:

$$
[M]\{\ddot{z}(t)\} + [C]\{\dot{z}(t)\} + [K]\{z(t)\} = F(t)
$$

(4.4)

Modal analysis was conducted and the results of modal analysis were used to generate the final solution of equations of motion in this research.

The damping matrix yields coupled differential equations and this complicates the solution of the problem. The initial step of solving the LHD vibration problem involves finding the response of an undamped free vibrations LHD system. Solving the undamped free vibrations system yields natural frequencies and the eigenvectors of the system. The resulting natural frequencies are then used to compute the damped frequencies. The results of the damped frequencies were be used to derive the generalized LHD system' displacement response to the vibration propagation on different components. The equations of motion for the free vibration problem in a compact matrix form are defined by equation (4.5):

$$[M]\{\ddot{z}(t)\} + [K]\{z(t)\} = 0 \tag{4.5}$$

The first step is to multiply Equation (4.5) by the inverse of mass matrix which yields Equation (4.6).

$$[I]\{\ddot{z}(t)\} + [A]\{z(t)\} = 0 \tag{4.6}$$

The dynamic matrix $[A]$ can be found as in Equation (4.7) by multiplying the inverse of the mass matrix by the stiffness matrix of the LHD system.

$$[M]^{-1}.[K] = [A] \tag{4.7}$$

$$\begin{bmatrix} \dfrac{K_6 + K_2 + K_3}{m_1} & 0 & -\dfrac{K_2}{m_1} & -\dfrac{K_3}{m_1} & -\dfrac{K_6}{m_1} & -\dfrac{aK_2 - bK_3}{m_1} \\[2ex] 0 & \dfrac{K_1}{m_2} & 0 & 0 & -\dfrac{K_1}{m_2} & 0 \\[2ex] -\dfrac{K_2}{m_3} & 0 & \dfrac{K_2 - K_4}{m_3} & 0 & 0 & -\dfrac{aK_2}{m_3} \\[2ex] -\dfrac{K_3}{m_4} & 0 & 0 & \dfrac{K_3 - K_5}{m_4}0 & 0 & -\dfrac{bK_3}{m_4} \\[2ex] -\dfrac{K_6}{m_5} & -\dfrac{K_1}{m_5} & 0 & 0 & \dfrac{K_6}{m_5} & 0 \\[2ex] \dfrac{aK_2 - bK_3}{I_6} & 0 & -\dfrac{aK_2}{I_6} & \dfrac{bK_2}{I_6} & 0 & -\dfrac{a^2K_2 + b^2K_3}{I_6} \end{bmatrix} \tag{4.8}$$

The aim is to get a harmonic solution of the form:

$$z_i(t) = Z_i e^{jw_{ni}t} \tag{4.9}$$

Where Z_i is the amplitude of system' response and ($i=1....6$), ω is the frequency of oscillations of the system.

Taking the second derivative of Equation (4.9) and substituting in the governing equation, Equation (4.5), the values of z and $\ddot{z}$ yields Equation (4.10):

$$([A] - \omega_{ni}^2[I])Z_i e^{jw_{ni}t} = \{0\} \tag{4.10}$$

To simplify the computational process of Equation (4.10), a change of variables is used, $\lambda = \omega_{ni}^2$ and this yields Equation (4.11):

$$([A] - \lambda[I])Z_i e^{jw_{ni}t} = \{0\} \tag{4.11}$$

Equation (4.11) has a non-trivial solution only if the determinant of the coefficients is equal to zero, $DET([A] - \lambda[I]) = 0$. The amplitude should not be zero otherwise a trivial solution will occur, and the LHD system will not vibrate.

This yields a 6x6 matrix that is equated to zero:

$$([A] - \lambda[I]) = 0 \tag{4.12}$$

$$
\begin{bmatrix}
\frac{K_6+K_2+K_3}{m_1} - \lambda & 0 & -\frac{K_2}{m_1} & -\frac{K_3}{m_1} & -\frac{K_6}{m_1} & -\frac{aK_2-bK_3}{m_1} \\
0 & \frac{K_1}{m_2} - \lambda & 0 & 0 & -\frac{K_1}{m_2} & 0 \\
-\frac{K_2}{m_3} & 0 & \frac{K_2-K_4}{m_3} - \lambda & 0 & 0 & -\frac{aK_2}{m_3} \\
-\frac{K_3}{m_4} & 0 & 0 & \frac{K_3-K_5}{m_4} - \lambda & 0 & -\frac{bK_3}{m_4} \\
-\frac{K_6}{m_5} & -\frac{K_1}{m_5} & 0 & 0 & \frac{K_6}{m_5} - \lambda & 0 \\
\frac{aK_2-bK_3}{I_6} & 0 & -\frac{aK_2}{I_6} & \frac{bK_2}{I_6} & 0 & -\frac{a^2K_2+b^2K_3}{I_6} - \lambda
\end{bmatrix} = 0
$$

$$\tag{4.13}$$

Solving Equation (4.13) above yields a characteristic equation to the sixth-order in terms of λ and this equation is solved for 6 different natural frequencies ω_{ni} of LHD system that describe different modes of vibration.

$$A\lambda^6 + B\lambda^5 + C\lambda^4 + D\lambda^3 + E\lambda^2 + F\lambda + G = 0 \tag{4.14}$$

Where A, B, C, D, E, F and G are the coefficients corresponding to terms developed numerically using MAPLE®.

The results of the 6-DOF analytical model developed on MAPLE® are in agreement with the results from the 6-DOF theoretical analysis using Lagrangian formulation. Table 4.1 gives the natural frequencies of the 6-DOF analytical model on MAPLE® for the LHD system.

Table 4.1. Natural frequencies of the simplistic 6-DOF analytical models

Frequency	Analytical Model (Hz) (MAPLE®)
f_1	0.66
f_2	0.79
f_3	0.87
f_4	1.01
f_5	2.00
f_6	4.06

4.5. SUMMARY

This section covers numerical solutions for the LHD vibrations. Numerical analysis of LHD vibrations start with a simple 6-DOF LHD system that is used in solving the undamped free vibrations problem. The input variables in solving the undamped free vibrations problem are the input force, mass matrix, damping matrix, and stiffness matrix. The RKF45 numerical method is used to solve the equations of motion in LHD vibrations analysis problem on MAPLE®. Kutta-Fehlberg method can only handle ordinary differential equations (ODEs) and cannot handle differential algebraic equations (DAEs).

The equations of motion derived are second-order coupled differential equations that are solved on MAPLE®, which offers robust and efficient numerical algorithms for solving equations of motion. Conducting normal-modes analysis yields eigenvalues and

eigenvectors of the model at a specific operating point. The results conducting normal-mode analysis are important because they help in understanding the natural modes of vibration for the model, and they are useful in determining the dynamic characteristics of the LHD model. Conducting a computational analysis on MAPLE® yields a characteristic equation that is equated to zero and solved for the natural frequencies of the 6-DOF system.

Accounting for the damping effect while solving the forced damped vibrations problem during the computational analysis of the EOMs adds difficulties in the solution process. Rayleigh dissipation function is introduced in numerical analysis of the damped vibrations problem to simplify the derivation of EOMs. Normal mode analysis is then conducted from the natural frequencies which yields the eigenvectors and eigenvalues of the model. The eigenvectors which correspond to the natural frequencies are then normalized to form the modal matrix.

5. BUILDING THE LHD VIRTUAL PROTOTYPE

This section covers the details of the virtual prototype simulator of LHD vehicle while in operation. The method and procedures used in building the complex dynamic model in MSC.ADAMS environment are covered in this section. All the constraints and dimensions of the prototype are covered and discussed in this section. Also, this section presents the limitations of the methods used in MSC.ADAMS environment to build a complex virtual prototype, as well as limitations in simulating the virtual prototype simulators.

5.1. VIRTUAL MODEL SIMULATION OF LHD VIBRATIONS

The LHD vehicle is a complex machine that is made up of rigid body components that are linked together to build one unit. Thus, the virtual model is built by connecting the different body parts of an LHD vehicle or the rigid body components together using joints. These different parts have dimensions, material properties, masses, and inertial properties which cannot be deformed by external forces.

The LHD virtual model is built, assembled, and simulated in the MSC.ADAMS®. The different parts of an LHD vehicle are drawn using MSC.ADAMS/View CAD capabilities. Then the dimensions, material properties, masses, and inertial properties are assigned to each part. The next step consists of linking these parts together to form one complete assembly.

The external forces are then applied to the model. The external forces applied to the model are the external excitations due to the material loaded into the LHD bucket while in operation. These external forces are regarded as 'custom forces' in MSC.ADAMS

environment because they are defined as impulsive forces and time dependent. The ADAMS/Solver chosen for this research adopts the cubic polynomial algorithm to interpolate between different points on the model. The magnitude of the external forces is a user written subroutine that defines a non-standard input into MSC.ADAMS® function. In AKISPL, the estimates for the first derivative of the approximated function are returned with evenly spaced data points. MSC.ADAMS/View evaluates the reactions in the joints, and evaluates the action and reaction forces that correspond to all spring-damper systems. After the virtual model has been completed, a static equilibrium simulation is performed with the initial conditions to ensure that all the system forces are balanced. A static equilibrium is carried first, and then it is followed by a dynamic equilibrium. A static equilibrium is basically undertaken with initial conditions to check and correct any geometric errors made while building the model. A dynamic simulation then follows that reduces some of the initial transient system responses.

During the simulation process many background analyses are performed by ADAMS/View, which formulates the equations of motion for various LHD components based on Newtonian Mechanics. EOMs are then solved by ADAMS/View for component displacements, velocities, and accelerations. The results can then be used for generating plots and numerical signal processing. The plots are useful because they provide a visual overall vibration response of the built virtual model.

Figure 5.1 shows the different steps followed during the development and simulation of the virtual prototype of LHD vehicle while in operation. After building the LHD model using MSC.ADAMS and then connecting different components together via joints and spring-damper system to add the necessary constraints to the model, static equilibrium simulation was then performed. The importance of the static equilibrium is to

verify the stability of the model. Static equilibrium simulation is then followed by the dynamic simulation while assigning step size and simulation end time parameters to the model.

Figure 5.1. General steps in building the LHD virtual model on MSC.ADAMS

A prototype simulator of LHD vibrations has been developed using MSC.ADAMS. The method adopted for developing this model uses a procedure for building a complex dynamic model with multi-degrees of freedom system that simulates the actual LHD vehicle while in operation. LHD is made up of rigid-body parts that are joined together to form one solid complex machine. The model has fixed inertia and mass properties that are not affected by external forces. Figure 5.2 is an illustration of the LHD model built on MSC.ADAMS.
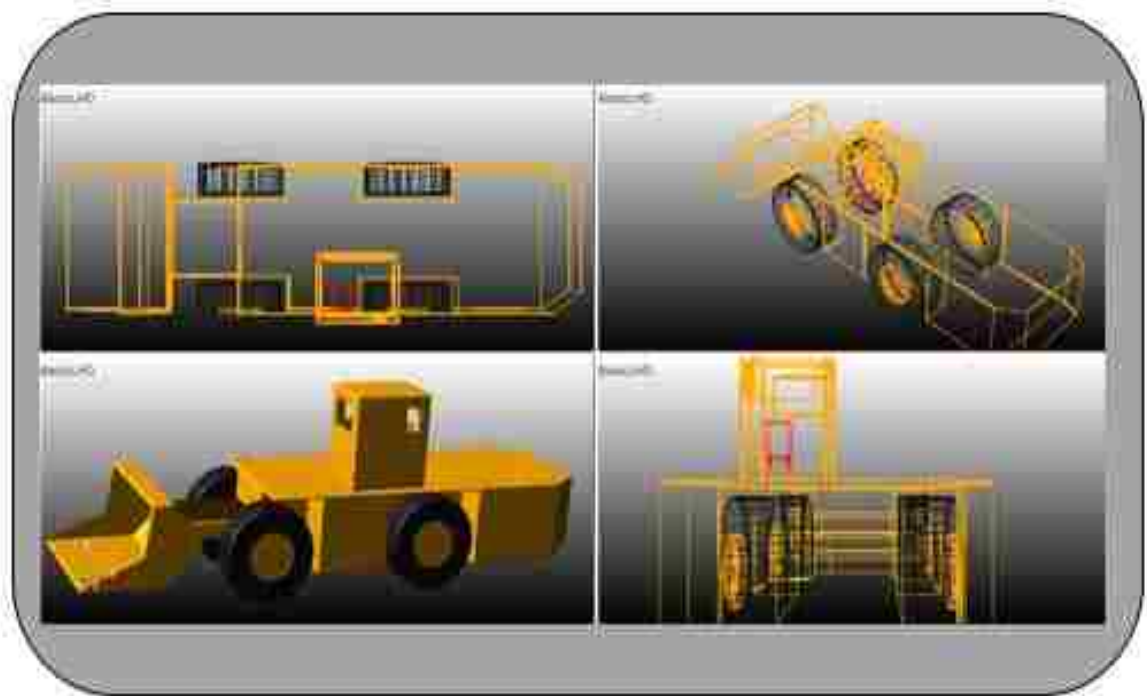
Figure 5.2 LHD virtual model in MSC.ADAMS environment

5.2. LHD VIRTUAL MODEL CONSTRAINTS

In building the LHD virtual model, different components were joined together in MSC.ADAMS to form one assembly. The components were linked together via joints and spring-damper system. The wheel assembly of the LHD system was connected to the LHD body, the driver's cabin was then connected to the LHD body and the driver's seat was connected to the cabin of the machine via joints and spring damper system. The joints used in this model allow the rotational and translational motion of the various LHD components relative to each other. Therefore, the joints on the LHD system determine the direction of motion of the LHD components and the overall machine motion. These joints introduce constraints to the LHD model because they define the number of DOF on the LHD system. The diagram shown in Figure 5.3 gives an example of how the LHD body is linked to the

driver's cabin. For this particular connection, a translational joint was used between the LHD body and the cabin.
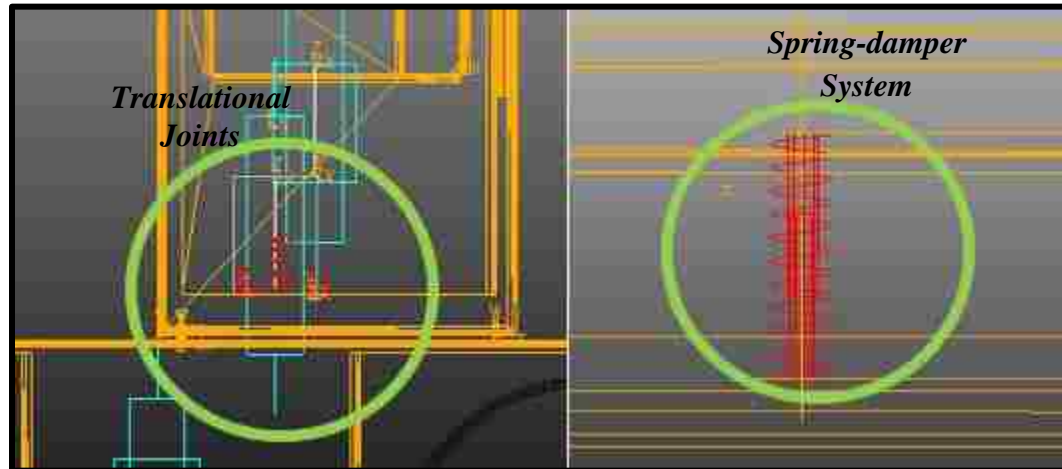
Figure 5.3. Joints and spring-damper system between the LHD body and the cabin

This translational joint is allowed to move only in one direction (vertical translation), and it has a restricted motion in the remaining five directions (two translational and three rotational directions). The spring-damper system mimics the physical link between the chassis and the cabin.

It is necessary that the LHD components are linked together using proper joints to produce realistic overall motion of the LHD system. The joints have to be assigned the proper and consistent coordinates for successful simulation results. The direction of motion for the various LHD components have to mimic the actual motion of an LHD vehicle during operations. While conducting static simulations of the LHD vibration during operations using MSC.ADAMS, investigations need a proper orientation of joints and proper direction of motion in the joints for a successful simulation. The stiffness and

damping coefficients were assigned for the various springs and dampers respectively based on the results of the mathematical estimations made during conducting numerical analysis of the LHD system. In Section 3 the spring-damper system is used to determine the reaction and action forces generated between various components of the LHD vehicle while in operation.

5.3. MSC.ADAMS METHODOLOGY IN VIBRATIONS ANALYSIS

MSC.ADAMS enables users to visualize results with realistic 3D physical animations and allows the user to plot the results. The MSC.ADAMS core products are ADAMS/View, ADAMS/Solver and ADAMS/PostProcessor. These core products were used in building the LHD vibrations model in this research. The LHD model was built on ADAMS/View, and ADAMS/Solver conducted background numerical computations to yield the output results.

ADAMS/View can be used to build a virtual prototype of a mechanical system that is similar to physical prototype. It allows for creating parts, connecting them with joints to form an assembly, and adding forces, as well as motions to the system to mimic the actual physical design behavior. Springs and dampers are then applied where necessary within a mechanical system for a successful simulation. ADAMS/View allows investigations to achieve fast simulations through advanced numerical solution techniques.

On the other hand, ADAMS/Solver performs numerical analysis by formulating the equations of motion using Euler-Lagrange formulation for this research. The solver has flexibility and it allows for customization of solutions. ADAMS/Solver has an in-built function expression language that allows solving complex functions that describe the

motions of the LHD system. ADAMS/Solver also allows for kinematic, static and dynamic solutions and this makes it a valuable tool for this research work.

ADAMS/PostProcessor is the graphical interface for visualizing MSC.ADAMS simulation results and it is integrated within ADAMS/View environment. It allows synchronized animations and plotting of the model results. The post processor results are displayed as either graphs or animations in viewports. The results of multiple simulations can also be superimposed for ease of comparison and evaluation. ADAMS/PostProcessor provides a very convenient tool for displaying the output simulation results in plots, reports and animations.

ADAMS/vibration provides an essential tool for studying vibrations within MSC.ADAMS models. It also conducts system modal analysis and individual mode responses for eigenvalues/eigenvector analysis. ADAMS/vibration is powerful in tabulating model elements to the static, kinetic, and dissipative energy distributions in system modes. This vibration analysis is vital because it investigates how parameter variation influences the vibratory behavior of a complete system. ADAMS/vibration is capable of linearizing the system and computing eigenvalues of the system, and hence, providing frequency response of the system under excitation.

Thus, MSC.ADAMS is fully capable of conducting an analysis on LHD vibrations during operations, and building a virtual model that can simulate the vibrations on LHD vehicle during operations and solve various frequency modes. Free and forced vibrations analysis was conducted for LHD vehicle to understand the dynamic characteristics of the machine while it is subjected to external forces during operation. The accompanying frequencies, as well as modes of response of the LHD system were the valuable output results during this vibration analysis study.

5.4. FORCED RESPONSE ANALYSIS OF AN LHD VEHICLE

An LHD model made up of basic geometrical components is constructed using MSC.ADAMS/View where physical properties of a real LHD vehicle are assigned. These physical properties are defined as positions, weights, damping and stiffness, forces, moments and joints. The dynamic behavior of a prototype is simulated with ADAMS/Solver using the numerical techniques within the software. ADAMS/Solver checks the model validity and stability, then formulates equations of motion for the LHD system for static, kinematic, quasi-static and dynamics simulations with both capabilities of fixed-step and variable step integrators.

ADAMS/Solver has the capability to indicate position and orientation. Different types of numerical analysis can be conducted on ADAMS/Solver. These include kinematic analysis, dynamic analysis, static analysis and quasi-static analysis. There are two main reliable methods for solving equations in ADAMS/Solver. The most common method is direct index 3 Differential-Algebraic Equations (DAE) solver, and the second algorithm reduces the original index 3 problem, and creates an analytically equivalent but numerically different index 2 DAE problem. Inputs and outputs to the linear model have to be defined by way of input and output channels in ADAMS/Vibration. A vibration analysis conducted on ADAMS/Vibration consists of input and output channels, a specified operating points, specific frequency range, and the accompanying number of steps within the range. ADAMS/Vibration can be used to compute the response of a system in the frequency domain. Normal-mode analysis and forced response analysis can be performed on ADAMS/Vibration. Conducting normal-modes analysis yields eigenvalues and eigenvectors of the model at a specific operating point. The results conducting normal-

modes analysis are important because they help in understanding the natural modes of vibration for the LHD model and they are useful in determining the dynamic characteristics of the LHD system. The result of eigenvalue analysis is independent of specific excitations or external forces acting on the system. Eigenvalues analysis helps in predicting the effects of applying dynamic loads to the LHD model.

On the other hand, conducting frequency-response analysis is a useful criteria to find the steady-state response of the LHD model to sinusoidal excitation. Frequency response is conducted on ADAMS/Vibration using linearized models. The specific details of linearization process on ADAMS/Solver (FORTRAN) are given by Sohoni (1986). Negrut and Ortiz (2005) have studied the details of the linearization process implemented on ADAMS/Solver (C++).

5.5. LIMITATIONS OF MSC.ADAMS LHD VIRTUAL MODEL

A virtual prototype is built on MSC.ADAMS in the same way as a physical prototype would be built. This is done by creating parts on ADAMS/View, and connecting them with the relevant joints. The parts created are then assigned proper forces and motions. As a result, an assembly model is created.

The accuracy of the simulation output results also depends on assigning the different parts of the LHD virtual model proper input parameters to mimic the actual physical characteristics of the real LHD vehicle. Existing literature lacks information on the physical characteristics of the different components of the LHD vehicle. The damping and stiffness coefficients of the LHD virtual model were estimated using computational analysis based on the physical characteristics of LHD vehicle. Therefore, the accuracy of assigned values could affect the LHD model simulation output results.

Moreover, the built-in Adams/Solver has a disadvantage because large models with heavy use of user-written subroutines run slower. Runge-Kutta 45 was used during numerical analysis in this study and its simulation results are slower than the default ADAMS/Solver. Nevertheless, the virtual model simulation results are expected to have a 95% confidence level.

5.6. SUMMARY

Section 5 covers the details of the virtual prototype simulator of LHD vehicle while in operation. The methods and procedures used in building the complex dynamic model in MSC.ADAMS environment are discussed in this Section. MSC.ADAMS package is chosen due to its full capabilities in conducting an analysis on LHD vibrations during operations, and building a virtual model that can be simulated during LHD vehicle operations. Free and forced vibrations analysis were conducted for the LHD vehicle to understand the dynamic characteristics of the machine while it is subjected to excitations during operation. The accompanying frequencies, as well as modes of response of the LHD system are valuable output results during this vibration analysis study.

This Section also discusses the constraints and dimensions of the LHD prototype and presents the limitations of methods used in MSC.ADAMS environment to build a complex virtual prototype. The limitations encountered while simulating the virtual prototype are also discussed in this Section. LHD vehicle is a complex machine made up of rigid body components linked together by joints and spring-damper system to build one complex unit.

The LHD virtual model is built and assembled in MSC.ADAMS®. The different LHD parts are drawn on MSC.ADAMS/View, and then dimensions, material properties,

masses, and inertial properties are assigned to each part. The relevant joints and spring-damper systems are used as a link to establish the DOFs of the LHD system. The external forces are then applied on the model mimicking external excitations due to the material loaded into the LHD bucket while in operation.

MSC.ADAMS/View evaluates the action-reaction forces in the joints to estimate the corresponding forces in all spring-damper systems. After the virtual model has been completed, a static equilibrium simulation is performed with the initial conditions to ensure that all the system forces are balanced. A static equilibrium is basically undertaken with initial conditions to check if there is any geometric miscalculations in the model that need to be corrected.

During the simulation process, background analysis is performed by ADAMS/View which sets the initial conditions for the various model objects. Then ADAMS/View formulates corresponding EOMs for various masses based on Newtonian Mechanics. The EOMs are then solved by MSC/Adams view for component displacements, velocities and accelerations. The results can then be used for generating plots and numerical signal processing. The plots provide a visual overall behavior of the model. The accuracy of the simulation output results also depend on assigning the different parts of the LHD virtual model proper input parameters to mimic the actual physical characteristics of the real LHD vehicle. Existing literature lacks information on the physical characteristics of the different components of the LHD vehicle. The damping coefficients and stiffness constants of the LHD virtual model were estimated based on computational analysis. Nevertheless, the virtual model simulation results are expected to have a 95% confidence level.

6. THE 24-DOF VIRTUAL PROTOTYPE SIMULATION MODEL

Section 6 discusses the details of the LHD virtual prototype simulation output results, and carries on discussions following the virtual model results. The LHD virtual model generated using MSC.ADAMS/View was simulated successfully for vibrations that reach the operator-seat interface of the LHD while in operation. This LHD virtual prototype model reproduces the actual LHD vibration mechanical response during operations. The LHD virtual prototype has a total of 24-degrees of freedom (24-DOF), and captures the complex vibration mechanics of the LHD vehicle while in operation, as well as vibrations reaching the operator seat-interface in the three dimensional directions (x, y, and z-directions).

6.1. LHD VIRTUAL PROTOTYPE SIMULATION RESULTS

The LHD virtual model was built by connecting the different components together using joints. These different parts have dimensions, material properties, masses and inertial properties which cannot be deformed by external forces. The LHD virtual model was built, assembled, and simulated in the MSC.ADAMS environment. The first step was to draw the different parts of an LHD vehicle using MSC.ADAMS/View CAD capabilities. Then the dimensions, material properties, masses, and inertial properties were assigned to each part.

The external forces were then applied to the model. These forces are the external excitations due to the material loaded into the bucket of the LHD vehicle while in operation. The external forces are regarded as custom forces in MSC.ADAMS because they are defined as impulsive forces and time dependent. MSC.ADAMS/View evaluated the

reactions in the joints, and evaluated the action and reaction forces that correspond to all spring-damper systems within the LHD model. After the virtual model was completed, a static equilibrium simulation was performed with the initial conditions to ensure that all the system forces were balanced. A static equilibrium was undertaken with initial conditions to check and correct any geometric errors made while building the model. A dynamic simulation then followed that reduced some of the initial transient system responses.

ADAMS/View formulated the equations of motion for various LHD components based on Newtonian Mechanics. EOMs were then solved by MSC.ADAMS/view for component displacements, velocities, and accelerations. The results were then used for generating plots, and these plots are useful because they provide a visual overall vibration response of the built virtual model.

The method adopted for developing the virtual model used a procedure for building a complex dynamic model with multi-degrees of freedom (MDOF) system that simulates the actual LHD vehicle while in operation. MSC.ADAMS enabled visualizing LHD results with realistic 3D physical animations and allows the user to plot the results. The results in Table 6.1 from the LHD virtual model conducted on MSC.ADAMS show that LHD vibrations are dominant in the vertical direction. Table 6.1 shows the RMS accelerations that reach the operator-seat interface in the x, y and z-directions. The RMS acceleration in the x-direction of the operator's seat is 0.62 m/s^2, and the peak acceleration recorded in the x-direction is 4.37 m/s^2. Also, the RMS acceleration in the y-direction is 0.51 m/s^2, and the peak acceleration recorded in the y-direction is 3.45 m/s^2. The RMS acceleration that reaches the operator-seat interface in the z-direction is 1.01 m/s^2, and the peak acceleration recorded in the z-direction is 7.44 m/s^2.

Table 6.1. LHD virtual model RMS acceleration results at the operator-seat interface

LHD	a_x (m/s^2)	a_y (m/s^2)	a_z (m/s^2)	Peak a_x (m/s^2)	Peak a_y (m/s^2)	Peak a_z (m/s^2)
R1700G	0.62	0.51	1.01	4.37	3.45	7.44

6.2. DISCUSSION OF THE VIRTUAL MODEL SIMULATION RESULTS

The LHD virtual prototype simulation results of this research effort are compared to the experimental results from a study on LHD vibration effects on human operators conducted by T. Eger et al. (2008) on various LHD models. The LHD virtual simulation results are also compared to the ISO standards to determine if harmful vibrations are generated by LHD vehicle while in operation. Moreover, the results of this research effort are compared to the harmful vibration frequency ranges established by other research studies on whole-body vibrations and musculoskeletal disorders that result from operating mining, tunneling, and construction equipment. Conducting LHD virtual model simulations eliminates the process of subjecting human operators to the harsh vibrations they face while conducting experimental results. Once the virtual model is built, operators do not have to interact with the LHDs, which prevents WBVs and MSDs problems. The LHD virtual model gives vibration results in a shorter time without subjecting any human operators to WBVs generated during operations. Moreover, experiments to gather LHD vibrations are costly and take too much time. Thus, building the virtual model is helpful in addressing the problem of longer research study resulting from experimental data collection, and the accompanying costs. Building the LHD virtual prototype expands the knowledge and understanding of vibration mechanics encountered during the operation of LHD vehicles by simulating the actual LHD vehicle while in operation.

The virtual prototype simulates vibrations of each LHD component relative to adjacent components connected to it via joints. This model also simulates the overall components motion within the LHD system. The results of the LHD virtual model capture the three-dimensional displacements, velocities, and accelerations of the seat, cabin, body, and the tires of the LHD vehicle relative to each other with the ground as a reference. Much focus is on the vibration frequencies that reach the operator seat-interface of the LHD vehicle during operations. The RMS accelerations values for the different components of the LHD vehicle are key to understanding the severity of vibrations generated while the LHD is in operation. The analysis conducted using MSC.ADAMS analysis comprises of plots and reports which give a visual representation of the vibration response for the various LHD components.

The 6-DOF virtual prototype model focuses more on the acceleration results as forces acting in the z-direction (upward and downward motion) of the LHD vehicle components. It is important to focus on the vertical direction of the LHD vehicle because the forces generated while the LHD vehicle is in operation are dominant in the vertical direction of the machine as a result of material loaded into the bucket of the LHD, and the mechanical orientation of the suspension system within the LHD vehicle. This LHD vehicle uses its wheels as dampers and shock absorbers with its front and rear wheels having the same specifications.

After conducting the 6-DOF analysis, more degrees of freedom are established for the LHD system to capture motions in all directions, and produce an LHD virtual prototype that mimics the actual vibrations behavior of a real LHD vehicle. The LHD virtual prototype has a total of 24-DOF and captures the complex vibration mechanics of the LHD

vehicle while in operation, as well as vibrations reaching the operator seat-interface in the three dimensions (3D), *x*, *y* and *z*-directions.

The LHD vibration study would be incomplete without considering the vibrations acting in the *x* and *y*-directions. The results from the 24-DOF LHD virtual prototype model showed that the front wheel assembly has an RMS acceleration value of 1.06 m/s^2 in the *z*-direction. Figure 6.1 is a visual illustration of the response of the front wheel assembly of the LHD vehicle while it is subjected to vibrations during operations in the vertical direction. The peak acceleration for the front wheel assembly is 12.58 m/s^2 and it occurs at 0.5 seconds at the beginning of the excitations.
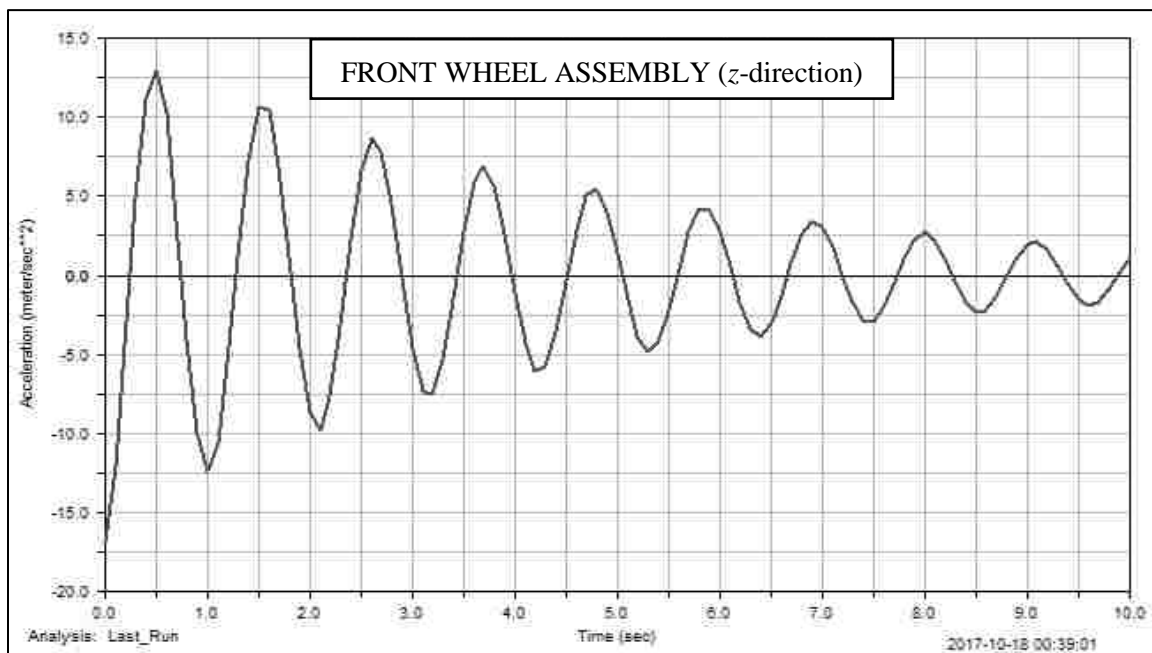
Figure 6.1. RMS acceleration of the front wheel assembly in the *z*-direction

The front wheel assembly oscillates until the vibrations decay to zero, and the system would go to rest if no external forces influence the motion after the initial

excitations. Viscous damping introduces resistance to the motion of the LHD system, and this resistance to motion results in energy loss which causes the LHD system to come to rest quicker. Acceleration is at its peak during the initial excitation, and it decays until it reaches zero due to damping.

Figure 6.2 shows the details of how the rear wheel assembly of the LHD vehicle respond to initial excitations and external forces during operations. Once the wheel assembly of the LHD vehicle starts to vibrate, the vibration frequencies propagate to other parts joined directly to the wheel assembly. These vibration excitations then cause these parts to vibrate. The weighted RMS acceleration value for the rear wheel assembly of the LHD vehicle is 1.03 m/s^2. The peak acceleration for the rear tires is 12.04 m/s^2 and it occurs at 0.5 seconds of initial excitations.
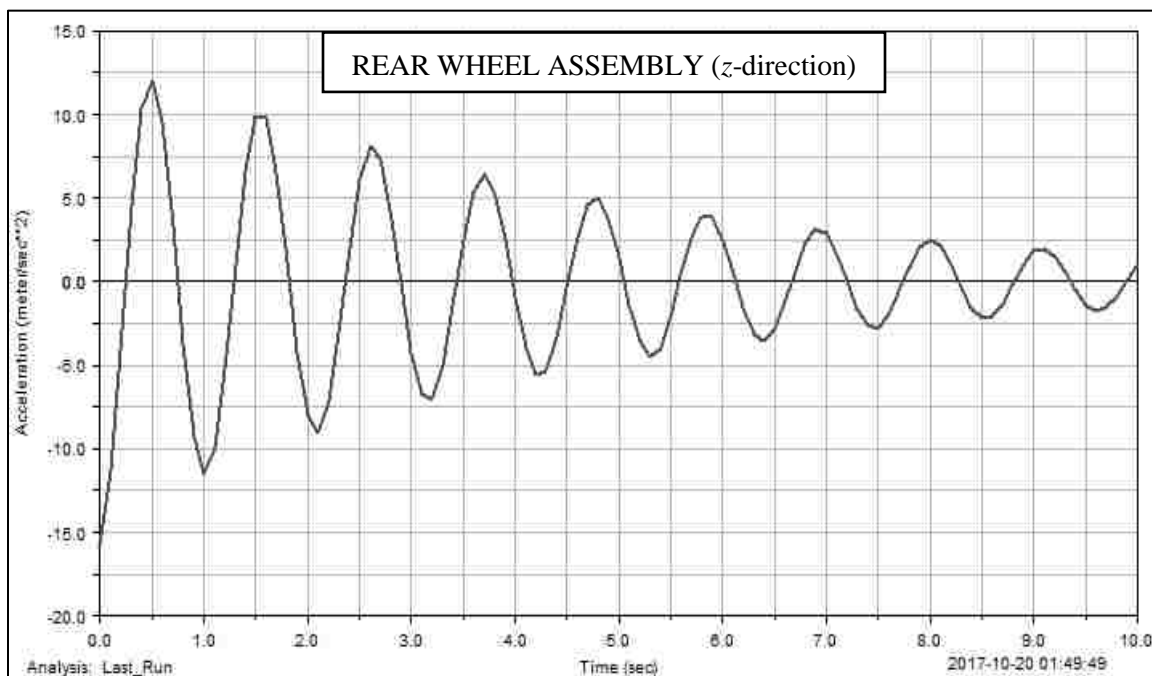
Figure 6.2. RMS acceleration of the rear wheel assembly in the vertical direction

Acceleration reduces as the system vibrates due to energy loss experienced in the LHD damping system. Viscous damping introduces friction within the suspension system, and some energy is lost within viscous damping due to friction while the LHD vehicle is in operation.

Once excited, the LHD body starts to vibrate as shown in Figure 6.3**.** The RMS acceleration value recorded for the LHD body is 0.96 m/s^2 in the vertical direction (z-direction) of the LHD vehicle while in operation. The peak acceleration for the LHD body is 11.16 m/s^2 and it occurs at 0.5 seconds. This reduction in the accelerations is because energy is dissipated in the spring-damper system that connects the wheel assembly to the LHD body.
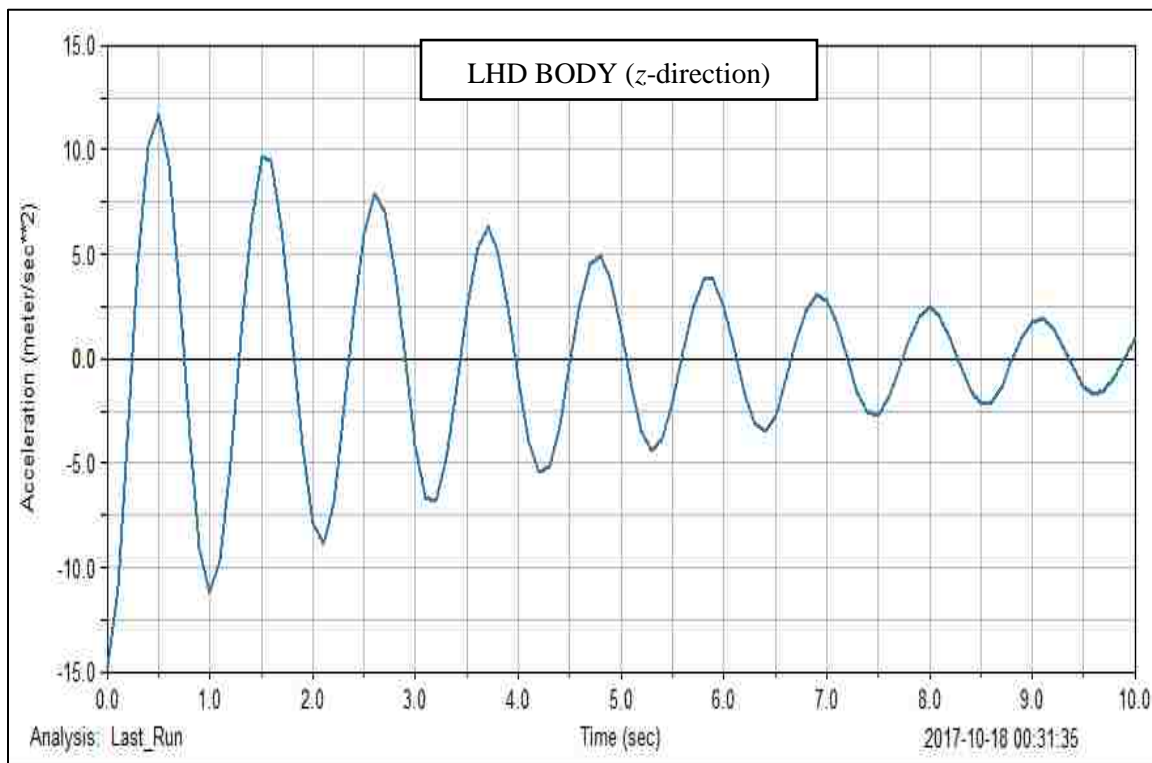
Figure 6.3. RMS acceleration of the LHD body in the vertical direction

When the four tires of the machine start to vibrate, the vibrations propagate to different LHD vehicle components through the joints and the spring-damper system that connect these different components to one another. The four LHD tires are linked directly to the LHD body via joints and spring-damper system, and the vibrations from the LHD tires propagate to the LHD body while it is excited.

The operator's cabin is directly linked to the body of the LHD vehicle by joints and spring-damper system. The vibrations propagate from the LHD body and then reach the cabin of the vehicle. Once the LHD cabin gets excited, it vibrates and displays a vibration behavior as shown in Figure 6.4. The RMS acceleration value experienced by the LHD cabin while in operation is 0.89 m/s^2, and the peak acceleration experienced by the cabin is 10.00 m/s^2 in the z-direction.
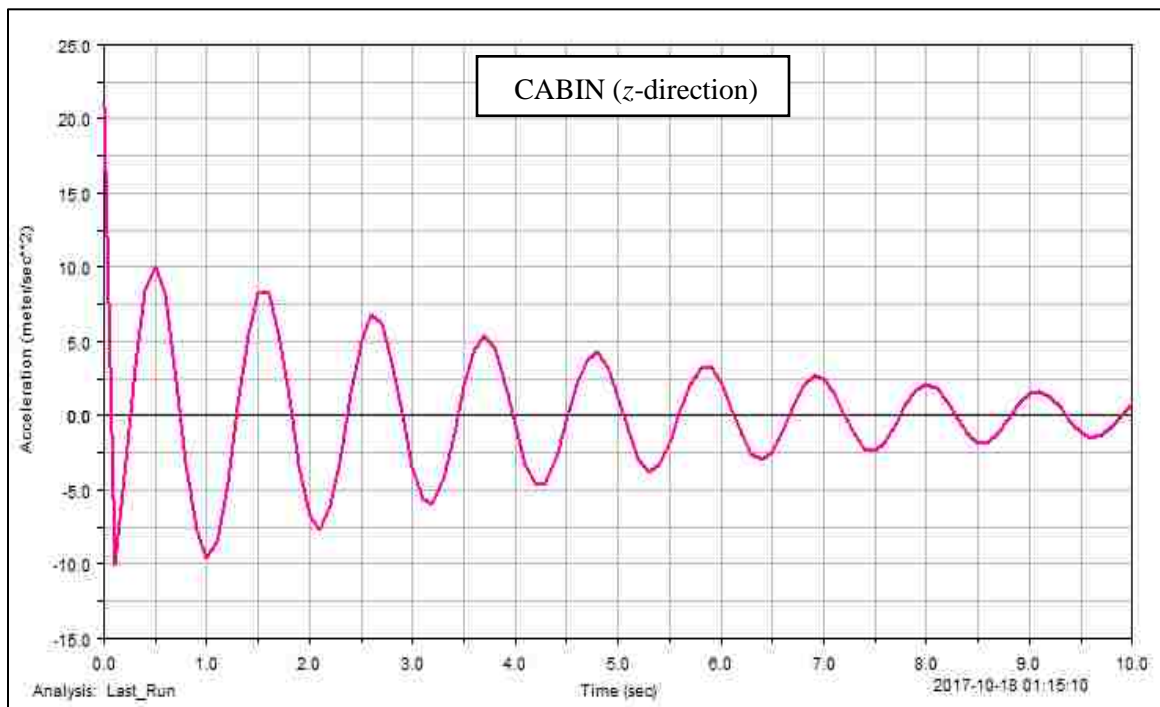
Figure 6.4. RMS acceleration of the operator's cabin in the vertical direction

The simulation results show that LHD vehicle gets exposed to repeated vibrations while it is in operation and it takes longer time for the different parts to come to rest once excited. LHD vehicle gets exposed to more vibration frequencies in the z-direction compared to the x and y-directions. Thus, experiencing more vibrations in the vertical direction is mainly due the mechanical build-up of the LHD vehicle in terms of the vertical orientation of the spring-damper system.

The driver's seat is located inside the cabin. The seat starts to vibrate immediately following the excitations from the cabin because the seat and the cabin are connected together by joints and spring-damper system. The seat has a different response as expected because its suspension system has characteristics different from other components of the LHD and their associated connections. Figure 6.5 shows the RMS acceleration of the seat in the vertical direction.
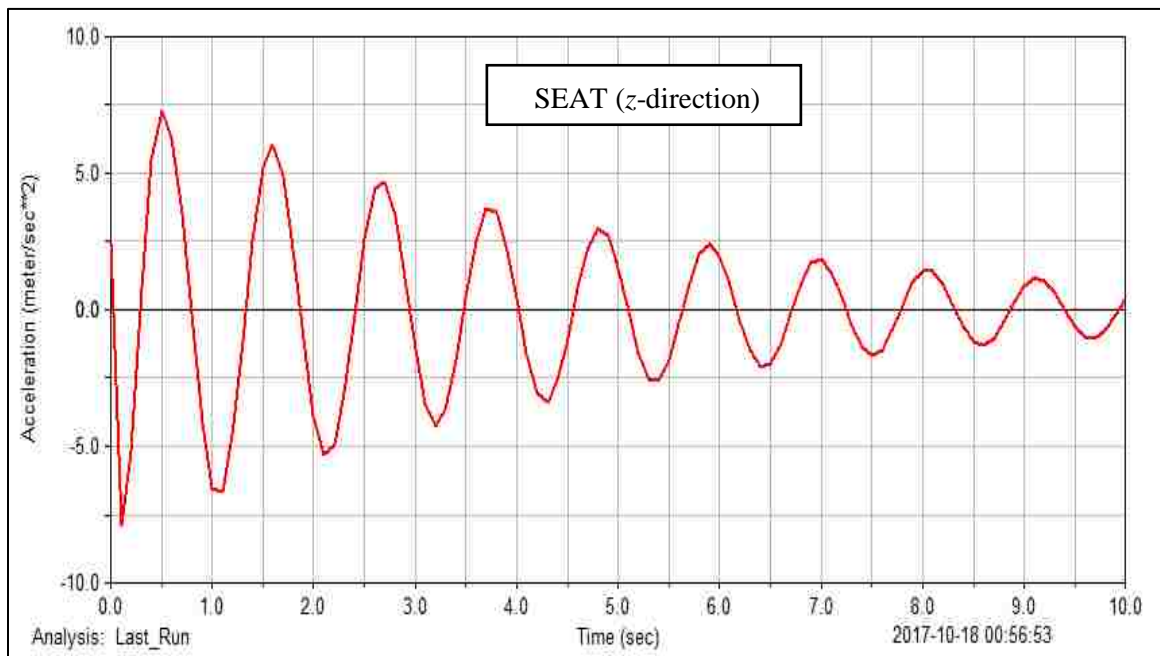
Figure 6.5. RMS acceleration of the driver's seat in the z-direction

The RMS acceleration value experienced by the LHD seat while in operation is 1.01 m/s^2 in the z-direction, and the peak acceleration experienced by the cabin is 7.44 m/s^2 occurring at the beginning of the excitation.

LHD vibration study would be incomplete without considering the vibrations acting on the x and y-directions. The vibrations generated in these directions contribute significantly to the total vibrations that reach the operator-seat interface of the LHD. Thus, it is important to account for these vibrations in the 3D virtual prototype model. The RMS accelerations in the x and y-directions are small compared to the RMS accelerations in the z-direction. Figure 6.6 shows the RMS accelerations in the x-direction of the operator seat. These vibrations are experienced by the LHD in the lateral direction of the operator seat. The RMS acceleration value recorded for the operator seat in the x-direction is 0.62 m/s^2, and the peak acceleration value recorded in the x-direction is 4.37 m/s^2, and it occurs at 0.25 seconds.
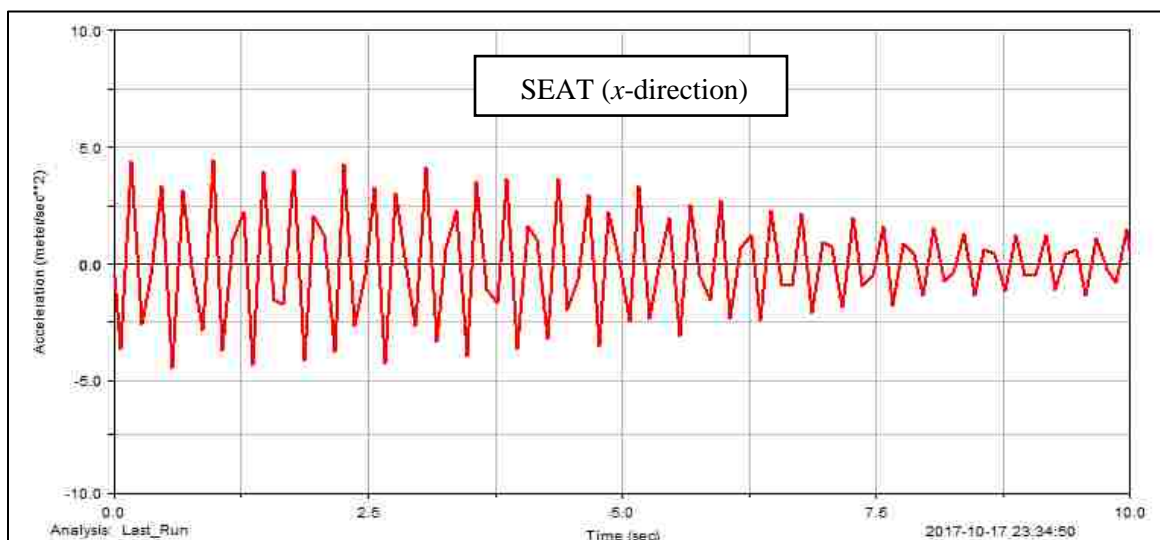
Figure 6.6. RMS acceleration of the driver's seat in the x-direction

Figure 6.7 shows the RMS acceleration values of the operator seat in the *y*-direction. The RMS acceleration value recorded for the operator seat in the *y*-direction is 0.51 m/s^2, and the peak acceleration value recorded in the *y*-direction is 3.45 m/s^2 and it happens within 1 second of the of the excitations.
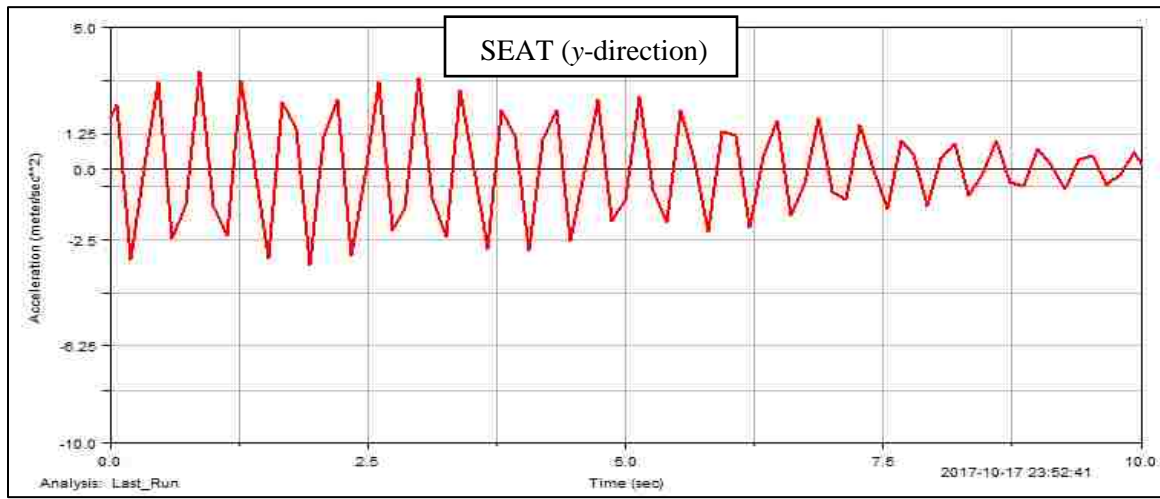
Figure 6.7. RMS acceleration of the driver's seat in the *y*-direction

The virtual prototype has to be connected to a reference point, in this case, the ground is considered as the fixed, which mimics the soil that the LHD operates on. Therefore, the ground is fixed and is assumed that it does not undergo permanent deformation. Figure 6.8 shows the acceleration response of the ground in the *x, y* and *z*-directions during LHD operations. The weighted RMS acceleration value experienced by the ground in all directions (a_x, a_y, a_z) while LHD vehicle is in operation is 0.0 m/s^2, and the peak acceleration value is also 0.0 m/s^2. This is because the ground is fixed during experimental analysis and is not affected by the forces exerted on LHD. Therefore, the

ground does not respond to any excitations and there is no motion taking place within the ground.
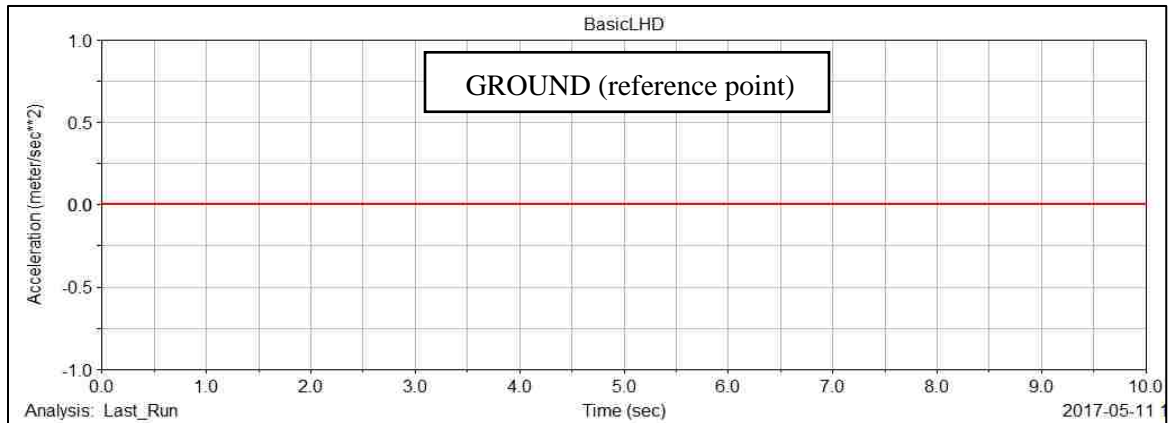
Figure 6.8. Response of the ground

The RMS values at the various LHD components of an LHD virtual prototype were recorded. Also, the peak accelerations for the different LHD components were recorded. Table 6.2 summarizes the RMS accelerations, and the peak accelerations of LHD components in the z-direction.

Table 6.2 RMS and peak accelerations of LHD virtual model components (z-direction)

LHD	a_z (m/s^2)	Peak a_z (m/s^2)
Front wheel assembly	1.06	12.58
Rear wheel assembly	1.03	12.04
LHD body	0.96	11.16
Cabin	0.89	10.00
Operator' seat	1.01	7.44
Ground (Reference point)	0.00	0.00

The study focused more on the vibrations that reach the operator-seat interface of the LHD vehicle while in operation. The RMS and peak accelerations at the operator seat for the LHD virtual prototype, and the experimental results conducted by T. Eger et al. (2008) are summarized in Table 6.3. Table also gives actual percentage difference between the experimental results and the LHD virtual prototype results conducted in this research study.

Table 6.3 RMS and peak accelerations of A-2 and R1700G LHDs (x, y, z-directions)

LHD	a_x (m/s^2)	a_y (m/s^2)	a_z (m/s^2)	Peak a_x (m/s^2)	Peak a_y (m/s^2)	Peak a_z (m/s^2)
A-2 (T. Eger,2008)	0.66	0.49	0.97	4.40	3.64	8.85
R1700G (MSC.ADAMS)	0.62	0.51	1.01	4.37	3.45	7.44
Actual Percentage Difference	6.1%	4.1%	4.1%	0.7%	5.2%	15.9%

6.3. DISCUSSION

The 24-DOF MSC.ADAMS virtual model was built and simulated successfully for the vibration frequencies that reach the operator-seat interface of the LHD vehicle during operations. This LHD virtual model mimics the physical characteristics and real vibration behavior of R1700G LHD while in operation. The output results from the LHD virtual model simulations show that there is an agreement, and there is a slight deviation from the site experimental results conducted on various LHDs by T. Eger et al. (2008). The MSC.ADAMS virtual prototype is a helpful tool for simulating the actual LHD mechanical

behavior, and responses of various LHD components while it is in operation. This virtual model gives useful 3D output results that show the displacements, velocities and accelerations of various LHD components, specifically at the operator-seat interface of the LHD vehicle without exposing human operators to the harmful vibration frequencies while conducting experimental research on the actual LHD vehicle.

The LHD virtual model shows that LHD vehicle operators are exposed to significant levels of vibrations during operations. The vibrations generated during operations of the LHD vehicle propagate throughout the machine until they reach the operator seat-interface. The results of the simulations conducted on LHD virtual prototype model showed that harmful vibrations reach the operator-seat interface.

The 24-DOF virtual prototype model focuses more on the acceleration results as forces acting in the z-direction (upward and downward motion) of the LHD vehicle components. It is important to focus on the vertical direction of the LHD vehicle because the forces generated while the LHD vehicle is in operation are dominant in the vertical direction of the machine as a result of material loaded into the bucket of the LHD. The front wheel assembly has RMS acceleration value of 1.06 m/s^2 in the z-direction, and a peak acceleration of 12.58 m/s^2. Viscous damping introduces resistance to the motion of the LHD system, and this resistance to motion results in energy loss which causes the LHD system to come to rest quicker if not subjected to repeated excitations. The weighted RMS acceleration value for the vibration frequencies on the rear wheel assembly of the LHD vehicle is 1.03 m/s^2, and the peak acceleration for the rear wheel assembly is 12.04 m/s^2.

Once the four tires of the LHD start to vibrate, the vibrations propagate to various components through the joints and the spring-damper system that connect these different components to one another. The four LHD tires are linked directly to the LHD body via

joints and spring-damper system and the vibrations from the LHD tires propagate to the LHD body. The RMS acceleration value recorded for the LHD body is 0.96 m/s^2 in the vertical direction of the LHD vehicle, and the peak acceleration for the LHD body is 11.16 m/s^2. This reduction in the accelerations is because energy is dissipated in the spring-damper system that connects the wheel assembly to the LHD body. The vibrations then propagate from the LHD body and reach the cabin of the vehicle. The RMS acceleration value experienced by the LHD cabin while in operation is 0.89 m/s^2, and the peak acceleration experienced by the cabin is 10.00 m/s^2. The driver's seat starts to vibrate immediately following the excitations from the cabin. The seat has a different response as expected because its suspension system has characteristics different from other components of the machine and their associated connections. The RMS acceleration value experienced by the LHD seat while in operation is 1.01 m/s^2, and the peak acceleration experienced by the seat is 7.44 m/s^2 occurring at the beginning of the excitation.

The LHD vibration study would be incomplete without considering the vibrations acting on the x and y-directions. The vibrations generated in these directions contribute significantly to the total vibrations that reach the operator-seat interface of the LHD. Thus, it is important to account for these vibrations in the 3D virtual prototype model. The RMS acceleration value recorded at the operator seat in the x-direction for the LHD virtual model is 0.62 m/s^2, and the peak acceleration value recorded is 4.37 m/s^2, whereas the RMS acceleration value recorded at the operator seat in the x-direction for the experimental results is 0.66 m/s^2, and the peak acceleration value recorded is 4.40 m/s^2. Moreover, the RMS acceleration value recorded for the operator seat in the y-direction is 0.51 m/s^2, and the peak acceleration value recorded is 3.45 m/s^2 for the LHD virtual model, whereas for the experimental results from T. Eger et al. (2008), the RMS acceleration value recorded

for the operator seat in the *y*-direction is 0.49 m/s^2, and the peak acceleration value recorded is 3.64 m/s^2 for the LHD virtual model.

The LHD virtual prototype simulation results of this research effort are compared to the experimental results from a study on LHD vibration effects on human operators conducted by T. Eger et al. (2008) on various LHD models. The LHD virtual simulation results are also compared to the ISO standards to determine if harmful vibrations are generated by LHD vehicle while in operation. The RMS acceleration value experienced by the LHD seat in the *z*-direction from the virtual prototype results is 1.01 m/s^2, and the peak acceleration experienced by the seat is 7.44 m/s^2, whereas the RMS acceleration value experienced by the LHD seat in the *z*-direction from experimental results by T. Eger et al. (2008) is 0.97 m/s^2, and the peak acceleration experienced by the cabin is 8.85 m/s^2 occurring at the 0.5 seconds of the excitations. The RMS accelerations that reach the operator-seat interface for the experimental results by T. Eger et al. (2008) and the LHD virtual model conducted in this research had a difference that ranged between 0.7 % and 6.1 %. The difference in the peak accelerations at the operator-seat interface for both studies was 15.9%. The acceleration values fall within an uncomfortable vibration zone as described in Table 7.8 that gives the ISO-2631 vibration exposure limits. Rasmussen (1982) conducted a study on human body vibrations exposure and measurement. He collected experimental data over years to help in defining the limits of human exposure to different levels of vibrations. The LHD virtual prototype model generates vibration frequencies that fall within a range that leads to WBVs and MSDs as detailed in Table 7.9. Kitazaki and Griffin (1998) showed that vibration frequencies that range between 1 Hz and 20 Hz are detrimental to the human health. These vibration frequencies cause the human body to resonate and cause structural damages, and damages to the organs. The human

back is also affected and this leads to lower back pains, degeneration of the spine, neck pains, leg pains and other MSDs. Beevis and Foreshaw (1985) and Shwarze et al. (1998) showed evidence of back and spinal problems in this frequency zone. The results show that f_5 and f_6 are uncomfortable, and can affect muscles and breathing (Rasmussen, 1982). Frequencies f_1 through f_4 cause motion sickness (ISO-2631). All the frequencies generated in this study (f_1 through f_6) are capable of causing musculoskeletal disorders (Kitazaki and Griffin, 1998).

Conducting virtual model simulations eliminates the process of subjecting human operators to the harsh vibrations they face while conducting experimental results. Once the virtual model is built, operators do not have to interact with the LHDs, which prevents WBVs and MSDs problems. The LHD virtual model gives vibration results in a shorter time without subjecting any human operators to WBVs generated during operations. Building the LHD virtual prototype expands the knowledge and understanding of vibration mechanics encountered during the operation of LHD vehicles by simulating the actual LHD vehicle while in operation. The virtual prototype simulates vibrations of each LHD component relative to adjacent components connected to it via joints. This LHD virtual model also simulates the overall components motion within the LHD system. The results of the LHD virtual model capture the three-dimensional displacements, velocities, and accelerations of the seat, cabin, body, and the tires of the LHD vehicle relative to each other with the ground as a reference. Much focus is on the vibration frequencies that reach the operator seat-interface of the LHD vehicle during operations. The RMS accelerations values for the different components of the LHD vehicle are key to understanding the severity of vibrations generated while the LHD is in operation.

6.4. SUMMARY

The LHD virtual prototype model was simulated successfully for vibrations generated while it is in operation, and ultimately reaching the operator seat-interface. This LHD virtual model represents the actual LHD vibration mechanical response while subjected to vibrations during operations. A total of 24 degrees of freedom were liberated in the LHD model to capture its complex vibration mechanics while in operation.

The front wheel assembly had an RMS acceleration value of 1.06 m/s^2 in the z-direction, and a peak acceleration of 12.58 m/s^2, and the rear wheel assembly had an RMS acceleration value of 1.03 m/s^2 in the z-direction, and a peak acceleration of 12.04 m/s^2. The RMS acceleration value recorded for the LHD body is 0.96 m/s^2 in the z-direction of the LHD vehicle, and the peak acceleration for the LHD body is 11.16 m/s^2. The reduction in the accelerations is because energy is dissipated in the spring-damper system that connects the wheel assembly to the LHD body. The RMS acceleration value experienced by the LHD cabin while in operation is 0.89 m/s^2, and the peak acceleration experienced by the cabin is 10.00 m/s^2. The driver's seat starts to vibrate immediately following the excitations from the cabin. The RMS acceleration value experienced by the LHD seat while in operation is 1.01 m/s^2, and the peak acceleration experienced by the seat is 7.44 m/s^2 occurring at the beginning of the excitation.

LHD vibration study would be incomplete without considering the vibrations acting in the x and y-directions. The RMS acceleration value recorded at the operator-seat interface in the x-direction for the LHD virtual model is 0.62 m/s^2, and the peak acceleration value recorded is 4.37 m/s^2, whereas the RMS acceleration value recorded at the operator seat in the x-direction for the experimental results is 0.66 m/s^2, and the peak

acceleration value recorded is 4.40 m/s^2. Moreover, the RMS acceleration value recorded for the operator seat in the y-direction is 0.51 m/s^2, and the peak acceleration value recorded is 3.45 m/s^2 for the LHD virtual model, whereas for the experimental results from T. Eger et al. (2008), the RMS acceleration value recorded for the operator seat in the y-direction is 0.49 m/s^2, and the peak acceleration value recorded is 3.64 m/s^2 for the LHD virtual model.

The LHD virtual prototype simulation results of this research effort are compared to the experimental results from a study on LHD vibration effects on human operators conducted by T. Eger et al. (2008). The LHD virtual simulation results are also compared to the ISO standards to determine if harmful vibrations are generated by LHD vehicle while in operation. The mean RMS acceleration value experienced by the LHD seat in the z-direction from the virtual prototype results is 1.01 m/s^2, and the peak acceleration experienced by the seat is 7.44 m/s^2, whereas the RMS acceleration value experienced by the LHD seat in the z-direction from experimental results by T. Eger et al. is 0.97 m/s^2, and the peak acceleration recorded for the seat was 8.85 m/s^2 occurring at the beginning of the excitation. The acceleration values fall within an uncomfortable vibration zone as described in Table 6.9 that gives the ISO-2631 vibration exposure limits. Rasmussen (1982) conducted a study on human body vibrations exposure and measurement, and collected experimental data to help in defining the limits of human exposure to different vibration levels. The LHD virtual prototype model generates vibration frequencies that fall within a range that leads to WBVs and MSDs as detailed in Table 7.9. Kitazaki and Griffin (1998) showed that vibration frequencies that range between 1 Hz and 20 Hz are detrimental to the human health. These vibration frequencies cause the human body to resonate and cause structural damages, and damages to the organs. The human back is also

affected and this leads to lower back pains, degeneration of the spine, neck pains, leg pains and other MSDs. Beevis and Foreshaw (1985) and Shwarze et al. (1998) showed evidence of back and spinal problems in this frequency zone. The results show that f_5 and f_6 are uncomfortable, and can affect muscles and breathing (Rasmussen, 1982). Frequencies f_1 through f_4 cause motion sickness (ISO-2631). All the frequencies generated in this study (f_1 through f_6) are capable of causing musculoskeletal disorders (Kitazaki and Griffin, 1998). The RMS accelerations that reach the operator-seat interface for the experimental results by T. Eger et al. and the LHD virtual model conducted in this research had a difference that ranged between 0.7 % and 6.1 %. The difference in the peak accelerations at the operator-seat interface for both studies was 15.9%

The results of the LHD virtual model capture the three-dimensional displacements, velocities, and accelerations of the seat, cabin, body, and the tires of the LHD vehicle relative to each other with the ground as a reference. The RMS accelerations values liberated at different LHD components are key to understanding the severity of vibrations generated while the LHD is in operation.

7. LHD MODEL VALIDATION AND EXPERIMENTAL RESULTS

Results from this research were compared to experimental results conducted by Eger et al. (2008) on various LHD models. The vibration shock waves reaching the operator-seat interface of the LHD vehicle while in operation were compared, and results from both studies had a convincing relationship. Section 7 discusses how the research results were validated using the experimental results conducted on LHDs, and highlights the deviation between the simulated virtual LHD model and the experimental results.

7.1. VALIDATION OF THE 24-DOF VIRTUAL PROTOTYPE

Validation is a necessary step used to verify the virtual prototype model by comparing outcomes between the actual model and the proposed virtual model. This validation process will ensure that the virtual prototype simulation results are reliable for analyzing real world LHD vehicle vibrations and ensuring that the model is robust enough for providing solutions within any parametric domains in question. In this research, validation is conducted by comparing the results of the LHD virtual model built on MSC.ADAMS to the experimental results gathered by Eger et al. (2008) where they conducted experimental research on the effects of whole-body vibrations on operators of LHD vehicles. The experimental research they conducted used ISO 2631-1 and ISO 2631-5 to evaluate the severity of vibrations generated while operating LHD vehicles, and to what extent these vibration levels reach the operator seat-interface of LHD vehicles. The process of validation entails recreating the experiment in MSC.ADAMS virtual environment that mimics the actual LHD operations using computer based software

without subjecting human operators to harmful shockwaves generated while operating LHDs.

The validation process for this research starts by replacing the LHD model component characteristics with the actual component characteristics of the Caterpillar R1700G LHD model. The masses of different components and their dimensions are taken from the Caterpillar R1700G brochure. Other values of significance such as, the stiffness and damping coefficients of the various suspensions are calculated theoretically as illustrated in Section 6. The complete validation process is then achieved by comparing the vibration frequencies measured at the operator-seat interface of the LHD during experimental analysis to the vibration frequencies reaching the operator-seat interface of the LHD vehicle model built in MSC.ADAMS.

7.2. MODEL DIMENSIONS

Understanding the LHD dimensions helps in building a virtual model simulator that is realistic relative to the actual LHD vehicle. The distance relationship between the different LHD components is useful in defining the positions of components relative to each other within the machine. The R1700G LHD vehicle model data is used to validate the virtual prototype model of LHD vehicle during operations. Figure 7.1 illustrates the details of inter-component dimensions. The LHD model used (R1700G) has an overall length of 11.03m and an overall machine height of 2.55m. Figure 7.1 also gives the important dimensions between the different components that are joined together within the LHD vehicle. Other dimensions given in Figure 7.1 include machine ground clearance, reach, wheelbase, maximum dump height, dump angle at maximum lift, height to top of hood, bucket pin height at maximum lift and digging depth. The dimensions were used to

build the virtual prototype on MCS.ADAMS. These LHD dimensions were also used to calculate the center of mass of the LHD vehicle. The LHD virtual prototype model built on ADAMS® used the exact dimensions of Caterpillar R1700G model.
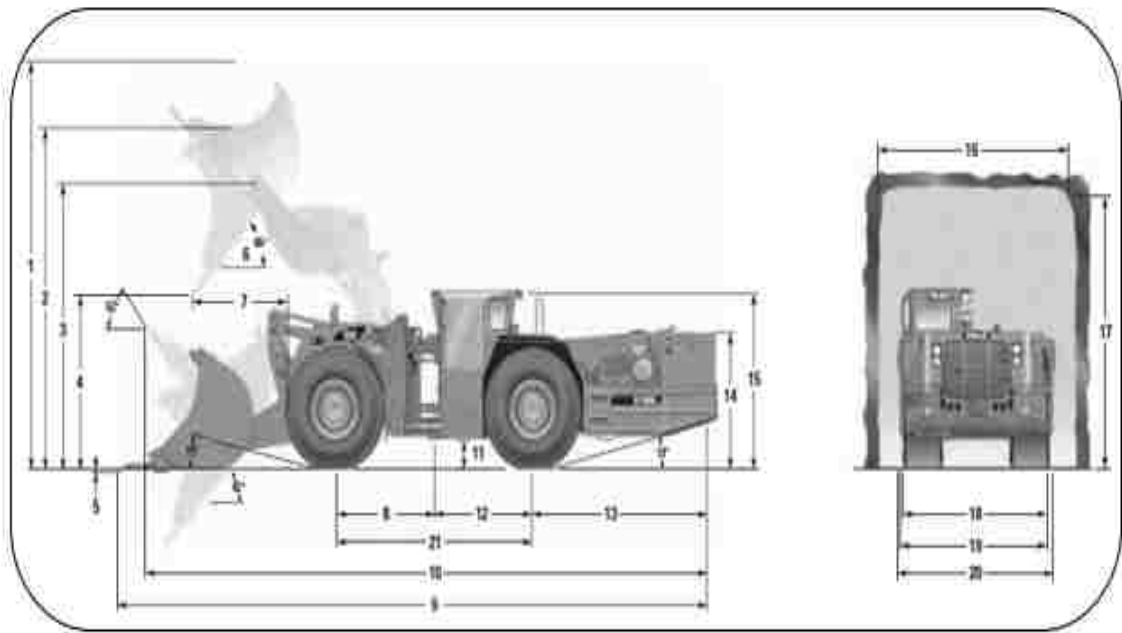

Figure 7.1. R1700G side and rear view dimensions

Table 7.1 gives the LHD vehicle numerical dimensions and all the dimensions between the machine components that were used to build the LHD virtual prototype on MSC.ADAMS. Table 7.1 gives the details of these R1700G LHD model dimensions which are useful in assembling the LHD virtual prototype.

Table 7.1. R1700G dimensions description

Bucket capacity	Bucket width over cutting edge	**1** Overall height – bucket raised	**2** Maximum dump height	**3** Bucket pin height at maximum lift
5.7 m^3	2772 mm	5606 mm	4899 mm	4104 mm
4 Dump clearance at maximum lift	**5** Digging depth	**6** Dump angle at maximum lift	**7** Reach	**8** Centerline of front axle to centerline of hitch
2443 mm	20 mm	46^0	1741 mm	1840 mm
9 Overall length (digging)	**10** Overall length (tramming)	**11** Ground clearance	**12** Centerline of back axle to centerline of hitch	**13** Length – rear axle to bumper
11035 mm	10589 mm	429 mm	1840 mm	3439 mm
14 Height to top of hood	**15** Height to top of ROPS	**18** Overall tire width	**20** Overall width including bucket	**20** wheelbase
1968 mm	2557 mm	2650 mm	2790 mm	3680 mm

It is also very important to know the specifications of various components of LHD vehicle in order to build a realistic model. Understanding the LHD vehicle specifications helps the investigators in knowing the mechanical dynamics of various parts that are interlinked and how the different components contribute to the general motion of the LHD vehicle. On the other hand, the engine specifications, transmission information, operating specifications and various weights of machine components are critical in vibrations analysis to identify the contribution of independent LHD parts to additional vibration frequencies that ultimately reach the operator-seat interface of the machine. Table 7.2 gives details of engine and transmission information for R1700G LHD vehicle.

Table 7.2. Engine and transmission information

R1700G Engine information		
Engine Model	Cat® C11 ACERT™	
Rated Power	1,800 rpm	
Gross Power – SAE J1995	241/263 kW	323/353 hp
Net Power – SAE J1349	218/241 kW	293/353 hp
Net Power – ISO 9249	218/241 kW	293/353 hp
Net Power – 80/1269/EEC	130 mm	5.1 in
Bore	140 mm	5.5 in
Stroke	11.1 L	680 in^3
R1700G Transmission information		
Forward 1	4.7 km/h	2.9 mph
Forward 2	8.3 km/h	5.2 mph
Forward 3	14.3 km/h	8.9 mph
Forward 4	24.1 km/h	15 mph
Reverse 1	5.4 km/h	3.3 mph
Reverse 2	9.4 km/h	5.8 mph
Reverse 3	16.4 km/h	10.2 mph
Reverse 4	25.3 km/h	15.7 mph

Table 7.3. Operating specifications and weights

Operating specifications	Operating weights	
Nominal Payload Capacity	12 500 kg	27,558 lb
Nominal Payload Capacity – Tramming	14 000 kg	30,865 lb
Gross Machine Operating Weight	52 500 kg	115,745 lb
Nominal Payload Capacity – Truck Loading	12 500 kg	27,558 lb
Static Tipping Load Straight Ahead Lift Arms	31 781 kg	70,065 lb
Static Tipping Load Full Turn Lift Arms Horizontal	26 306 kg	57,995 lb
Breakout Force (SAE)	20 885 kg	46,051 lb
Empty	38 500 kg	84,878 lb
Front Axle	16 940 kg	37,346 lb
Rear Axle	21 560 kg	47,532 lb
Loaded	51 000 kg	112,436 lb
Front Axle	37 077 kg	81,741 lb
Rear Axle	13 923 kg	30,695 lb
Loaded – Tramming	52 500 kg	115,743 lb

(Ref: www.cat.com)

7.3. MODEL PARAMETER DETERMINATION

It is necessary that the correct values for the stiffness coefficients and damping constants are used in this study in order to produce a realistic virtual model that mimics the actual vibration response of the LHD vehicle during operations. Because of company policies and confidentiality, the values for the damping coefficients and stiffness constants have not been made available to the public. Thus these parameters were estimated from computational analysis in this study. The stiffness constants for LHD suspensions have been derived using Hooke's Law as shown in Equation (7.1).

Hook's Law:

$$F = K\Delta z \qquad (7.1)$$

where F is the force as a result of the weight of the sprung mass and Δz is equal to the effective cylinder stroke. Equation (7.1) can be re-written to solve for the stiffness coefficients as shown in Equation (7.2):

$$K = F\Delta z \qquad (7.2)$$

Equation (7.3) is used to calculate the damping coefficients of the suspension system using the results of the stiffness constants calculated by using Equation (7.2):

$$C = 2\zeta\sqrt{KM} \qquad (7.3)$$

where ζ is damping ratio and it is equal to 0.4 for most commercial cars and trucks (Gillespie, 1992), K= stiffness constant, C= damping coefficient, and M= component mass.

The stiffness constants of the body, the cabin and the seat are calculated using Equation (7.4) as follows:

$$f_n = \frac{1}{2\pi}\sqrt{\frac{K}{M}}$$

(7.4)

Equation (7.4) is re-arranged to solve for the stiffness constant (K), and the value of f_n is equal to 1 Hz for optimum vehicles design according to Gillespie (1992).

$$K = (2\pi f_n)^2 M$$

(7.5)

The weights of various LHD components that are important in vibrations analysis are listed in Table 7.4. These weights include gross machine weight, front axle weight, rear axle weight, cabin weight, seat weight and tire/wheel assembly weight. The gross machine weight of R1700G LHD vehicle is 38,500 kg and the combined weight of the front and rear axles is equal to the gross machine weight (38,500 kg). Thus, the LHD vehicle is divided into two important mechanical articulations, the front axle and the rear axle. The front wheels of the LHD vehicle do not turn independently with respect to the front axle. Instead the turning motion while LHD vehicle is in operation occurs at the articulation joints located between the front and rear axle. These joints allow LHD side-ways motion to maneuver the road turns within an underground mining environment. Table 7.4 lists the different LHD components and their corresponding weights as specified in Caterpillar for R1700G LHD model brochure.

Table 7.4. R1700G component weights

Component	Weight (KG)
Gross machine weight	38 500
Front Axle	16 940
Rear Axle	21 560
Cabin	700
Seat	121
Tire/Wheel Assembly	1736

(Ref: www.cat.com)

7.4. LHD EXPERIMENTAL RESULTS FROM T. EGER ET AL.

T. Eger et al. (2008) conducted a study to determine health effects on operators of load-haul-dump vehicles. The operators are exposed to whole-body vibrations during operations, and their study aims at predicting the effects associated with operating LHDs. Eger et al. outline that health risks associated with operating LHDs have not been studied using ISO 2631-5. They argue that predictions of health risks that result from operating LHDs are limited while using ISO 2631-1 standards. When conducting their experimental study, they used tri-axial accelerometers to measure vibrations at the operator seat-interface of the LHD vehicles. They used ISO 2631-1 and ISO 2631-5 criteria in their study on LHDs and then compared the results the collected using the two criteria.

7.4.1. LHDs and Mine Site Selection. This experimental research study focused on the health effects of operating LHDs with bucket capacities ranging from 5.7 m^3 to 7.6 m^3. The LHDs used in their study had overall machine length ranging between 10.6 m^3 and 11.0 m^3. Also, the height of the LHDs used ranged between 2.6 m and 2.7 m, and the width between 2.8 m and 3.0 m. Eger et al. asked for help in conducting their research study from northern Ontario mine companies, and asked for their contribution in the

research. These LHDs were used to move material throughout an underground mine. LHD vehicles, A-1, A-2 and B-1 had a KAB 525 suspension system on their seats. Throughout data collection operators were not allowed to rise voluntarily from the seats.

7.4.2. WBVs Data Collection. Test subjects (LHD operators) had to load, haul, and dump material using an assigned LHD vehicle at designated work areas for one hour period. Before conducting the load haul dump activities, testing equipment was installed on LHDs at the operator seat-interface to capture whole-body vibrations in the x, y and z axis. Measurements of exposure to whole-body vibrations were recorded at the operator-seat interface using the ISO 2631-1 (1997). Vibration measurements were recorded at the operator-seat interface of the LHD vehicles using tri-axial accelerometers and data loggers. The accelerometers measured vibrations in the $x, y,$ and z axis. The series 2 tri-axial accelerometer was secured in the seat pad and placed firmly between the operators' buttocks and the seat. The LHD vibration data was then recorded using a 13 bit analog to digital conversion and a resolution of 0.0025 g at ±10 g full-scale range at 500 Hz.

7.4.3. WBV Analysis using ISO 2631-1. ISO standards were used to analyze whole-body vibrations in this research study. Procedures and guidelines of the ISO standards were adopted in this study to analyze LHD vibrations. Following ISO 2631-1 guidelines, the frequency-weighted RMS accelerations were calculated. In this analysis, appropriate frequency-weighting curves and scaling factors were applied to each of the orthogonal axis, and a vector summation of frequency-weighted RMS acceleration was computed. The presence of transient shocks was at first determined by computing the peak accelerations in all the axis (x, y, z). Vibrations at the operator-seat interface were recorded, vibration measures and peak accelerations were also calculated for consecutive 5-minute

interval and their average was recorded throughout the trial to yield more representative crest factor values. T. Eger's research team estimated that LHD vehicles are engaged in operations for about 7 hours in an 8 hours shift. This is because LHDs lose time during breaks, travel time to and from the underground site, as well as time lost moving the LHD vehicle to designated work areas.

7.4.4. ISO 2631-5 Analysis. This standard is covers probable health risks to the human backbones as a result of exposure to vibrations that contain multiple shocks. In this analysis tri-axial accelerometers are used at the operator-seat interface of LHDs to analyze the number, and size of vibration peaks as a results of exposure to WBVs. The data collected is used to compute the daily equivalent static compression dose at the lumbar-spine area of the LHD operators. Individual operator profile was derived from each operator's age and lifelong exposure to WBVs and this profile is used to calculate the risk factor. Operators' health risks were also determined using the known characteristics of exposure associated with specific LHD operator profile.

An evaluation of health risks of studies conducted in accordance ISO 2631-1 and ISO 2631-5 criteria was conducted for different LHD models. After conducting experimental analysis, the probability of health risks to the LHD operators was greatest using daily exposure criterion measurements that are published in ISO 2631-1. The probability of health risks was lowest while using ISO 2631-5 criterion measurements. According to Eger, a more conservative ISO 2631-1 should be adopted in evaluating the potential serious health risks to the operators, and other methods that focus a decreasing vibration reaching the operator-seat interface should be implemented for LHD operations.

7.4.5. Summary of LHD Experimental Results Conducted by Eger et al.

Frequency-weighted RMS accelerations (a_x, a_y, a_z) were measured at operator-seat interface of the LHD vehicle while in operations. The vibration results conducted on LHD model A-2 are shown in the Table 7.5. These results from experimental vibration study on LHDs are compared with this research results of a numerical and virtual analyses conducted in this study for LHD vibrations. The RMS acceleration in the *x*-direction is 0.66 m/s^2, and the peak acceleration recorded in the *x*-direction is 4.40 m/s^2. Also, the RMS acceleration in the *y*-direction is 0.49 m/s^2, and the peak acceleration recorded in the *y*-direction is 3.64 m/s^2. The peak acceleration recorded in the vertical (*z*-direction) at the operator-seat-interface direction is 8.85 m/s^2, and the RMS value recorded in the vertical direction at the operator seat interface of LHD B-1 is 0.97 m/s^2.

Table 7.5. RMS and peak accelerations at the operator-seat interface

LHD	a_x (m/s^2)	a_y (m/s^2)	a_z (m/s^2)	*Peak* a_x (m/s^2)	*Peak* a_y (m/s^2)	*Peak* a_z (m/s^2)
A-2	0.66	0.49	0.97	4.40	3.64	8.85

Table 7.6 shows the resulting mean (mean), standard deviation (SD), minimum (min), and maximum (max) values of accelerations measured in different directions at the operator-seat interface of various models of LHD vehicles. The results show that peak accelerations are dominant in the vertical (*z*) direction of the LHD vehicles at the operator-seat interface. The vertical direction experienced high accelerations measured at operator-seat interface for every LHD trial conducted on different models of LHDs used.

Table 7.6. RMS and peak accelerations at operator-seat interface of different LHDs

LHD Model		a_x (m/s^2)	a_y (m/s^2)	a_z (m/s^2)	Peak a_x (m/s^2)	Peak a_y (m/s^2)	Peak a_z (m/s^2)
B-1	*Mean*	0.49	0.42	0.65	3.26	4.68	6.80
	SD	0.13	0.15	0.19	0.63	2.56	2.66
	Min.	0.24	0.16	0.24	2.19	1.17	2.75
	Max.	0.60	0.63	0.83	4.43	11.94	13.21
A-1	*Mean*	0.68	0.46	0.78	4.59	3.81	6.70
	SD	0.20	0.12	0.23	1.12	0.64	1.86
	Min.	0.10	0.18	0.16	1.61	3.09	4.65
	Max.	0.90	0.66	1.03	6.30	5.81	11.42
A-2	*Mean*	0.66	0.49	0.97	4.40	3.64	8.85
	SD	0.15	0.12	0.23	1.40	1.21	5.93
	Min.	0.25	0.18	0.35	0.64	0.45	0.93
	Max.	0.86	069	1.28	6.34	4.66	28.07
F-2	*Mean*	0.65	0.43	0.61	4.17	3.72	5.79
	SD	0.18	0.11	0.16	1.01	0.99	1.50
	Min.	0.01	0.01	0.03	0.24	0.22	1.29
	Max.	0.80	0.56	0.76	5.35	5.63	9.51
C-2	*Mean*	0.65	0.56	1.06	4.91	4.68	13.31
	SD	0.24	0.20	0.34	1.51	1.51	4.68
	Min.	0.11	0.12	0.35	0.85	1.37	2.18
	Max.	0.98	0.90	1.55	7.78	8.08	20.93
C-3	*Mean*	0.62	0.53	0.74	4.89	4.37	16.11
	SD	0.21	0.19	0.26	1.88	1.73	15.68
	Min.	0.07	0.04	0.21	1.11	0.71	3.39
	Max.	0.77	0.68	1.06	8.49	7.28	56.59
H-3	*Mean*	0.60	0.55	0.56	3.93	4.29	6.76
	SD	0.12	0.09	0.09	0.78	1.23	2.98
	Min.	0.27	0.34	0.26	2.94	2.83	3.88
	Max.	0.71	0.66	0.65	5.75	7.60	14.75
Overall mean		**0.45**	**0.37**	**0.58**	**3.32**	**3.53**	**11.80**
Overall SD		**0.30**	**0.25**	**0.41**	**2.39**	**2.80**	**11.80**

The study showed discrepancies on the health effects to the operators when comparing the health effects given by ISO 2631-1 analysis and ISO 2631-5 evaluation methods, and this lack of agreement is a concern. For example, three out of seven LHD

operators used as test subjects in the study conducted by T. Eger et al. (2008) were placed above the health guidance caution zone (HGCZ) limits and the other four test subjects were placed within the HGCZ while using ISO 2631-1 standard. ISO 2631-5 predicted health risks lower than health risks predicted by ISO 2631-1 (T. Eger et al, 2008). Thus, there is a likelihood to misuse the standards and conclude that LHDs are safe and the vibrations reaching the operator-seat interface of the LHDs are harmless while using ISO 2631-5, and it can be concluded that there is extreme health risks while using ISO 2631-1 standard. Eger et al. (2008) concluded that the two criteria need to be revised.

7.5. COMPARISON OF LHD EXPERIMENTAL AND VIRTUAL MODEL RESULTS

The virtual model was built to mimic the actual LHD operating conditions. Vibration shocks reaching the operator seat interface of the LHD vehicle were captured. The overall values of the accelerations in different directions at the operator-seat interface of the machine conducted in this research study are consistent with the experimental results from LHD study by T. Eger et al. (2008).

The results of A-2 LHD model were compared to the results of this study. From the experimental results conducted on A-2 LHD model, RMS accelerations recorded at the operator-seat interface are 0.66 m/s^2 in the x-direction, 0.49 m/s^2 in the y-direction, and 0.97 m/s^2 in the z-direction, whereas the simulated LHD model RMS accelerations recorded at the operator-seat interface are 0.62 m/s^2 in the x-direction, 0.51 m/s^2 in the y-direction, and 1.01 m/s^2 in the z-direction. The peak acceleration recorded for the A-2 LHD model at the operator seat was 8.85 m/s^2, whereas 7.44 m/s^2 was recorded in the vertical direction at the operator-seat interface for the LHD virtual model. Table 7.7 illustrates the

RMS accelerations and peak accelerations recorded at the operator-seat interface for A-2 (T. Eger et al., 2008) and R1700G LHD virtual model used in this study.

Table 7.7. RMS and peak accelerations at operator-seat interface

LHD	a_x (m/s^2)	a_y (m/s^2)	a_z (m/s^2)	Peak a_x (m/s^2)	Peak a_y (m/s^2)	Peak a_z (m/s^2)
A-2 (T. Eger, 2008)	0.66	0.49	0.97	4.40	3.64	8.85
R1700G (MSC.ADAMS)	0.62	0.51	1.01	4.37	3.45	7.44
Actual Difference	0.04	0.02	0.04	0.03	0.19	1.41
Percentage Difference (%)	6.1%	4.1%	4.1%	0.7%	5.2%	15.9%

Table 7.7 also includes the actual percentage difference values between the results of both studies conducted on vibrations that reach the operator seat interface during LHD operations. The percentage difference from both studies on the results of vibrations reaching the operator-seat interface is between 0.7 % and 6.1 %, and only the peak acceleration percentage difference in the z-direction was 15.9 %.

7.6. CLASSIFYING COMFORT LEVELS AND VIBRATION FREQUENCIES

ISO suggests a level of 0.315 m/s^2 as a guideline for an eight hour per day exposure as shown in Table 7.8. Accelerations less than 0.315 are classified as not uncomfortable in accordance with ISO-2631-1 standards. Accelerations between 1.25m/s^2 and 2.5 m/s^2 are classified as very uncomfortable and accelerations greater than 2 m/s^2 are classified as extremely uncomfortable vibration levels. These guidelines were estimated on an 8 hours vibrations exposure time.

Table 7.8. ISO-2631 (1997) guideline for an 8 hour per day exposure

ACCELERATION (m/s^2)	COMFORT LEVEL
Less than 0.315 m/s^2	Not uncomfortable
0.315 m/s^2 to 0.63 m/s^2	A little uncomfortable
0.5 m/s^2 to 1.0 m/s^2	Fairly uncomfortable
0.8 m/s^2 to 1.6 m/s^2	uncomfortable
1.25 m/s^2 to 2.5 m/s^2	Very uncomfortable
Greater than 2.0 m/s^2	Extremely uncomfortable

Rasmussen (1982), conducted a study on human body vibrations exposure and measurement. Experimental data has been collected over years to help in defining the limits of human exposure to different levels of vibrations.

Thus, knowledge on vibration related comfort and fatigue-decreased proficiency is based on statistics collected over time while conducting practical and experimental research studies. Symptoms for vibration exposure frequencies in the range 1 Hz to 20 Hz are shown in Table 7.9. The table gives frequency ranges the vibrations are most dominant and the associated symptoms operators can feel. Vibration frequencies between 4 and 8 Hz affects breathing, and vibrations between 4-9 Hz result in a general feeling of discomfort and affect muscle contractions. A person that experiences vibration frequencies between 4 and 10 Hz experiences abdominal pains, and chest pains can be felt between 5 to 7 Hz frequency exposures. Lower jaw symptoms can be felt between 6 and 8 Hz. At a frequency range of 10 to 18 Hz the human body experiences an urge to urinate. Head symptoms, increased muscle tone, and influence on speech symptoms can be felt at frequencies between 13 and 20 Hz.

Table 7.9. Symptoms of exposure at frequencies of 1 to 20 Hz

SYMPTOMS	FREQUENCY
Influence on breathing movements	4-8
General feeling of discomfort	4-9
Muscle contractions	4-9
Abdominal pains	4-10
Chest pains	5-7
Lower jaw symptoms	6-8
Urge to urinate	10-18
lump in the throat	12-16
Head symptoms	13-20
Influence on speech	13-20
Increased muscle tone	13-20

(G. Rasmussen, 1982)

Table 7.10 shows the natural frequencies of the simplified 6-DOF LHD system analyzed in this research and their classification according to Rasmussen and ISO.

Table 7.10. Natural frequencies of the 6-DOF LHD system

Frequency (rad/sec)		Frequency (Hertz)		Rasmussen (1982)
$\omega_{n,1}$	4.56	f_1	0.66	Motion sickness
$\omega_{n,2}$	6.84	f_2	0.79	Motion sickness
$\omega_{n,3}$	13.54	f_3	0.87	Motion sickness
$\omega_{n,4}$	16.39	f_4	1.01	Motion sickness
$\omega_{n,5}$	18.19	f_5	2.00	Uncomfortable
$\omega_{n,6}$	26.00	f_6	4.06	General feeling of discomfort, influence on breathing movements, muscle contractions

Fundamental studies were conducted in this research work on LHD vibrations during operations with a practical aim to identify harmful vibration frequencies that reach the operator-seat interface of the machine during operations. Six natural frequencies were recorded for the 6-DOF LHD system. The highest frequency recorded on the LHD virtual prototype was 4.06 Hz and the lowest frequency recorded was 0.66 Hz.

The spine is susceptible to vibrations within frequencies of 4 to 8 Hz (ISO 2631-1, 1997). Very low-frequency accelerations (0.1 Hz to 0.5 Hz) experienced by machine operators when vertical forces are applied may cause kinetosis (ISO). Equations of motion were derived for the LHD system and solved for the vibration frequencies using MAPLE®. A virtual prototype LHD model was also built on MSC.ADAMS to identify the harmful frequency spectrum on the LHD vehicle during operations. The results of the LHD numerical models using MAPLE® and the virtual model using MSC.ADAMS show vibration frequencies within frequency spectrum and their associated symptoms identified by Rasmussen (1982). The human body harmlessly attenuates most vibration effects, but exposure to machine vibrations affects human health. Kitazaki and Griffin (1998) showed that vibration frequencies that range between 1 Hz and 20 Hz are detrimental to the human health. These vibration frequencies cause the human body to resonate and cause structural damages, and damages to the organs. The human back is also affected and this leads to lower back pains, degeneration of the spine, neck pains, leg pains and other MSDs. Beevis and Foreshaw (1985) and Shwarze et al. (1998) showed evidence of back and spinal problems in this frequency zone. The results show that f_5 and f_6 are uncomfortable, and can affect muscles and breathing (Rasmussen, 1982). Frequencies f_1 through f_4 cause motion sickness (ISO-2631). All the frequencies generated in this study (f_1 through f_6) are capable of causing musculoskeletal disorders (Kitazaki and Griffin, 1998).

7.7. SUMMARY

Results from this research were compared to experimental results conducted by Eger et al. (2008) on various LHD models. Section 7 discusses how the research results were validated using the experimental results conducted on LHDs, and highlights the deviation between the simulated virtual LHD model and these experimental results. In this research, validation is conducted by comparing the results of the LHD virtual model built on MSC.ADAMS to the experimental results gathered by Eger et al. (2008) where they conducted experimental research on the effects of whole-body vibrations on operators of LHD vehicles. The experimental research they conducted used ISO 2631-1 and ISO 2631-5 to evaluate the severity of vibrations generated while operating LHD vehicles, and to what extent these vibration levels reach the operator seat-interface of LHD vehicles.

The validation of the results in this research is achieved by comparing the LHD vehicle weighted RMS acceleration values at the operator-seat interface from the experimental results conducted by T. Eger et al. (2008) with the results of the virtual model. The masses of different components and their dimensions are taken from the Caterpillar brochure of R1700G. Other values of significance such as the stiffness constants and damping coefficients of the various suspensions are calculated theoretically. The results of A-2 LHD model were compared to the results of this study. From the experimental results conducted on A-2 LHD model, RMS accelerations recorded at the operator-seat interface are 0.66 m/s^2 in the x-direction, 0.49 m/s^2 in the y-direction, and 0.97 m/s^2 in the z-direction, whereas the simulated LHD model RMS accelerations recorded at the operator-seat interface are 0.62 m/s^2 in the x-direction, 0.51 m/s^2 in the y-direction, and 1.01 m/s^2 in the z-direction. The peak acceleration recorded for the A-2 LHD model at the operator-seat interface was 8.85 m/s^2, whereas 7.44 m/s^2 was recorded in the vertical direction at the

operator-seat interface for the LHD virtual model. Also, fundamental studies were conducted in this research work on LHD vibrations during operations with a practical aim to identify harmful vibration frequencies that reach the operator-seat interface of the machine during operations. The results show that f_5 and f_6 are uncomfortable, and can affect muscles and breathing (Rasmussen, 1982). Frequencies f_1 through f_4 cause motion sickness (ISO-2631). All the frequencies generated in this study (f_1 through f_6) are capable of causing musculoskeletal disorders (Kitazaki and Griffin, 1998).

8. SUMMARY, CONCLUSIONS AND RECOMMENDATIONS

8.1. SUMMARY

Load-haul-dump vehicles are used in mining, tunneling, and construction industries as the primary loading machines. This is because they have proven to be vigorous, highly productive, and reliable in these industries. About 75% of underground metal mines in the world use LHDs to move rocks from small drives, large tunnels, and wide excavations (Ratan, 2013). LHDs generate vibration frequencies while they are in operation, and the vibrations propagate to different components of the machine such as the tire assembly, LHD body, and driver's cabin, and ultimately reach the operator-seat interface. Exposure to high vibration frequencies affect the efficiency, lifespan, and the health of the operators of these machines. About 4% to 7% of the labor force within the United States, Canada, and Australia is affected by whole-body vibrations (Bovenzi, 1998). The human body harmlessly attenuates most vibration effects, but exposure to machine vibrations affects human health. Kitazaki and Griffin (1998) showed that vibration frequencies that range between 1 Hz and 20 Hz are detrimental to the human health. These vibration frequencies cause the human body to resonate and cause structural damages, and damages to the organs. The human back is also affected and this leads to lower back pains, degeneration of the spine, neck pains, leg pains and other MSDs. Beevis and Foreshaw (1985) and Shwarze et al. (1998) showed evidence of back and spinal problems in this frequency zone.

There is a need to build a dynamic virtual model that would help to solve vibration problems within LHD vehicles and help to promote solutions that would reduce human exposure to harmful frequencies. This research highly impacts the study of innovation processes for manufacturing vibration mitigated machines. Vibrations generated while

LHDs are in operation have not been exposed in depth to promote solutions that would reduce MSDs and WBVs that operators of these machines are exposed to during operations. The aim of this research is to identify the forces acting on LHDs while in operation and link them to impact forces propagating throughout the entire LHD, and ultimately reaching the operator-seat interface. Also, this study developed a complete analytical vibration model used in describing vibration problems encountered in LHD operations. The last objective of this study was to create an LHD virtual model to simulate various frequency exposures upon LHD operations. The mechanics of the LHD vehicle is based on a multi-degree of freedom system (MDOF) where components are connected together by joints and spring-damper systems. Mathematical models derived describing the LHD motion are used to generate the EOMs and thus, analyze the free and forced vibration problem of the LHD vehicle.

Valid mathematical models for describing the propagation of vibrations on the LHD vehicle was developed and solved using MAPLE® to identify the frequency spectrum on the machine and thus, filter the harmful ones. Virtual 3D model of the LHD vehicle was built on MSC.ADAMS® to identify the harmful vibrations LHD operators are exposed to during operations. The complete dynamic virtual prototype captures the three-dimensional displacement, velocities, accelerations, profiles, as well as moments and forces acting on the various LHD components. The virtual model was validated using the experimental results from a research studies conducted by T. Eger et al. (2008). The standards of permissible vibration limits a human body is allowed to be exposed to as set by the ISO was used as a benchmark to the vibration exposure limit on the human operators for this research.

8.2. CONCLUSIONS

The main objectives of this research have been successfully accomplished. Mechanics of the LHD vehicle were studied to determine frequencies that reach the operator-seat interface while the machine is in operation. Numerical analysis was conducted for the LHD vehicle to study the vibrations generated and propagating throughout the LHD body, and ultimately reaching the operator-seat interface. The LHD vehicle was dissected into different components, and free-body diagrams were drawn for the associated components to identify all the external and internal forces acting on each of these components. The forces identified on the free-body diagrams were then used to derive the equations of motion for the LHD system. At first, a 6-DOF LHD system was established using Lagrangian formulation and then it was solved for the undamped free vibrations. The undamped free vibration LHD model generates the natural frequencies and mode shapes of different LHD components. The results from the undamped free vibration problem were then used to develop the numerical LHD model for the forced vibrations problem.

The following conclusions can be drawn from the results of undertaking this research work:

1) This research successfully developed a 6-DOF and 24-DOF numerical models for LHD vibrations mechanics. The 24-DOF virtual prototype captures the complex vibration mechanics of the LHD vehicle while in operation and all the vibrations at the various LHD components, as well as vibrations that reach the operator seat-interface in the three dimensions (3D) x, y and z-directions.

2) The complex dynamic model developed in this study is a MDOF system that simulates the actual LHD behavior while in operation and captures associated vibrations propagating throughout the machine. This complex model is a platform for design optimization, and could be used to improve LHDs at a design stage.

3) The developed LHD virtual model for this research was successful in predicting the RMS acceleration values at the operator-seat interface within a range between 0.7 % and 6.1 % error compared to the experimental results by T. Eger et al. (2008). From the experimental results conducted on A-2 LHD model, RMS accelerations recorded at the operator-seat interface are 0.66 m/s^2 in the x-direction, 0.49 m/s^2 in the y-direction, and 0.97 m/s^2 in the z-direction, whereas the simulated LHD model RMS accelerations recorded at the operator-seat interface are 0.62 m/s^2 in the x-direction, 0.51 m/s^2 in the y-direction, and 1.01 m/s^2 in the z-direction.

4) The generic model can capture vibration behavior of all the machine components and mimic the actual behavior of the LHD vehicle while in operation. This complex virtual model built on MSC.ADAMS will become a generic model that can accommodate various loaders for underground mining applications, as well as construction applications.

5) The LHD virtual model built on MSC.ADAMS provides a powerful tool to innovation-based technology in the field of heavy mining equipment design and optimization. Vibration simulations can be carried out on heavy mining machines to obtain necessary data without exposing human operators to the harmful vibration shocks.

6) This research gives a baseline tool accessible to the public in understanding the behavior of vibrations within LHD vehicles and how they propagate until they reach the operator-seat interface. Also, this analysis highlights vibrations propagation through the different components linked together. The results of this research initiative will be helpful to equipment manufacturers by enhancing their future LHD designs and building vibration mitigated machines that perform within the ISO limits.

7) This fundamental research study conducted on LHD vibrations was successful in identifying harmful vibration frequencies that reach the operator-seat interface of the LHD during operations. The RMS accelerations at the operator seat-interface of the simulated virtual Caterpillar R1700G LHD model show that there are harmful RMS accelerations that reach the operator seat-interface of the machine. These RMS accelerations exceed the ISO limits, thus there is a health and safety concern amongst the operators of the CAT R1700G LHD model.

8.3. RECOMMENDATIONS

The results of this research initiative have been successful. The model simulated (Caterpillar R1700G), produces a vibration frequency spectrum that falls within a range of harmful vibration frequency limits to the human body. Vibrations generated while the LHD vehicle is in operation propagate throughout the entire body until they reach the operator-seat interface of the machine. This research can be refined more to improve the accuracy of the results since various machine parameters were not provided and had to be assumed or derived from theoretical analysis. More research efforts need to be conducted in the field

of LHD vibrations to expand knowledge on how vibrations propagate throughout the LHD vehicle while in operation.

The structural design of the LHD vehicle could be modified in the future to account for unwanted frequency spectrums generated during operations. The LHD vehicle has the chassis directly fixed to the body of the machine and has no suspension system between the chassis and the body of the machine. It uses its wheels as shock absorbers to dampen the harmful vibration frequencies it is exposed to while in operation. A suspension system could be incorporated in future designs of LHD vehicles to reduce vibrations that are generated while in operation, and ultimately reduce vibrations reaching the operator seat-interface of the machine.

The suspension system characteristics of springs and dampers (damping coefficients and stiffness constants) used in this research were estimated based on computational analysis because manufacturers keep their information confidential and do not release it to the public. For more accurate results, future research studies in this field must use the exact parameters of the suspension system to improve the overall reliability of the results from this research. Exact characteristics of the suspension system would help to produce an accurate virtual model that will simulate the actual behavior of the LHD vehicle while it is subjected to vibrations during operation.

The digging forces generated when the LHD bucket is loading material have not been studied and numerically modeled to understand how they influence the overall LHD system vibrations behavior. Thus, it is necessary for future work to take into account the mechanical behavior of the LHD bucket with a practical aim to understand the forces generated while digging the material.

New LHD vehicles that do not need to be operated by way of human interaction with the machine could be adapted. LHD vehicles can also be fully automated or be remote controlled while in operation to avoid using human operators. This would help to avoid human interaction with the machine, and eliminate the possibility of operators being exposed to harmful vibration frequencies that lead to MSDs in the long run.

Moreover, the operator's seat can be modified filter the harmful vibration spectrum generated while the LHD is in operation. This modified seat design would absorb the harmful vibration frequencies and keep the operator of the LHD vehicle safe from unwanted vibrations. The modifications to the seat could include an additional spring-damper system to the LHD seat and different characteristics of a spring-damper system of the LHD vehicle. More cushioning could be added to the LHD seat to help it absorb more vibrations generated during operations.

APPENDIX A.

NUMERICAL MODEL OF THE 6-DOF LHD SYSTEM

The code generated on MAPLE® for the damping matrix is shown in Equation (A.1):

```
Damping matrix
> CC:=linalg[matrix](6,6,[C__6+C__2+C__3,0,-C__2,-C__3,-C__6,a*C__2-b*
  C__3,0,C__1,0,0,-C__1,0,-C__2,0,C__2-C__4,0,0,-aC__2,-C__3,0,0,C__3-
  C__5,0,b*C__3,-C__6,-C__1,0,0,C__6,0,a*C__2-b*C__3,0,-a*C__2,b*C__3,0,
  a^2*C__2+b^2*C__3]);
```

$$(A.1)$$

Equation (A.2) shows the code used in this study to compute the inverse of mass matrix.

```
Inverse of a MASS matrix
> BB:=linalg[matrix](6,6,[1/m__1,0,0,0,0,0,0,1/m__2,0,0,0,0,0,0,1/m__3,
  0,0,0,0,0,0,1/m__4,0,0,0,0,0,0,1/m__5,0,0,0,0,0,0,1/I__5]);
```

$$(A.2)$$

The code generated on MAPLE® for the stiffness matrix is given by Equation (A.3)

```
Stiffness matrix
> DD := linalg[matrix](6, 6, [K_6+K_2+K_3, 0,-K_2,-K_3,-K_6, a*K_2-b*K_3, 0, K_1, 0, 0,
    -K_1, 0,-K_2, 0, K_2-K_4, 0, 0,-aK_2,-K_3, 0, 0, K_3-K_5, 0, b*K_3,-K_6,-K_1, 0, 0,
    K_6, 0, a*K_2-b*K_3, 0,-a*K_2, b*K_3, 0, a^2*K_2+b^2*K_3]);
```

$$(A.3)$$

The inverse of mass matrix is multiplied by the stiffness matrix as one of the series of steps conducted to compute the determinant matrix as shown in equation (A.4).

```
> EE:=(linalg[matrix](6,6,[1/m__1,0,0,0,0,0,0,1/m__2,0,0,0,0,0,0,1/m__3,
  0,0,0,0,0,0,1/m__4,0,0,0,0,0,0,1/m__5,0,0,0,0,0,0,1/I__5]))*(linalg
  [matrix](6,6,[K__6+K__2+K__3, 0, -K__2, -K__3, -K__6, K__2*a-K__3*b,
  0, K__1, 0, 0, -K__1, 0, -K__2, 0, K__2-K__4, 0, 0, -aK__2, -K__3, 0,
  0, K__3-K__5, 0, b*K__3, -K__6, -K__1, 0, 0, K__6, 0, K__2*a-K__3*b,
  0, -a*K__2, b*K__3, 0, K__2*a^2+K__3*b^2]));
```

$$(A.4)$$

The solution for the determinant of coefficients yields a characteristic Equation A.5. Solving the characteristic equation yields the natural frequencies of the LHD system on MAPLE®, which are compared to the frequencies from the 6-DOF model from hand calculations.

$$DET = 1.00000000000453\ \lambda^6 - 77.0957146260868\ \lambda^5 + 1430.96483742329\ \lambda^4 + 2841.67825954566\ \lambda^3$$
$$-1.88439334215140\ 10^5\ \lambda^2 + 1.45444606304800\ 10^5\ \lambda + 5.02666044399330\ 10^6 = 0$$

(A.5)

APPENDIX B.

NUMERICAL MODELING OF THE 6-DOF FEL SYSTEM

The numerical approach used for load-haul-dumps was repeated on front-end-loaders (FELs) to check if the approach is flexible for use on other heavy machines as tool for studying vibrations propagation. FELs have a mechanical structure and build-up that is similar to the LHDs. Thus, the approach adopted in this research, and the numerical algorithms used in this research can be used to analyze FEL vibrations during operations FEL was dissected into various components as shown in Figure (B.1). The spring-damper system was established oriented vertically on the FEL vehicle the same way as the approach used in LHD vehicle vibrations analysis. The tires of the FEL vehicle were fixed to the ground for the 6-degree of freedom model, and the ground was not allowed to deform due to the weight of the FEL (the tires were fixed to the ground).
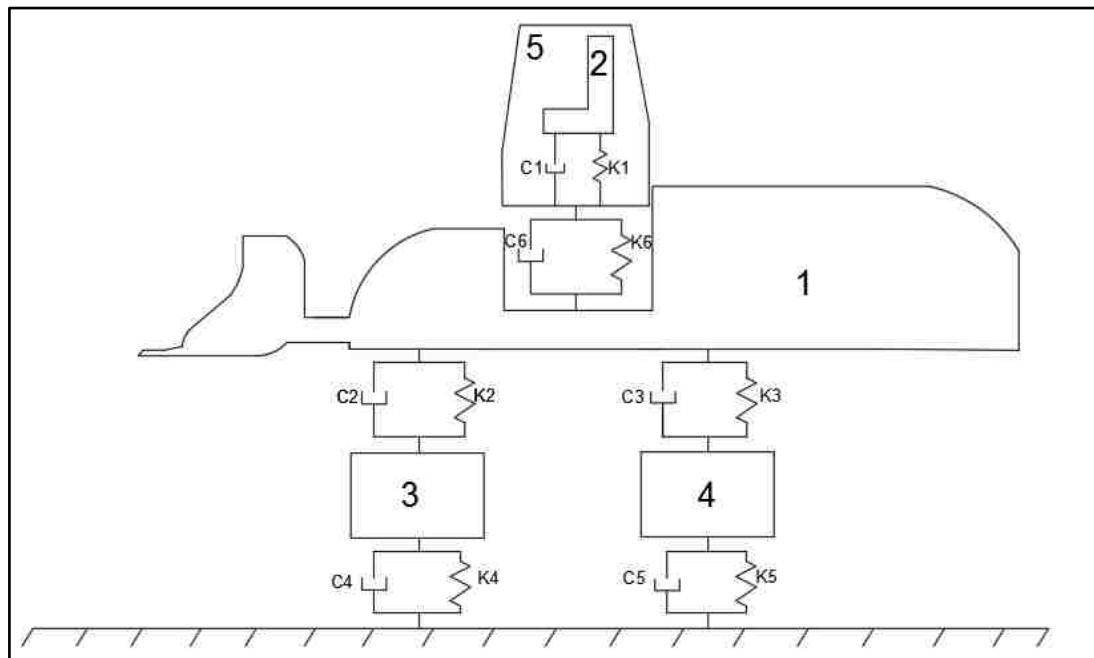
(B.1)

Figure B.1. Spring damper system oriented in the vertical direction on an FEL vehicle

The steps used for identifying various forces acting on LHD components were repeated for the FEL system. A basic 6-DOF system was established, and all the action–reaction forces acting on the different FEL components were identified. Also, the center of mass of the FEL vehicle was established. The established FBDs in Figures (B.1) and (B.2) form the basis of deriving the equations of motion using the Lagrangian formulation. Figure (B.2) gives the details of the action–reaction forces acting on the FEL components, and the external forces acting each components.
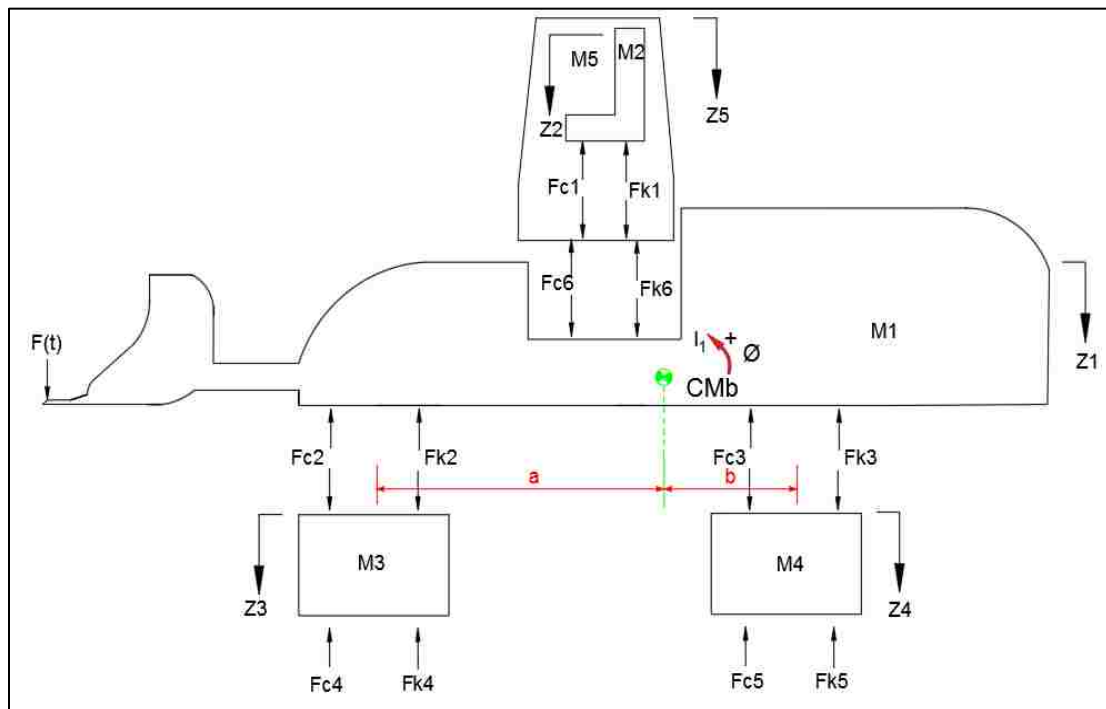
(B.2)

Figure B.2. Action-reaction forces identified on FEL components

The inverse of mass matrix was multiplied by the stiffness matrix as shown in the Equation (B.3) as one of the steps leading to computing the natural frequencies of the front-end-loader system.

```
> EE:=(linalg[matrix](6,6,[1/m__1,0,0,0,0,0,0,1/m__2,0,0,0,0,0,0,1/m__3,0,0,0,0,0,
  0,0,1/m__4,0,0,0,0,0,0,1/m__5,0,0,0,0,0,0,1/I__5]))*(linalg[matrix](6,6,[K__6+
  K__2+K__3, 0, -K__2, -K__3, -K__6, K__2*a-K__3*b, 0, K__1, 0, 0, -K__1, 0, -
  K__2, 0, K__2-K__4, 0, 0, -a*K__2, -K__3, 0, 0, K__3-K__5, 0, b*K__3, -K__6, -
  K__1, 0, 0, K__6, 0, K__2*a-K__3*b, 0, -a*K__2, b*K__3, 0, K__2*a^2+K__3*b^2]))
  ;
```

$$(B.3)$$

The characteristic Equation (B.4) was finally derived and solved for the natural frequencies.

$$DET = 0.999999512566461 \, \lambda^6 - 153.386511548360 \, \lambda^5 - 19450.8191917207 \, \lambda^4 + 2.84181104676851 \, 10^6 \, \lambda^3$$
$$+ 6.39278567351087 \, 10^7 \, \lambda^2 - 1.13246548799045 \, 10^{10} \, \lambda + 1.86867116210858 \, 10^{11} = 0$$

$$(B.4)$$

APPENDIX C.

24-DOF LHD VIRTUAL MODEL SIMULATION RESULTS

Figures (C.1) and (C.2) show the RMS acceleration responses of the front wheel assembly in the *x*, and *y*-directions, respectively.
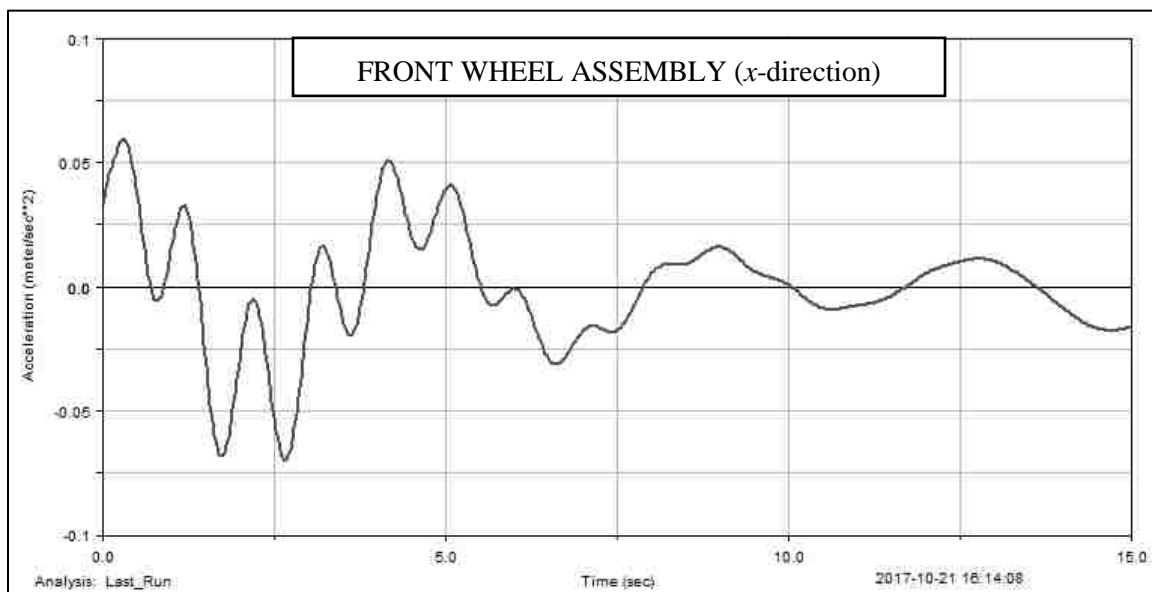
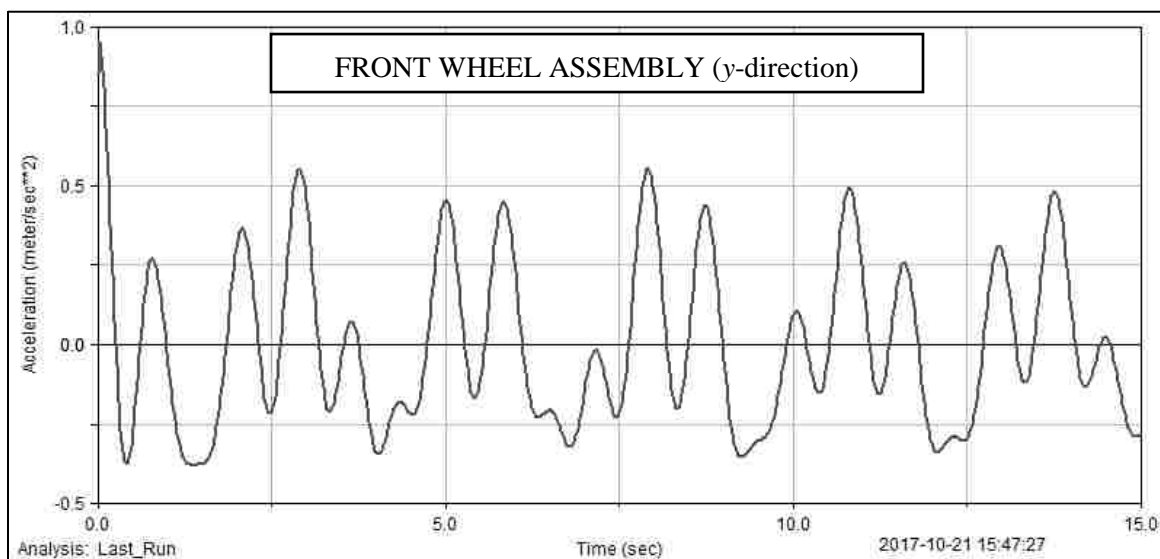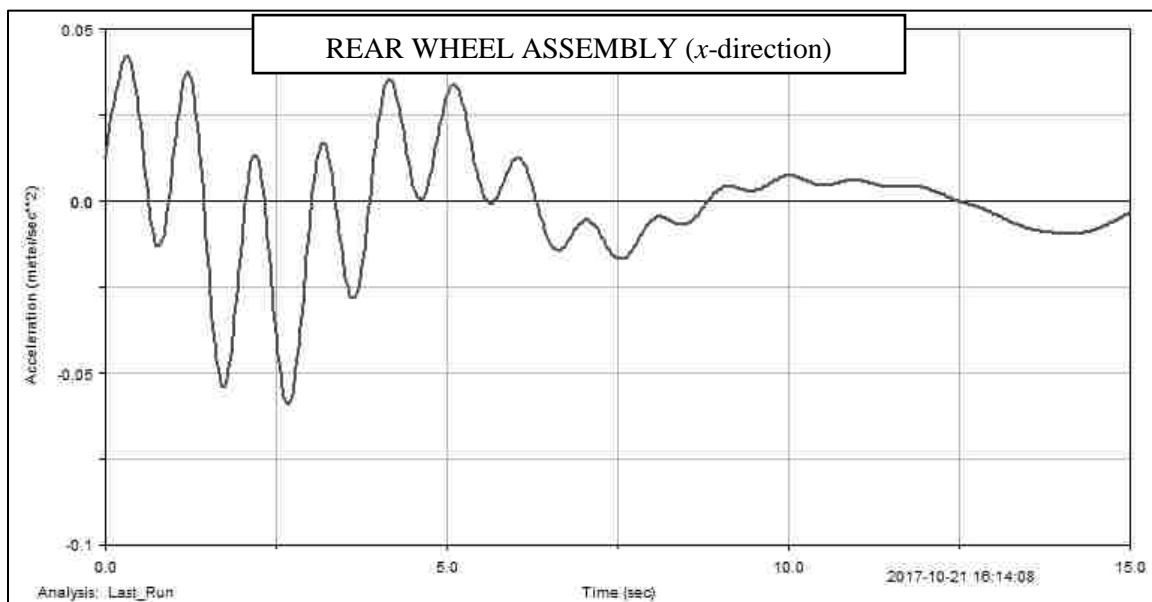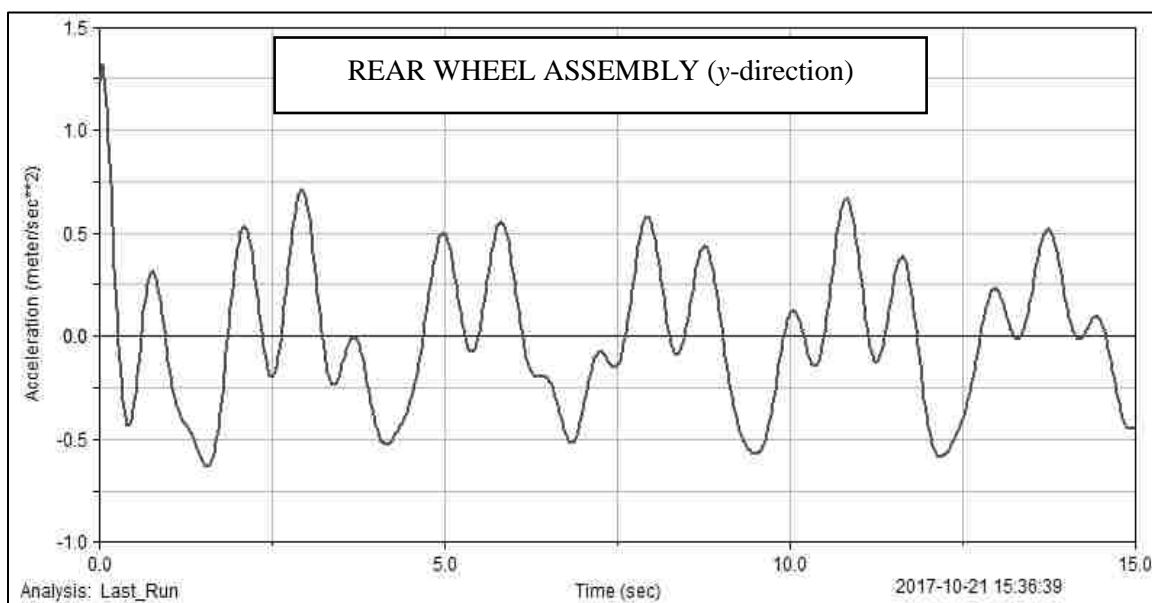Figure C.1. RMS acceleration of the front wheel assembly in the *x*-direction

Figure C.2. RMS acceleration of the front wheel assembly in the *y*-direction

Figures (C.3) and (C.4) show the RMS acceleration responses of the rear wheel assembly in the *x*, and *y*-directions, respectively.

Figure C.3. RMS acceleration of the rear wheel assembly in the *x*-direction

Figure C.4. RMS acceleration of the rear wheel assembly in the *y*-direction

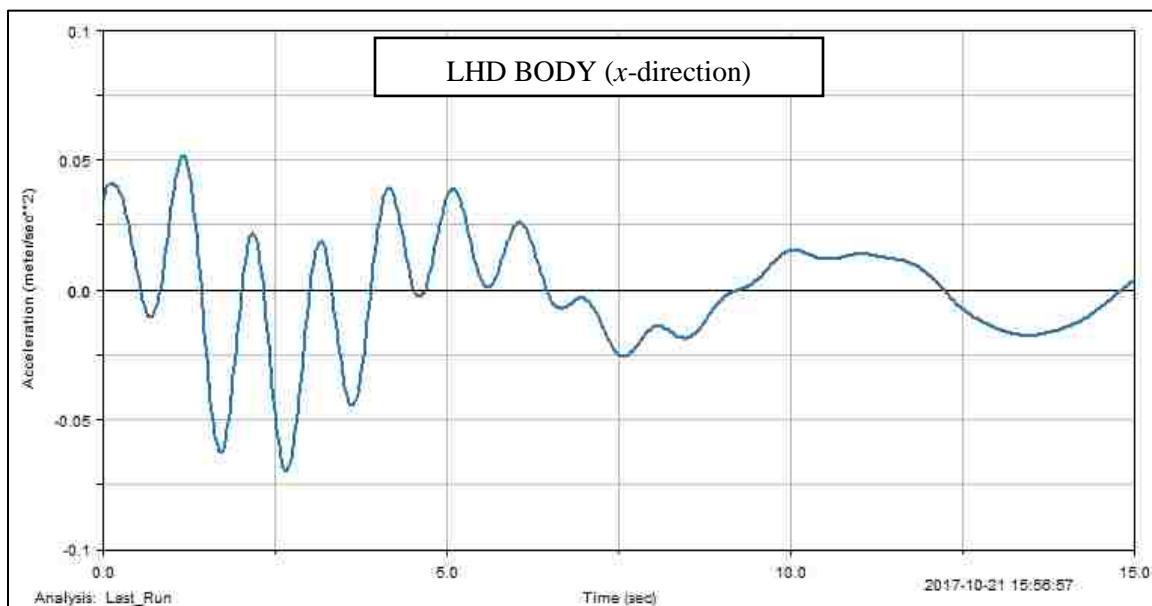Figures (C.5) and (C.6) show the RMS acceleration responses of the LHD body in the *x*, and *y*-directions, respectively.

Figure C.5. RMS acceleration of the LHD body in the *x*-direction
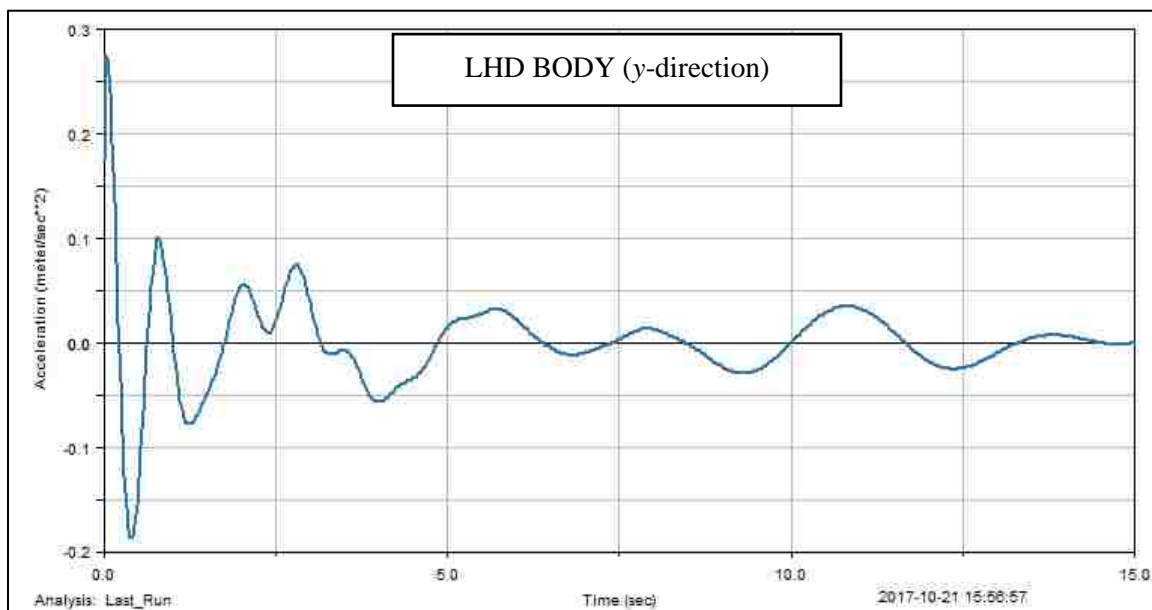
Figure C.6. RMS acceleration of the LHD body in the *y*-direction

Figures (C.7) and (C.8) show the RMS acceleration responses of the cabin in the *x*, and *y*-directions, respectively.
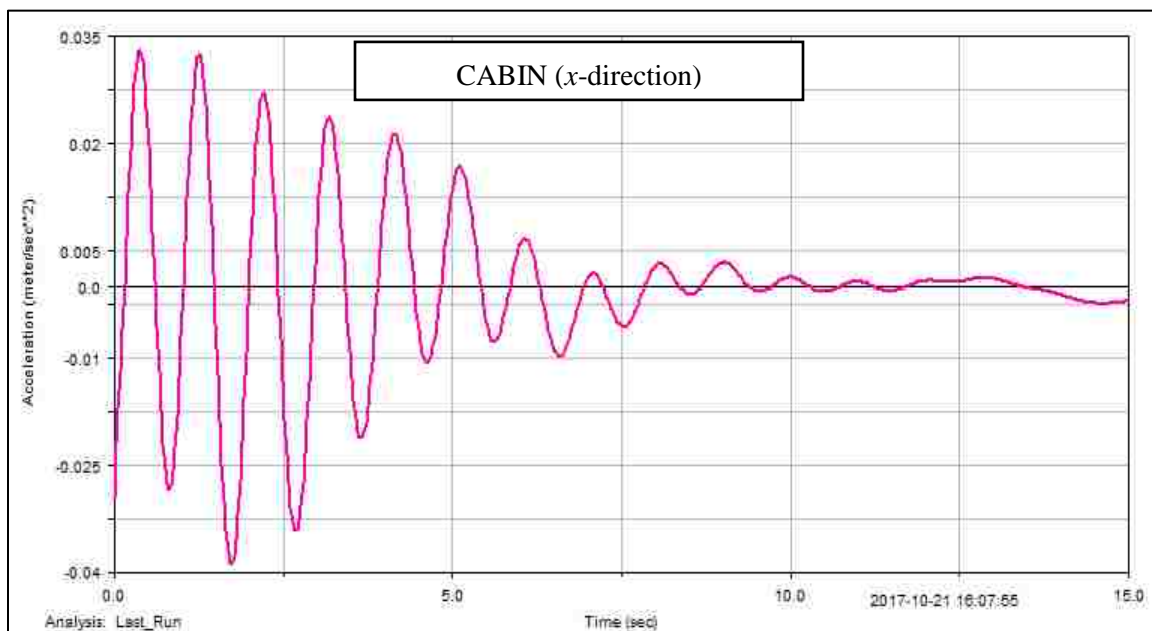

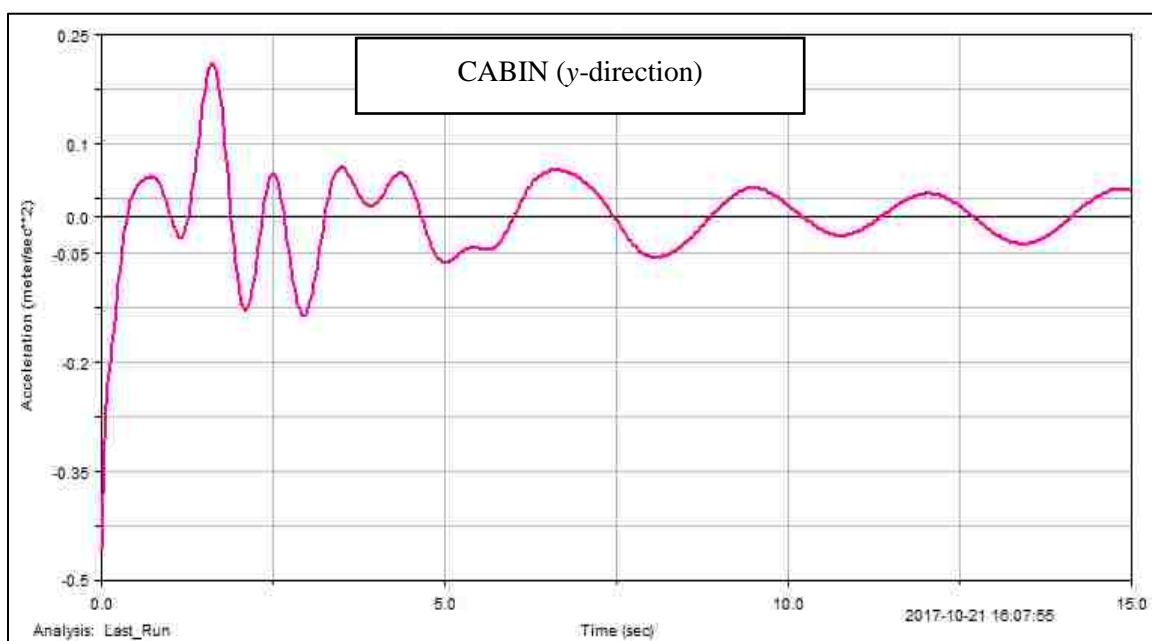Figure C.7. RMS acceleration of the cabin in the *x*-direction

Figure C.8. RMS acceleration of the cabin in the *y*-direction

Figures (C.9), (C.10) and (C.11) show the displacement responses of the driver's seat in the *x*, *y,* and *z*-directions, respectively.
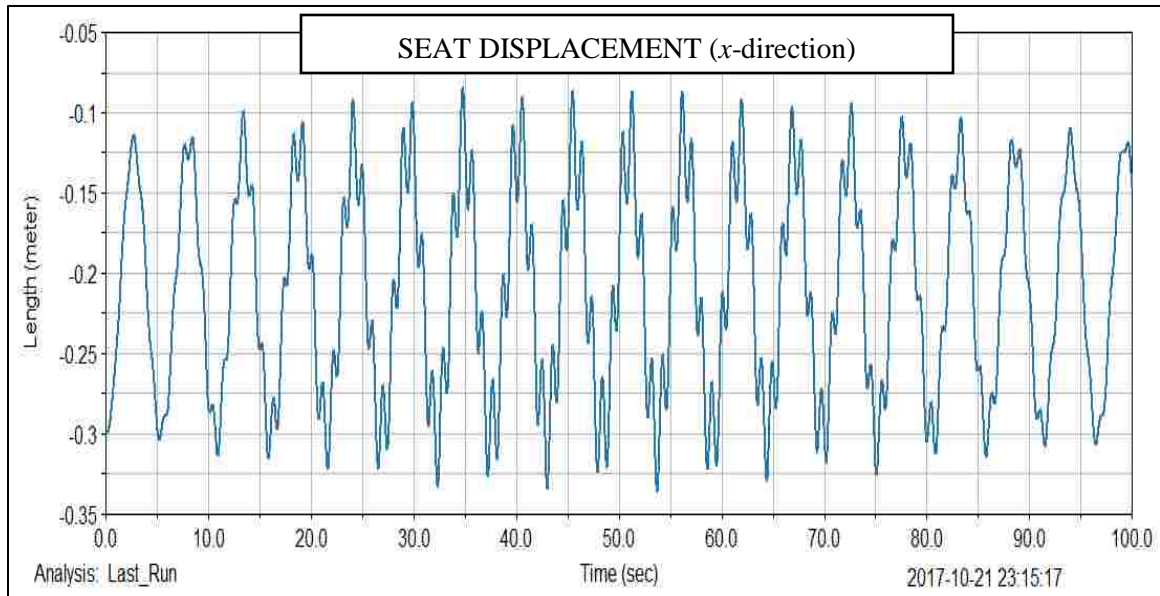

Figure C.9. Displacement of the operator's seat in the *x*-direction
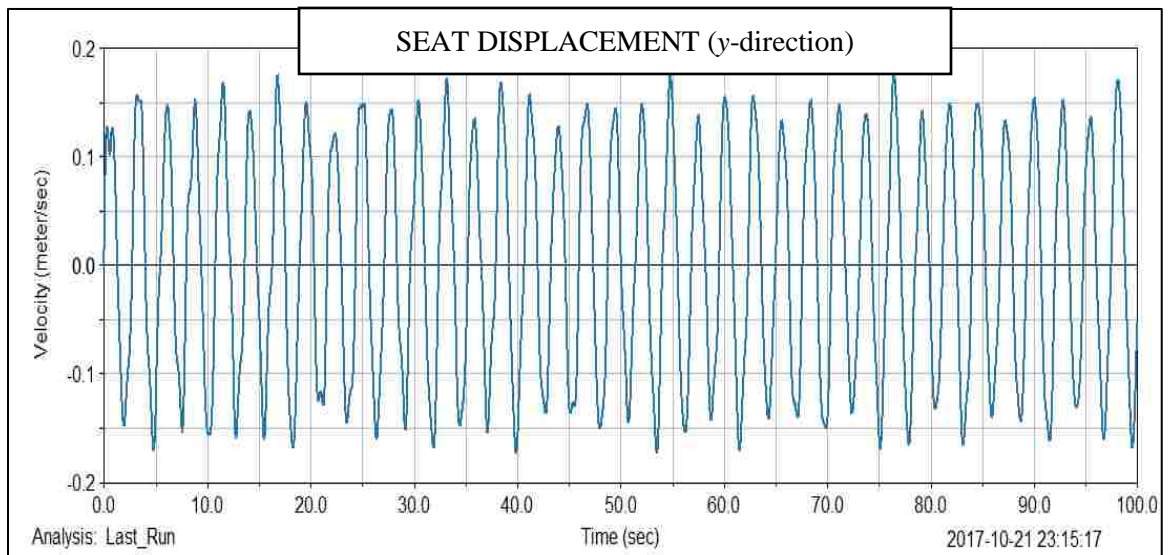

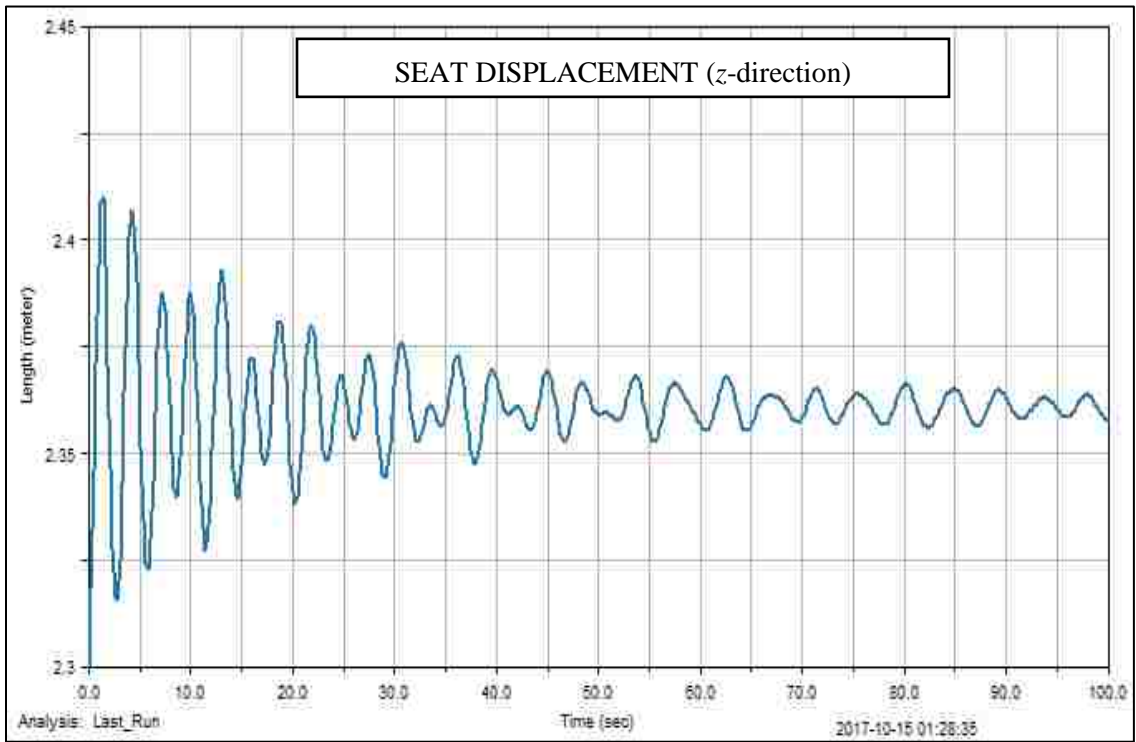Figure C.10. Displacement of the operator's seat in the *y*-direction

Figure C.11. Displacement of the operator's seat in the *z*-direction

BIBLIOGRAPHY

Alem, N. (2005), "Application of the new ISO 2631–5 to health hazard assessment of repeated shocks in U.S. army vehicles. Ind. Health" *43*, 403–412.

Andrew J. Kowalyshyn, and Jeffrey P. Kwolkoski, (2008), "Mitigation of excessive vibration induced by commercial washers on elevated post-tensioned concrete slab," Dearborn, Michigan.

Aouad, N., (2008), "Mechanics of Dump Truck Vibrations in High Impact Shovel Loading Operations, "Ph.D. thesis, Missouri University of Science and Technology, Rolla, MO.

Aouad, N., and Frimpong, S. (2011) "Research and Engineering Solutions for Dump Truck Vibration Problems in HISLO," Proceedings of the 140th SME Annual Meeting & Exhibit and CMA 113th National Western Mining Conference, Denver, CO, February 27-March 2, Curran Associates, Inc.,Red Hook, NY, Vol. 1, pp.548-551.

Benaroya, H. (2004), "Mechanical vibration Analysis, Uncertainties, and Control,"Second Edition, Published by Marcel Dekker Inc., New York, USA 712pp.

Blood, R. P., Ploger, J. D., Yost, M.G., Ching, R. P., & Johnson, P. W. "Whole Body Vibrations Exposures In Metropolitan Bus Driver: A Comparison of Three Seats," *Journal of Sound And Vibration Journal of Sound and Vibration*, *329* (2010) 109–120.

Boileau P.E. & Rakheja S. (1990), "Vibration attenuation performance of suspension seats for off-road forestry vehicles," *International Journal of Industrial Ergonomics*, Vol. 5, No. 3, pp. 275-29.

Boileau, P.E., Boutin, J., Eger, T. & Smets, M. (2006) "Vibration Spectral Class Characterization of Load-Haul-Dump Mining Vehicles and Seat Performance Evaluation" *In Proceedings of the First American Conference on Human Vibration*, Morgantown, WV, USA, 5-7.

Bovenzi M. (1996), "Low back pain disorders and exposure to whole-body vibration in the workplace," *Seminars in Perinatology*, Vol. 20, No. 1, pp. 38-53.

C. Yipeng, Z. Dayuan, G. Huijun, & M. Xiuzhen, (2014), "Study On Vibration Control Methods of Diesel Engine Fuel Injection System*," The 21st International Congress on Sound and Vibration,* Beijing, China,13-17.

Cann A.P., Salmoni A.W., Vi P., and Eger T.R., An exploratory study of whole-body vibration exposure and dose while operating heavy equipment in the construction industry, Applied Occupational and Environmental Hygiene, 2003, Vol. 18, No. 12, pp. 999-1005.

Cartwright, J. H. E. and Piro, 0. (1992), "The dynamics of Runge-Kutta methods," *International Journal of Bifurcation and Chaos*, *Vol. 2*(3), pp. 427-449.

E. Johanning, (1998), (1998), "Back disorder intervention strategies for mass transit operators exposed to whole-body vibration-comparison of two transit system approaches and practices," *Journal of Sound and Vibration*, *215* (4), 629–634.

Eger, T., Aaron M. Kociolek & James P. Dickey., (2013) "Comparing Health Risks to Load Haul Dump Vehicle Operators Exposed to Whole-Body Vibration Using EU Derective 2002/44EC, ISO 2631-1 and ISO 2631-5, Minerals 2013, Ontario, Canada.

Eger, T., Smets, M., Grenier, S., Vibration Research Group (2005), "Whole-body vibration exposure experienced during the operation of small and large load-haul-dump vehicles" *Proceedings of the 36th Annual Conference of Canadian Ergonomists, Halifax, NS.*

Eger, T., Stevenson, J., Boileau, Pe., & Salmoni, A. (2008), "Predictions of health risks associated with the operation of load-haul-dump mining vehicles: Part 1 Analysis of wholebody vibration exposure using ISO2631-1 and ISO 2631-5 standards". *International Journal of industrial Ergonomics*, 38(9-10), 726-738.

Eger, T., Stevenson, J., Grenier, S., Boileau, P.-É., Smets, M., (2006) "Whole-body vibration exposure and driver posture evaluation during the operation of LHD vehicles in underground mining," *Proceedings of the First American Conference on Human Vibration, Morgantown*, WV.

Eger, T.; Stevenson, J.; Grenier, S.; Boileau, P.E.; Smets, M. Influence of vehicle size, haulage capacity and ride control on vibration exposure and predicted health risks for LHD vehicle operators. J. Low Freq. Noise V. A. 2011, 30, 45-62.

Eger. T., Grenier, S & Salmoni, A. (2004) Whole-Body Vibration exposure experienced by mining equipment operators. Proceedings of Fifth Canadian Rural Health Research Society Conference and the Fourth International Rural Nurses Congress, Sudbury, ON.

Fairley, T. E., (1995) "Predicting the discomfort caused by tractor vibration", *Ergonomics*, 38(10), 2091-2106.

Friesenbichler, B., Lienhard, K., Vienneau, J., & Nigg, B. M. (2014), "Vibration Transmission to Lower Extremity Soft Tissues During Whole-Body Vibration," *Journal of Biomechanics,* 47 (2014) 2858–2862.

George Gazetas, 1983, "Analysis of machine foundation vibrations," *Soil Dynamics and Earthquake Engineering*, Troy, New York Vol. 2, No. 1.

Gillespie, T. D. (1999), "Fundamentals of Vehicle Dynamics," *Published by Society of Automotive Engineers, Inc*., Warrendale, PA, USA, 495pp.

Griefahn, B., Bröde, P., (1993) "The Significance Of Lateral Whole-Body Vibrations Related To Separately And Simultaneously Applied Vertical Motions," *Applied Ergonomics*, 1999, 3.

Griffin, M. J. (1998), "A Comparison of Standardized Methods for Predicting the Hazards of Whole-Body Vibration and Repeated Shocks," *Journal of Sound and Vibration, Vol.* 215, pp. 88-914.

Grube, G.J., & Ziperman, H.H. "Relationship between Whole-Body Vibration and Morbidity Patterns among Motor Coach Operators," *National Institute of Occupational Safety and Health*, Cincinnati, Ohio, 1992.

H. Choi, D. Lim, S. Hwang, Y. Kim, H. Kim, A Study Of Biomechanical Response In Human Body During WBV Through Musculoskeletal Model Development, Journal Of The Korean Society For Precision Engineering,Vol 25,2008.

Hoy, J., N. Mubarak, S. Nelson, M. Sweertsdelandas, M. Magnusson, O. Okunribido, and M. Pope, (2005), "Whole Body Vibration and Posture as Risk Factors for Low Back Pain among Forklift Truck Drivers." *Journal of Sound and Vibration*, 284 (3– 5), pp. 933–946.

International Standards Organization, "(1997) ISO 2631-1: Mechanical vibration and shock-Evaluation of human exposure to whole-body vibration-Part 1: General requirements," *International Standards Organization*, Geneva, Switzerland.

Ishikawa F. Development of vibration protection seats for agricultural machinery. Industrial Health. 1998, 36:133-139.

ISO-2631, (1997), "Evaluation of Human Exposure to Whole Body Vibration," *International Standards Organization.* Available from: International Standards Organization. Specific to ISO-2631, Geneva.

James P. Dickey, Tammy R. Eger, Michele L. Oliver, Paul-Emile Boileau, Lana M. Trick, A. Michelle Edwards, (2007) "Multi-axis sinusoidal whole-body vibrations: part ii - relationship between vibration total value and discomfort varies between vibration axes," *Journal of Low Frequency Noise, Vibration And Active Control, 26* (3) 195 – 204.

Johanning, E., Fischer, S., Christ, E., Gores, B., & (2006) "Luhrman, R. Railroad Locomotive Whole-Body Vibration Study: Vibration, Shocks and Seat Ergonomics," *In Proceedings of the First American Conference on Human Vibration*, Morgantown, WV, USA, 5–7.

Kamenskii, Y. & Nosova, I. (1989), "Effects of whole-body vibration on certain indicators of neuro-endocrine processes," *Noise and Vibration Bulletin*, pp205-206.

Khatake, P. &P. T. Nitnaware, (2013), "Vibration mitigation using passive damper in machining," *International Journal of Modern Engineering Research*, pp-3649-3652.

Kitazaki, S. & Griffin, M. (1998), "Resonance behavior of the seated human body and effects of posture," *3*, 143–149.

Kittusamy, N. K. (2003), "Self-Reported Musculoskeletal Symptoms among Operators of Heavy Construction Equipment," XVth Triennial Congress, *International Ergonomics Association*, Seoul, Korea, August 24-29.

Kumar A, Puneet M, Mohan D. & Vargese M. (2001), "Tractor vibration severity and Driver health," *A study from Rural India*, *80*(4), 313 – 328.

Lagrange, J. L. (1788), "Mecanique Analytique (Analytical Mechanics)," Fourth Edition, 1888-89, Published by Gauthier-Villars & fils, Paris, First Edition in 1788.

Larsson, P. (2011), "Prevention of Servo-Induced Vibrations in Robotics," *Maters Thesis, Department of Automatic Control*, Lund University, Sweden.

Law, S. S., Wu, Z. M. and Chan, S. L. (2004), "Vibration Control Study of a Suspension Footbridge Using Hybrid Slotted Bolted Connection Elements," *Engineering Structures*, Vol. 26, pp. 107-116.

Matthew Dunbabin, Stephen Brosnan, Jonathan Roberts and Peter Corke, 2004, "Vibration Isolation for Autonomous Helicoter Flight," International Conference on Robotics and Automation, New Orleans, LA, April 2004.

McPhee, B. (2004) "Ergonomics in mining," *Occ. Med., 54*, 297-303.

Negrut, D. and Ortiz, J.L. (2005), "An Approach for the Linearization of the Differential Algebraic Equations of Multi-Body Dynamics," *ASMEIIEEE International Conference on Mechatronic and Embedded Systems and Applications.*

Paddan, G.S. & M.J. Griffin, "Evaluation of Whole-Body Vibration in Vehicles," *Journal of Sound and Vibration*, *253* (1) (2002) 195–213.

Park C. H., Park, D. & Park, J. (2013), "Vibration Control of Flexible Mode for a Beam-Type Substrate Transport Robot," *International Journal of Advanced Robotic Systems*, Korea.

Punnett L., Pruss-Utun A., Nelson D.l., Fingerhut M.A., Leigh J., Tak S., & Phillips S., (2005) "Estimating the global burden of low back pain attributable to combined occupational exposures," *American Journal of Industrial Medicine,* Vol. 48, No. 6, pp. 459–469.

Ramachandran, T., & Padmanaban, K. P., (2012), "Review on Internal Combustion Engine Vibrations and Mountings," *International Journal of Engineering Sciences & Emerging Technologies*, pp.63-73.

Rehn B, Bergdahl I, Ahlgren C, From C, Jarvholm B, Lundstrom R, Nilsson T & Sundelin G. (2002), "Musculo-skeletal symptoms among drivers of all-terrain vehicles," *Journal of sound and vibration*, 253 (1), 21-29.

Riihimaki H, Tola S, Videman T, & Hanninen K. (1989) "Low Back Pain and Occupation. A cross-sectional questionnaire study of men in machine operating, dynamic physical work and sedentary work Spine, 14:204-209.

Saleh, K. (2013), "Modelling and Analysis of Chatter Mitigation Strategies in Milling*," Ph.D. Thesis,* Sheffield, UK.

Seidel, H. (1993), "Selected health risks caused by long-term whole-body vibration," *American Journal of Industrial Medicine*, 23(4), 589-604.

Sharad Kumar Shukla, and Akhilesh Lodwal, 2013, "Experimental Analysis of Vibration On Radial Drilling Machine Using Piezoelectric Sensor," Bookman International Journal of Mechanical and Civil Engineering, Vol. 2 No. 1 Jan-Feb-Mar 2013.

Shoenberger R.W. (1980), "Psychophysical comparison of vertical and angular vibrations," *Aviation, Space and Environmental Medicine*, 1980, Vol. 51, No. 8, pp. 759-762.

Singh, K. V. and Ram, Y. M. (2000), "Dynamic Absorption by Passive and Active Control," *Journal of Vibration and Acoustics, American Society of Mechanical Engineers*, Vol. 122, pp. 429 - 433.

Smith, S. D. (1998), "The Effect of Prototype Helicopter Seat Cushion Concepts on Human Body Vibration Response," *Journal of Low Frequency Noise, Vibration and Active Control*, Vol. 17(1), Multi - Science Publishing Co. Ltd., United Kingdom.

Soedel, W. (2004), "Vibrations of Shells and Plates," Third Edition, Revised and Expanded, *Published by Marcel Dekker Inc.*, New York, USA 592pp.

Suzuki, H. (1997) "A Study on the Vibrational Factors Determining the Riding Comfort of Railway Vehicle," *The Japanese Journal of Ergonomics,* Vol. 33(6), pp. 349 – 355.

T. Hansson, M. Magnusson & H. BromanBack (1991), "muscle fatigue and seated whole body vibrations: an experimental study in man Clinical Biomechanics," *6*, pp. 173-178.

Tiemessen, I. J. H., Hulshof C. T. J., & Frings-Dresen M. H. W. (2008). "Low Back Pain in Drivers Exposed to Whole Body Vibration: Analysis of a Dose-Response Pattern." *Occupational and Environmental Medicine*, *65* (10): 667 –675.

Village, J, Morrison J. & Leong D. (1989) "Whole-body vibration in underground load haul dump vehicles," *Ergonomics*, 31 (10), 1167-1183. IS0 2631-1 (1997).

Village, J. Morrison, J.B. & Leong, D. (1989), "Whole-body vibration in underground load-haul-dump vehicles," *Ergonomics, 32*, 1167-1183.

Wikström, B.O., Kjellberg A., & Landström, U. (1994), "Health effects of long-term occupational exposure to whole-body vibration," *International Journal of Industrial Ergonomics,* 14 (1994), pp. 273-292.

Yamakawa, H., Sakai, Y., Yamamoto, Y., Barber, A. J. & Wakabayashi, Y. (2002), "An Application of Full Vehicle ADAMS Modeling with Detailed Force Elements: Collaborative activity among Design, Experiment & CAE in the field of vehicle dynamics," *International Symposium on Advanced Vehicle Control (AVEC-02), Society of Automotive Engineers of Japan (JSAE)*, Hiroshima, Japan, September 2002.

Yangmin LI, Yugang Liu & Xiaoping Liu, (2005), "Active Vibration Control of a Modular Robot Combining a Back-Propagation Neural Network with a Genetic Algorithm," *Journal of Vibrations and Control*, Beijing, China, January 24- April 7, 2004.

VITA

Kgosietsile Kolobe was born and raised in a mining town of Selebi-Phikwe, Botswana. He obtained his Bachelor of Science in Mining Engineering from Missouri University of Science and Technology (Rolla, USA). He has worked for RESPEC consulting (Kentucky, USA), Casteel Mine (Doe Run company, USA), BCL Mine (Botswana) and he is one of the pioneers of Diamond Mine in Botswana (Gem Diamonds Mining) where he started with the company from bush clearing to the production of first diamonds. Kolobe Has also worked as a teaching fellow for Saudi Mining Polytechnic (Ar'ar, Saudi Arabia), and as a research and teaching assistant at Missouri University of Science and Technology. He received his PhD in Mining Engineering in December 2017 from Missouri S&T.